

Lithiated Imines:
Solvent-Dependent Aggregate Structures and
Mechanisms of Alkylation

Stephan J. Zuend, Antonio Ramírez, Emil Lobkovsky, and David B. Collum*

Contribution from the Department of Chemistry and Chemical Biology

Baker Laboratory, Cornell University

Ithaca, New York 14853-1301

Supporting Information

	Page
Part 1: Experimental Procedures	S5
Part 2: NMR Spectroscopic Studies	
I ^1H NMR and ^{13}C NMR spectra of [^{15}N]cyclohexylcarboxamide	S7
II ^1H NMR and ^{13}C NMR spectra of [^{15}N]cyclohexylammonium tosylate	S8
III ^1H NMR and ^{13}C NMR spectra of [^{15}N]5	S9
IV Syn/anti selectivities for the alkylation of 3 with $n\text{-C}_7\text{H}_{15}\text{I}$	S10
V ^1H NMR and ^{13}C NMR spectra of 2-heptyl cyclohexanone	S12
VI ^1H NMR and ^{13}C NMR spectra of 2-octyl cyclohexanone	S13
VII ^6Li NMR spectra of [$^6\text{Li},^{15}\text{N}$] 3 in $n\text{-BuOMe}$ /toluene at $-90\text{ }^\circ\text{C}$	S14
VIII ^{15}N NMR spectra of [$^6\text{Li},^{15}\text{N}$] 3 in $n\text{-BuOMe}$ at $-90\text{ }^\circ\text{C}$	S14
IX ^6Li NMR spectra of [$^6\text{Li},^{15}\text{N}$] 3 in $n\text{-BuOMe}$ at variable temp	S15
X ^6Li NMR spectra of [$^6\text{Li},^{15}\text{N}$] 3 in $n\text{-BuOMe}$ /THP/toluene	S17
XI ^6Li NMR spectra of [$^6\text{Li},^{15}\text{N}$] 3 in $n\text{-BuOMe}$ /THP at variable temp	S18
XII ^6Li NMR spectra of [$^6\text{Li},^{15}\text{N}$] 3 in Et_2O /toluene at $-90\text{ }^\circ\text{C}$	S19
XIII ^{15}N NMR spectra of [$^6\text{Li},^{15}\text{N}$] 3 in Et_2O at $-90\text{ }^\circ\text{C}$	S19
XIV ^6Li NMR spectra of [$^6\text{Li},^{15}\text{N}$] 3 in Et_2O at variable temp	S20
XV ^6Li NMR spectra of [$^6\text{Li},^{15}\text{N}$] 3 in $t\text{-BuOMe}$ /toluene at $-90\text{ }^\circ\text{C}$	S21

XXVI	^{15}N NMR spectra of $[^6\text{Li},^{15}\text{N}]\mathbf{3}$ in <i>t</i> -BuOMe at $-90\text{ }^\circ\text{C}$	S21
XXVII	^6Li NMR spectra of $[^6\text{Li},^{15}\text{N}]\mathbf{3}$ in 2,2-Me ₂ THF / toluene at $-90\text{ }^\circ\text{C}$	S22
XXVIII	^{15}N NMR spectra of $[^6\text{Li},^{15}\text{N}]\mathbf{3}$ in 2,2-Me ₂ THF at $-90\text{ }^\circ\text{C}$	S22
XIX	^6Li NMR spectra of $[^6\text{Li},^{15}\text{N}]\mathbf{3}$ in 2-MeTHF / toluene at $-90\text{ }^\circ\text{C}$	S23
XX	^{15}N NMR spectra of $[^6\text{Li},^{15}\text{N}]\mathbf{3}$ in 2-MeTHF recorded at $-90\text{ }^\circ\text{C}$	S24
XXI	^6Li NMR spectra of $[^6\text{Li},^{15}\text{N}]\mathbf{3}$ in 2-MeTHF / toluene at variable temp	S25
XXII	^6Li NMR spectra of $[^6\text{Li},^{15}\text{N}]\mathbf{3}$ in 2-MeTHF / THP / toluene at $-90\text{ }^\circ\text{C}$	S26
XXIII	^6Li NMR spectra of $[^6\text{Li},^{15}\text{N}]\mathbf{3}$ in 2-MeTHF / THP at variable temp	S27
XXIV	^6Li NMR spectra of $[^6\text{Li},^{15}\text{N}]\mathbf{3}$ in THP / toluene at $-90\text{ }^\circ\text{C}$	S28
XXV	$^6\text{Li}\{^{15}\text{N}\}$ NMR spectra of $[^6\text{Li},^{15}\text{N}]\mathbf{3}$ in 5.0 M THP / toluene at $-90\text{ }^\circ\text{C}$	S29
XXVI	$^6\text{Li}\{^{15}\text{N}\}$ NMR spectra of $[^6\text{Li},^{15}\text{N}]\mathbf{3}$ in 1.6 M THP / toluene at $-90\text{ }^\circ\text{C}$	S30
XXVII	^{15}N NMR spectra of $[^6\text{Li},^{15}\text{N}]\mathbf{3}$ in 5.0 M THP / toluene at $-90\text{ }^\circ\text{C}$	S31
XXVIII	Selective ^{15}N decoupled ^6Li NMR spectra of $[^6\text{Li},^{15}\text{N}]\mathbf{3}$ in THP / toluene	S32
XXIX	^6Li NMR spectra of $[^6\text{Li},^{15}\text{N}]\mathbf{3}$ in 5.0 M THP / toluene at variable temp	S33
XXX	^6Li NMR spectra of $[^6\text{Li},^{15}\text{N}]\mathbf{3}$ in THF / toluene at $-90\text{ }^\circ\text{C}$	S34
XXXI	^6Li NMR spectra of $[^6\text{Li},^{15}\text{N}]\mathbf{3}$ in THF / toluene at $-90\text{ }^\circ\text{C}$	S35
XXXII	^{15}N NMR spectra of $[^6\text{Li},^{15}\text{N}]\mathbf{3}$ in THF / toluene at $-90\text{ }^\circ\text{C}$	S36
XXXIII	^6Li NMR spectra of $[^6\text{Li},^{15}\text{N}]\mathbf{3}$ in 5.0 M THF / toluene at variable temp	S37
XXXIV	$J(^6\text{Li},^{15}\text{N})$ -resolved NMR spectrum of $[^6\text{Li},^{15}\text{N}]\mathbf{3}$ in THP / toluene	S38

Part 3: Rate Studies

XXXV	Plot of k_{obsd} vs $[n\text{-BuOMe}]$ for the alkylation of $\mathbf{3}$ with $n\text{-C}_7\text{H}_{15}\text{I}$	S39
XXXVI	Plot of k_{obsd} vs $[\mathbf{3}]$ in 2.10 M <i>n</i> -BuOMe / toluene for the alkylation of $\mathbf{3}$	S40
XXXVII	Plot of k_{obsd} vs $[\mathbf{3}]$ in 6.10 M <i>n</i> -BuOMe / toluene for the alkylation of $\mathbf{3}$	S41
XXXVIII	Plot of k_{obsd} vs $[t\text{-BuOMe}]$ for the alkylation of $\mathbf{3}$ with $n\text{-C}_7\text{H}_{15}\text{I}$	S42
XXXIX	Plot of k_{obsd} vs $[\mathbf{3}]$ in 2.10 M <i>t</i> -BuOMe / toluene for the alkylation of $\mathbf{3}$	S43

XL	Plot of k_{obsd} vs [3] in 6.10 M <i>t</i> -BuOMe/toluene for the alkylation of 3	S44
XLI	Plot of k_{obsd} vs [2-MeTHF] for the alkylation of 3 with <i>n</i> -C ₈ H ₁₇ Br	S45
XLII	Plot of k_{obsd} vs [2-MeTHF] for the alkylation of 3 with <i>n</i> -C ₇ H ₁₅ I	S46
XLIII	Plot of k_{obsd} vs [3] in 1.10 M 2-MeTHF/toluene for the alkylation of 3	S47
XLIV	Plot of k_{obsd} vs [3] in 4.10 M 2-MeTHF/toluene for the alkylation of 3	S48
XLV	Plot of k_{obsd} vs [3] in 8.10 M 2-MeTHF/toluene for the alkylation of 3	S49
XLVI	Plot of k_{obsd} vs [Et ₂ O] for the alkylation of 3 with <i>n</i> -C ₇ H ₁₅ I	S50
XLVII	Plot of k_{obsd} vs [3] in 2.10 M Et ₂ O/toluene for the alkylation of 3	S51
XLVIII	Plot of k_{obsd} vs [3] in 8.10 M Et ₂ O/toluene for the alkylation of 3	S52
XLIX	k_{obsd} in various ethereal solvents for the alkylation of 3 with <i>n</i> -C ₇ H ₁₅ I	S53
L	Representative decays of <i>n</i> -C ₈ H ₁₇ Br relative to an internal standard	S53

Part 4: DFT Computational Studies

LI	Geometries and energies of monomers AS_n	S54
LII	Selected bond lengths and angles of monomers AS_n	S55
LIII	Geometries and energies of dimers A₂S_n	S56
LIV	Selected bond lengths and angles of dimers A₂S_n	S59
LV	Geometries and energies of trimers A₃S_n	S62
LVI	Selected bond lengths and angles of trimers A₃S_n	S66
LVII	Geometries and energies of monomer-based transition structures	S68
LIVIII	Selected bonds and angles of monomer-based transition structures	S69
LIX	Geometries and energies of dimer-based transition structures	S70
LX	Selected bond lengths and angles of dimer-based transition structures	S75

Part 5: GIAO Computational Studies

LXI	Calculated δ and J for monomers AS_n	S76
LXII	Calculated δ and J for dimers A₂S_n	S77

LXIII	Calculated δ and J for trimers A_3S_n	S78
LXIV	Effect of solvation and π -complexation upon δ and J for dimers A_2S_n	S79
LXV	Effect of solvation and π -complexation upon δ and J for trimers A_3S_n	S79
Part 6: X-Ray Crystal Data		
LXVI	X-ray crystal data for lithioimine <i>trans</i> - 12 (A_2S_2 , $S = Me_2EtN$)	S80
LXVII	Ortep drawing of lithioimine <i>trans</i> - 12	S87
Part 7: References		S88

Part 1: Experimental Procedures

[¹⁵N]Cyclohexylcarboxamide.^[S-1] A 250 mL round bottom flask containing a small stir bar was charged with ¹⁵NH₄Cl (3.01 g, 55.2 mmol) and 15 mL of distilled water. Cyclohexylcarbonyl chloride (11.0 g, 77.1 mmol) in 30 mL anhydrous Et₂O was layered on to the aqueous solution. The reaction mixture was cooled in an ice bath and 50 % aq NaOH (30 mL) was added via syringe with slow stirring to avoid mixing the layers. The reaction mixture was warmed to room temperature and stirred slowly for an additional 15 min. The reaction mixture was then stirred vigorously for 5 min, capped with a glass stopper, and shaken with frequent venting. The white solid that formed was extracted with 3 x 500 mL CH₂Cl₂, washed with 200 mL brine, dried over Na₂SO₄, filtered, and dried in vacuo. The resulting solid was dissolved in hot CH₃CN, filtered, and crystallized at -20 °C to yield 5.65 g of [¹⁵N]cyclohexylcarboxamide (44.4 mmol, 80 %) as white flakes (see S7 for spectral data).

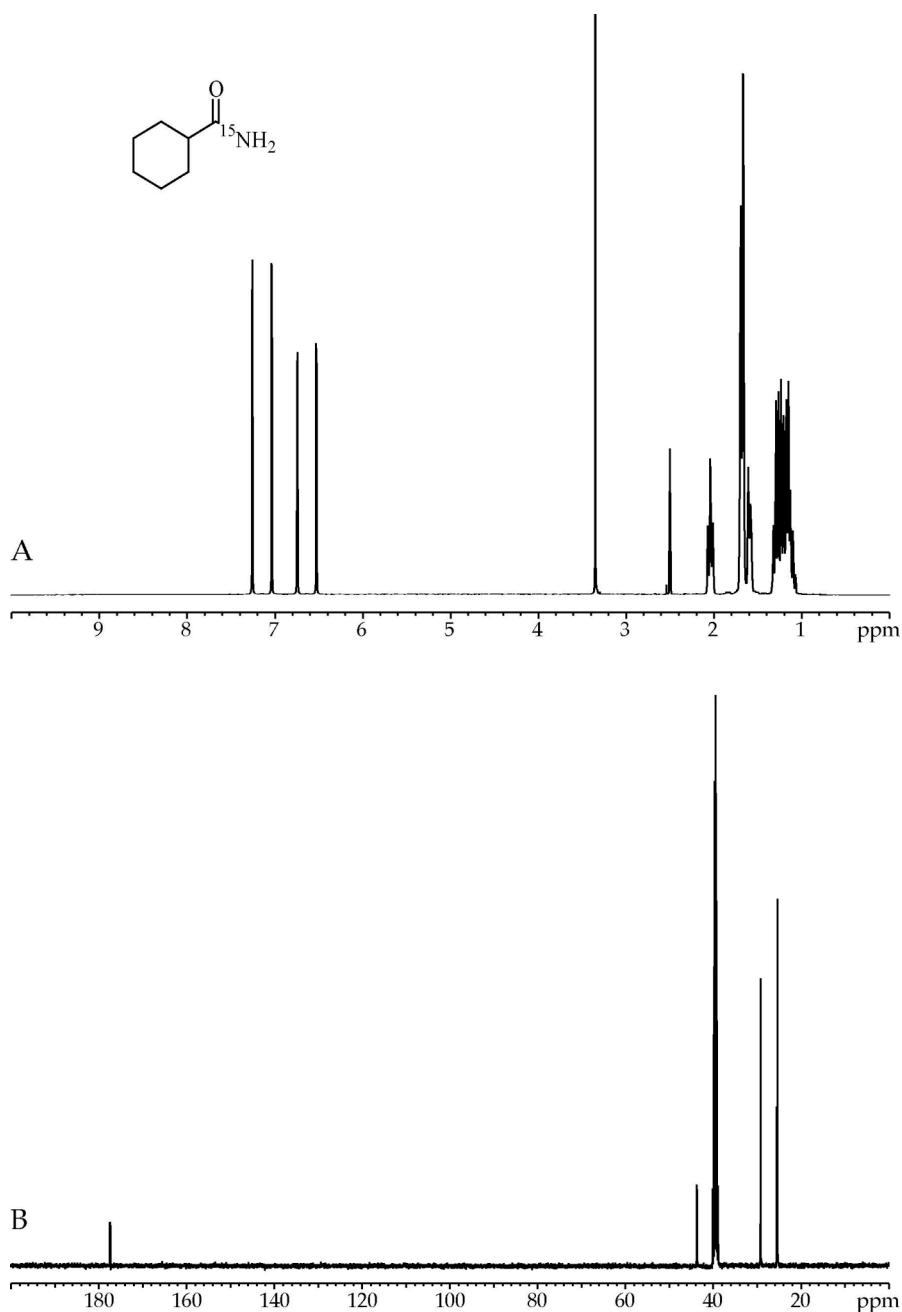
[¹⁵N]Cyclohexylammonium tosylate.^[S-2] A 500 mL round bottom flask was charged with [hydroxyl(tosyloxy)iodo]benzene^[S-3] (18.5 g, 47.6 mmol) and 50 mL CH₃CN. [¹⁵N]cyclohexylcarboxamide (5.55 g, 43.6 mmol) was added dissolved in hot CH₃CN (150 mL), and the reaction mixture was heated at reflux for 1 h to give a yellow solution that yielded a white precipitate upon standing at room temperature. The reaction mixture was cooled to -20 °C to complete precipitation. Filtration, drying, and recrystallization from 10:1 THF/EtOH yielded 10.1 g of [¹⁵N]cyclohexylammonium tosylate (37.1 mmol, 85 %) as white needles (see S8 for spectral data).

[¹⁵N]Cyclohexanone cyclohexylimine ([¹⁵N]5). A flame dried 50 mL round bottom flask was charged with [¹⁵N]cyclohexylammonium tosylate (3.05 g, 11.2 mmol) and 3 Å molecular sieves (3.5 g). The flask was evacuated, and freshly distilled Et₃N (25 mL) and cyclohexanone (2.50 mL, 2.37 g, 24.2 mmol) were added under an argon purge. The reaction mixture was stirred for 40 h under argon and filtered to remove the molecular sieves. Distillation (0.1 torr, b.p. 70-72 °C) yielded 1.72 g of [¹⁵N]cyclohexanone cyclohexylimine (9.6 mmol, 86 %) as

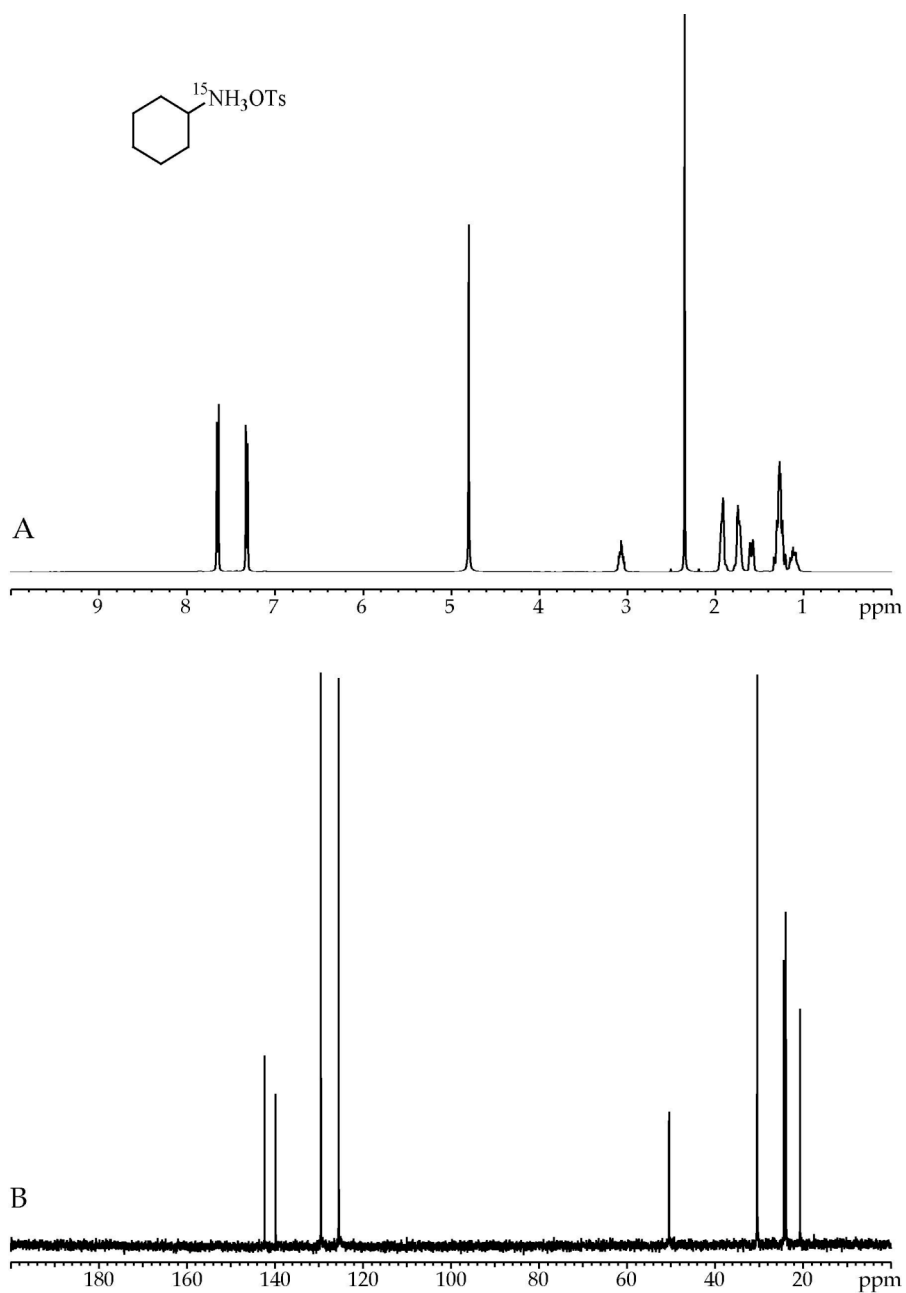
a colorless oil (see S9 for spectral data). Unlabelled **5** was prepared by methods described previously.^{5a}

[⁶Li, ¹⁵N]Lithiated cyclohexanone cyclohexylimine ([⁶Li, ¹⁵N]3**).** A flame dried 100 mL round bottom flask was charged with recrystallized [⁶Li]LDA^[5-4] (0.50 g, 4.7 mmol) and 20 mL of freshly distilled hexanes under argon. After heating to dissolve the LDA and cooling to room temperature, [¹⁵N]**3** (1.0 g, 5.6 mmol) was added neat. The solution immediately turned yellow and a precipitate was observed after ~ 5 min. Stirring for 1 h led to significant formation of a white solid. Further precipitation was achieved by cooling the reaction mixture to -78 °C for 2 h. Filtration, washing with 2 x 10 mL fresh hexanes, and drying in vacuo yielded 0.73 g of [⁶Li, ¹⁵N]**3** (3.9 mmol, 84 %) as a white powder which was stored in a dry box. Unlabelled **3** for use in rate studies was prepared on multigram scales (5.0 g LDA) using the method described above with a 250 mL round bottom flask and 200 mL hexanes.

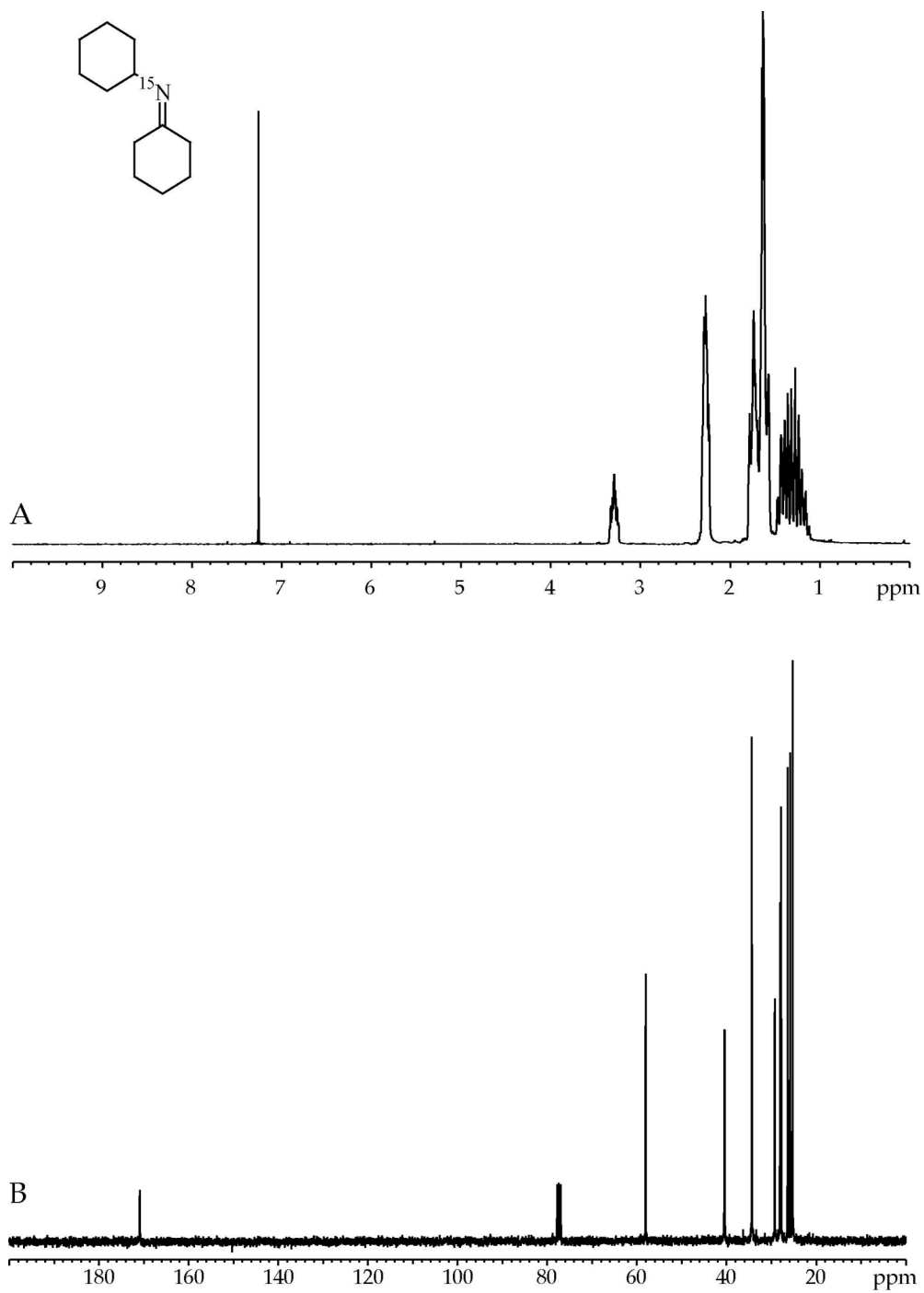
Part 2: NMR Spectroscopic Studies



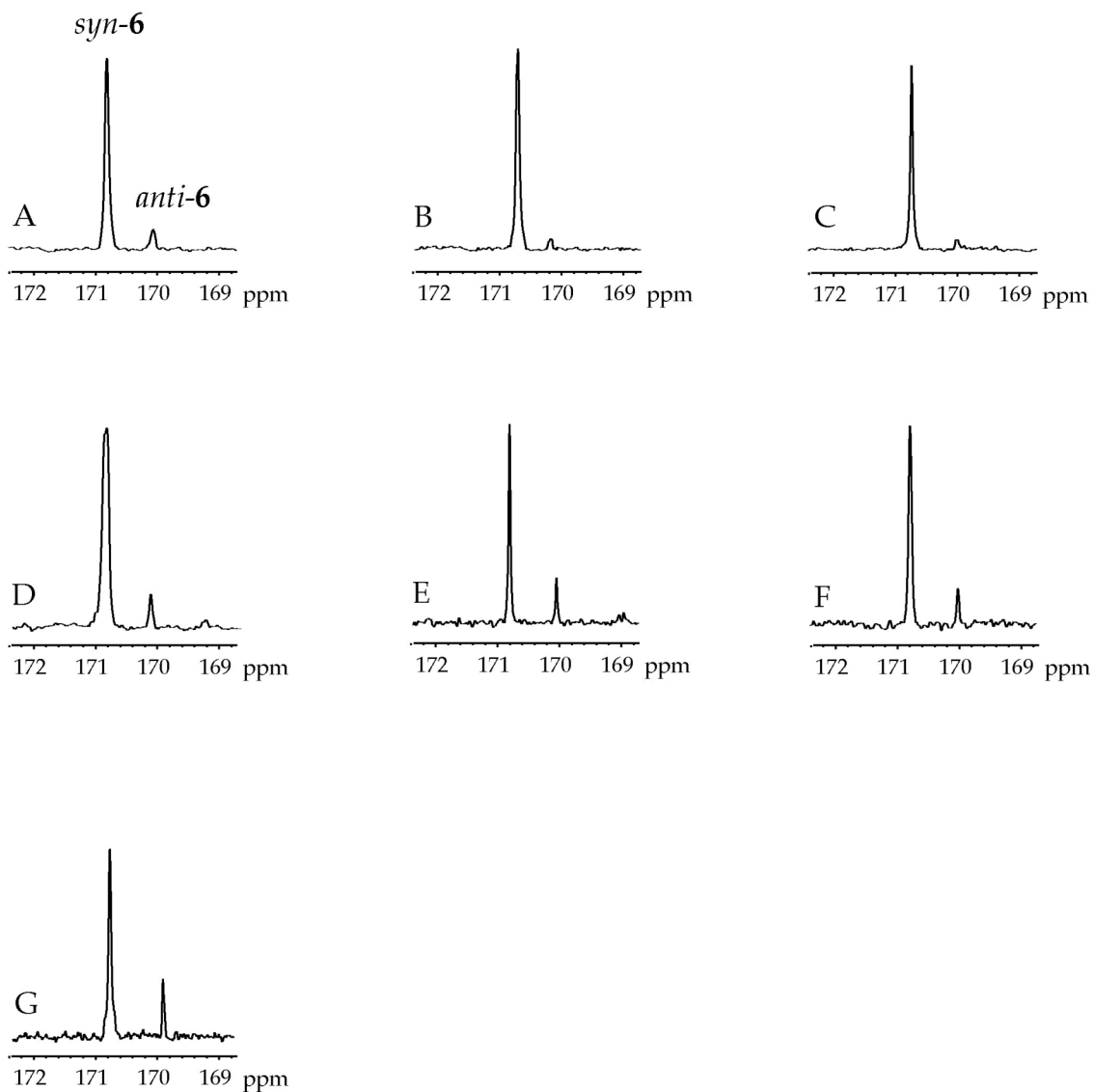
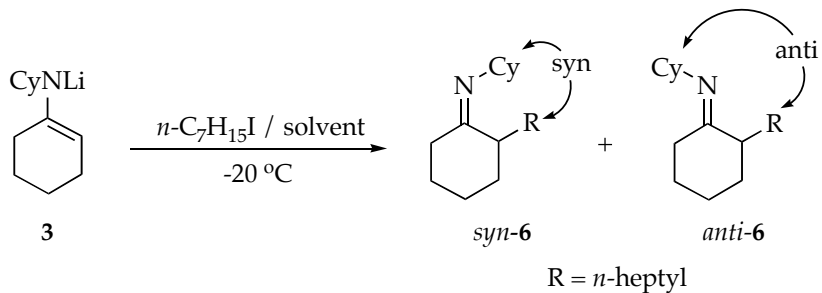
I. NMR spectra of [¹⁵N]cyclohexylcarboxamide. (A) ¹H NMR (400 MHz, DMSO-*d*₆, 20 °C) δ 1.06-1.33 (m, 5H), 1.56-1.62 (m, 2H), 1.64-1.71 (m, 3H), 2.04 (tt, J = 11.4, 3.1 Hz, 1H), 6.64 (dd, J = 87.3, 2.4 Hz, 1H), 7.15 (dd, J = 89.2, 2.4 Hz, 1H). (B) ¹³C{¹H} NMR (100 MHz, DMSO-*d*₆, 20 °C) δ 25.4, 25.6, 29.2, 43.7 (d, J = 7.5 Hz), 177.4 (d, J = 13.9 Hz).



II. NMR spectra of [^{15}N]cyclohexylammonium tosylate. (A) ^1H NMR (400 MHz, D_2O , 20°C) δ 1.05-1.16 (m, 1H), 1.19-1.34 (m, 4H), 1.55-1.63 (m, 1H), 1.68-1.77 (m, 2H), 1.87-1.96 (m, 2H), 2.35 (s, 3H), 3.03-3.11 (m, 1H), 7.32 (d, $J = 8.3$ Hz, 2H), 7.65 (d, $J = 8.3$ Hz, 2H). (B) $^{13}\text{C}\{^1\text{H}\}$ NMR (75 MHz, D_2O , 20°C) δ 20.7, 23.9, 24.4, 50.4 (d, $J = 4.6$ Hz), 125.5, 129.5, 139.8, 142.3.



III. NMR spectra of [^{15}N]5. (A) ^1H NMR (400 MHz, CDCl_3 , 20 °C) δ 1.30-1.47 (m, 6H), 1.56-1.81 (m, 11H), 2.22-2.31 (m, 4H), 3.23-3.34 (m, 1H). (B) $^{13}\text{C}\{^1\text{H}\}$ NMR (75 MHz, CDCl_3 , 20 °C) δ 25.3, 25.8, 26.4, 27.8, 28.1, 29.2 (d, $J = 2.9$ Hz), 34.3 (d, $J = 2.9$ Hz), 58.0, 170.9 (d, $J = 7.0$ Hz).



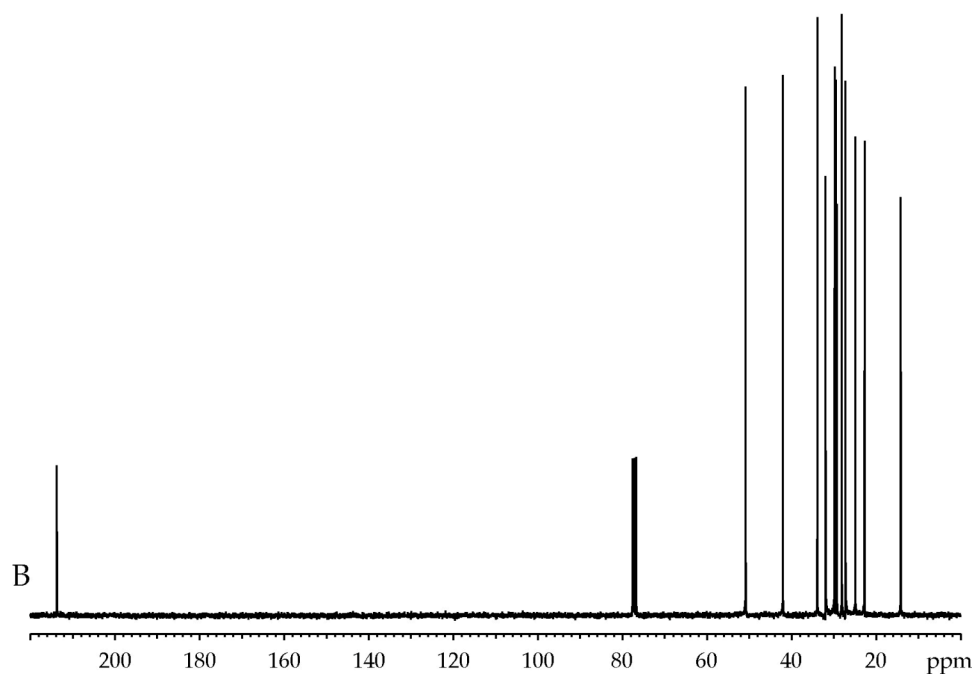
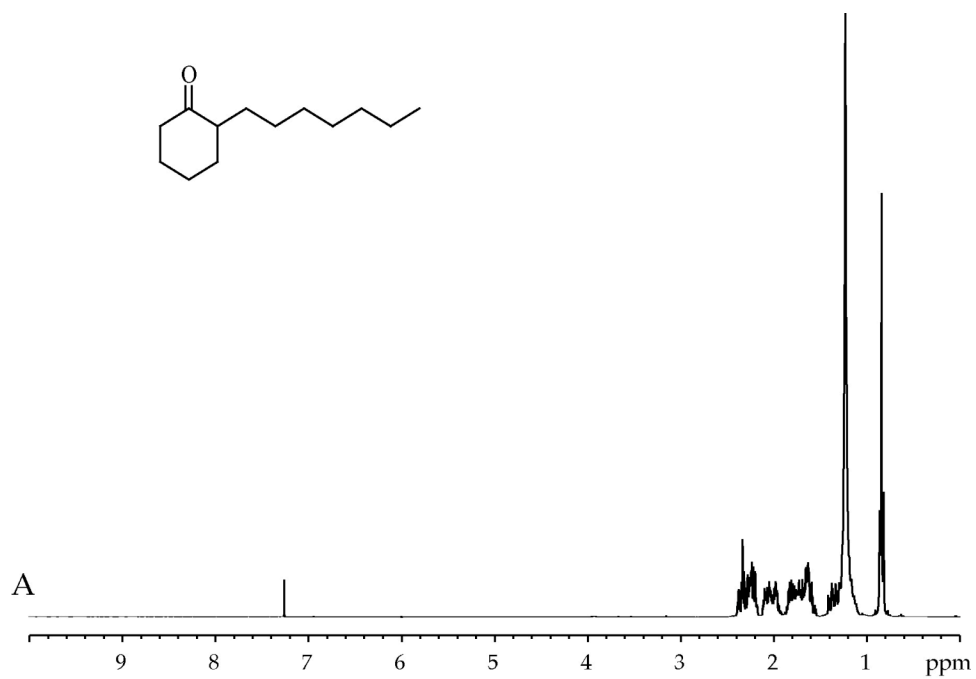
IV. C=N region of the ^{13}C spectra of *syn/anti* mixtures of imine **6** resulting from the alkylation of **3** with 1.1 equiv of $n\text{-C}_7\text{H}_{15}\text{I}$ in: (A) THF; (B) THP; (C) 2-MeTHF; (D) $n\text{-BuOMe}$; (E) 2,2-Me₂THF; (F) Et₂O; (G) $t\text{-BuOMe}$.

IV. (Continued) Syn/anti stereoselectivity of the alkylation of lithiated *N*-alkylimine **3** with *n*-C₇H₁₅I^a

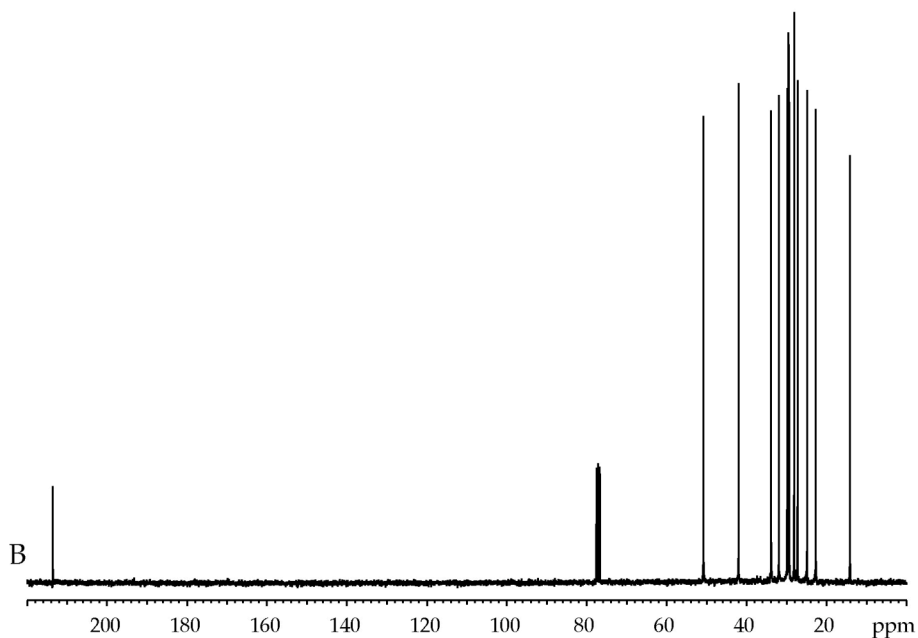
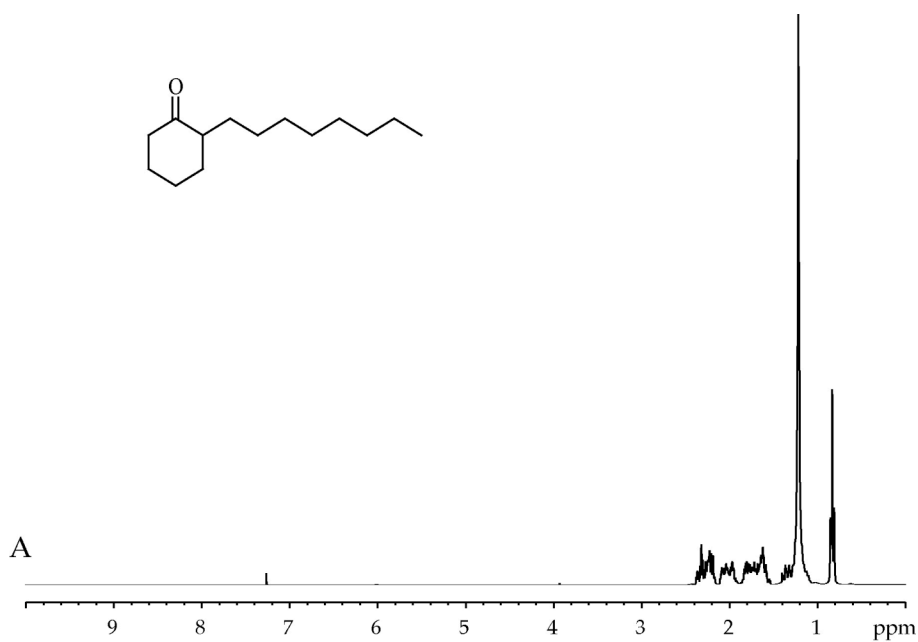
entry	solvent	syn/anti ^b
1	THF	10:1
2	THP	>20:1
3	2-MeTHF	>20:1
4	<i>n</i> -BuOMe	8:1
5	2,2-Me ₂ THF	6:1
6	Et ₂ O	6:1
7	<i>t</i> -BuOMe	5:1

^a Reactions were carried out at -20 °C using 0.1 M solutions of **3** in neat solvent and 1.1 equiv of *n*-C₇H₁₅I. The sample was sealed in an NMR tube under Ar and kept at -78 °C until the spectra were recorded. Under these conditions, the isomerizations (*t*_{1/2} > 6 h at 40 °C) proved to be slower than the alkylations.

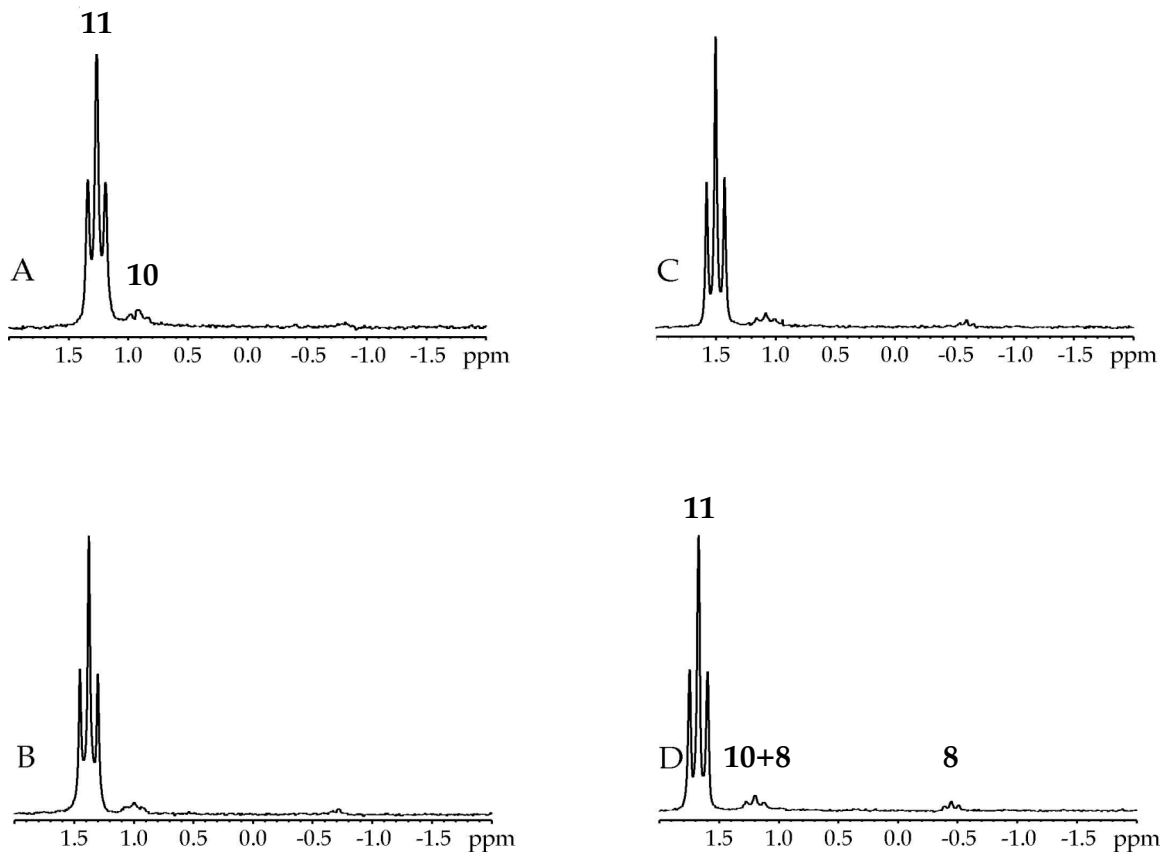
^b Numerical ratios were obtained from ¹³C NMR spectra. The syn and anti orientations in 2-heptyl imine **6** (R = *n*-C₇H₁₅) were assigned following protocols described elsewhere.^{5a}



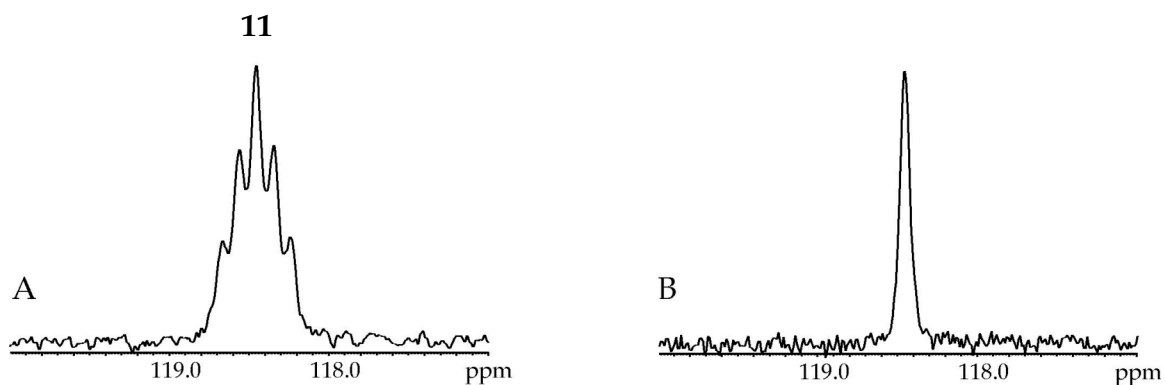
V. NMR spectra of 2-heptylcyclohexanone. (A) ¹H NMR (300 MHz, CDCl₃, 20 °C) δ 0.84 (t, *J* = 6.6 Hz, 3H), 1.16-1.42 (m, 12H), 1.55-1.87 (m, 4H), 1.94-2.12 (m, 2H), 2.17-2.40 (m, 3H). (B) ¹³C{¹H} NMR (75 MHz, CDCl₃, 20 °C) δ 14.2, 22.8, 24.9, 27.3, 28.1, 29.3, 29.5, 29.8, 31.9, 33.9, 42.0, 50.9, 213.7.



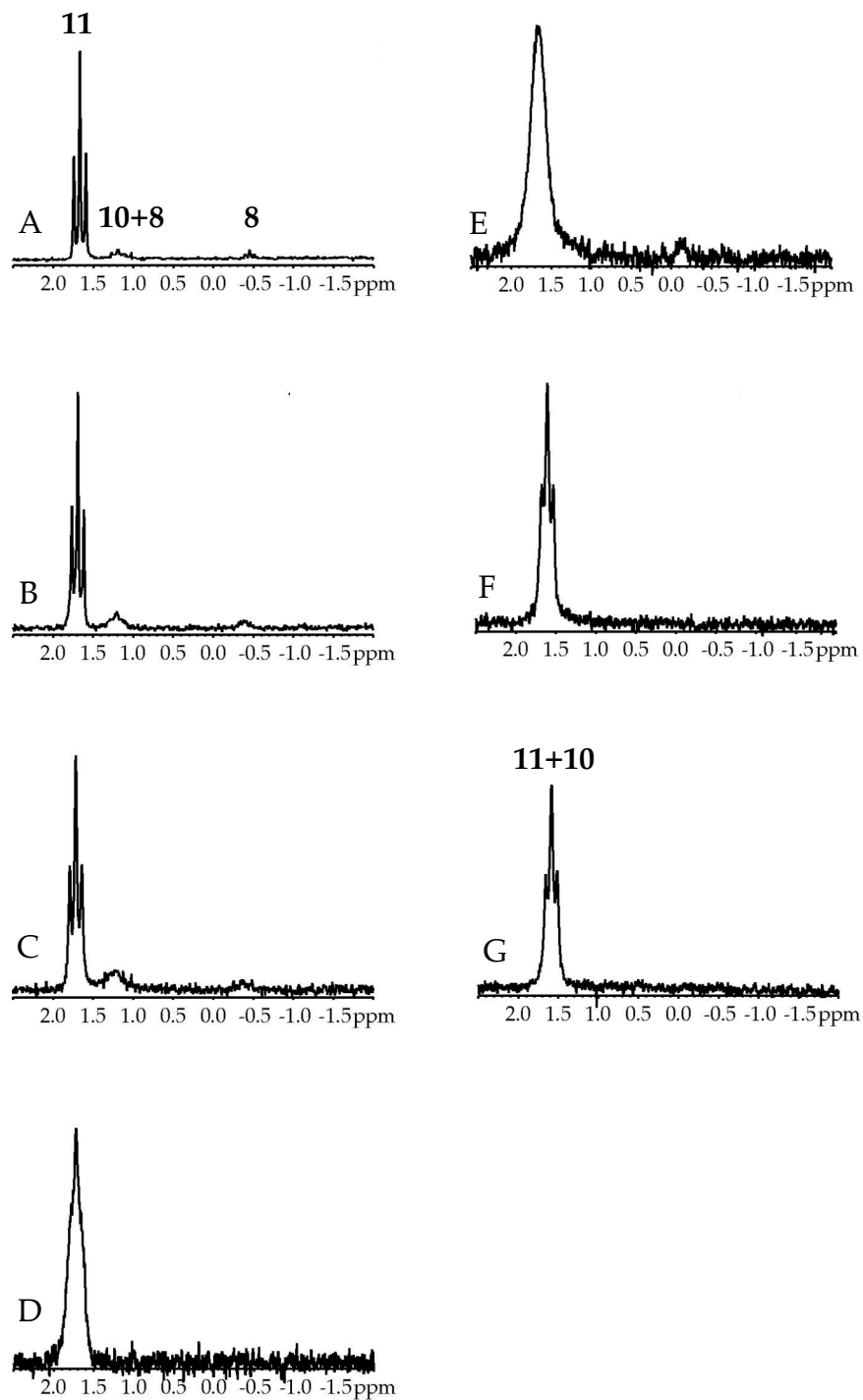
VI. NMR spectra of 2-octyl cyclohexanone. (A) ^1H NMR (300 MHz, CDCl_3 , 20 $^\circ\text{C}$) δ 0.83 (t, $J = 6.5$ Hz, 3H), 1.16-1.41 (m, 14H), 1.54-1.84 (m, 4H), 1.93-2.11 (m, 2H), 2.17-2.38 (m, 3H). (B) $^{13}\text{C}\{^1\text{H}\}$ NMR (75 MHz, CDCl_3 , 20 $^\circ\text{C}$) δ 14.2, 22.7, 24.9, 27.3, 28.1, 29.4, 29.5, 29.6, 29.9, 32.0, 33.9, 42.0, 50.8, 213.6.



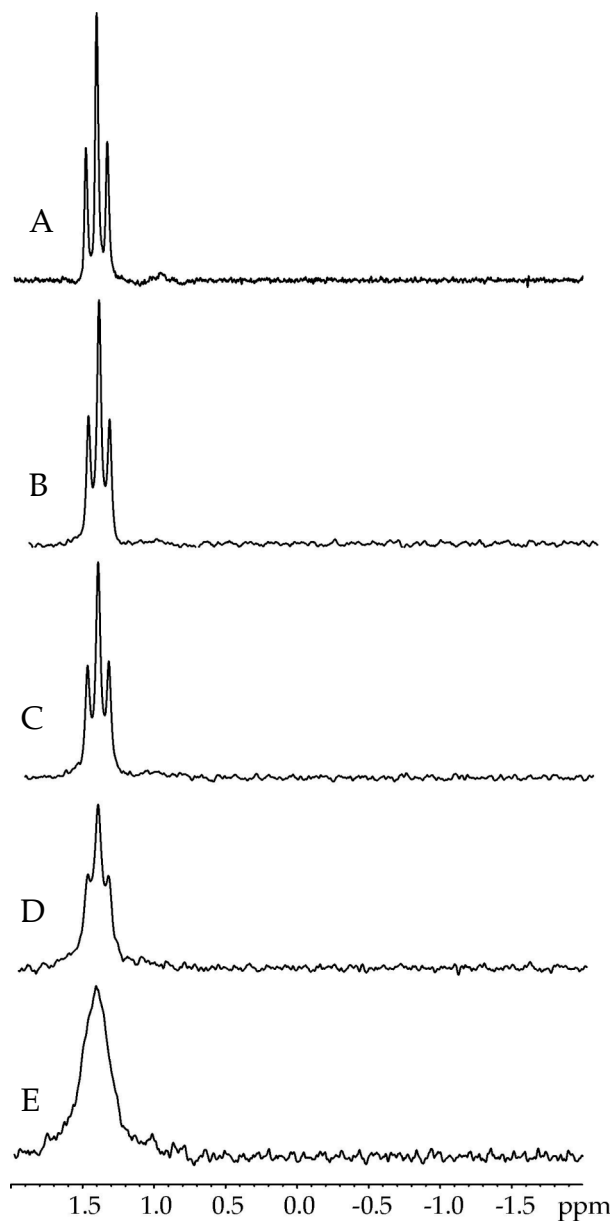
VII. ${}^6\text{Li}$ NMR spectra of 0.10 M $[{}^6\text{Li}, {}^{15}\text{N}]\mathbf{3}$ in *n*-BuOMe/toluene recorded at -90 °C: (A) 2.0 M *n*-BuOMe; (B) 4.0 M *n*-BuOMe; (C) 6.0 M *n*-BuOMe; (D) 8.1 M *n*-BuOMe.



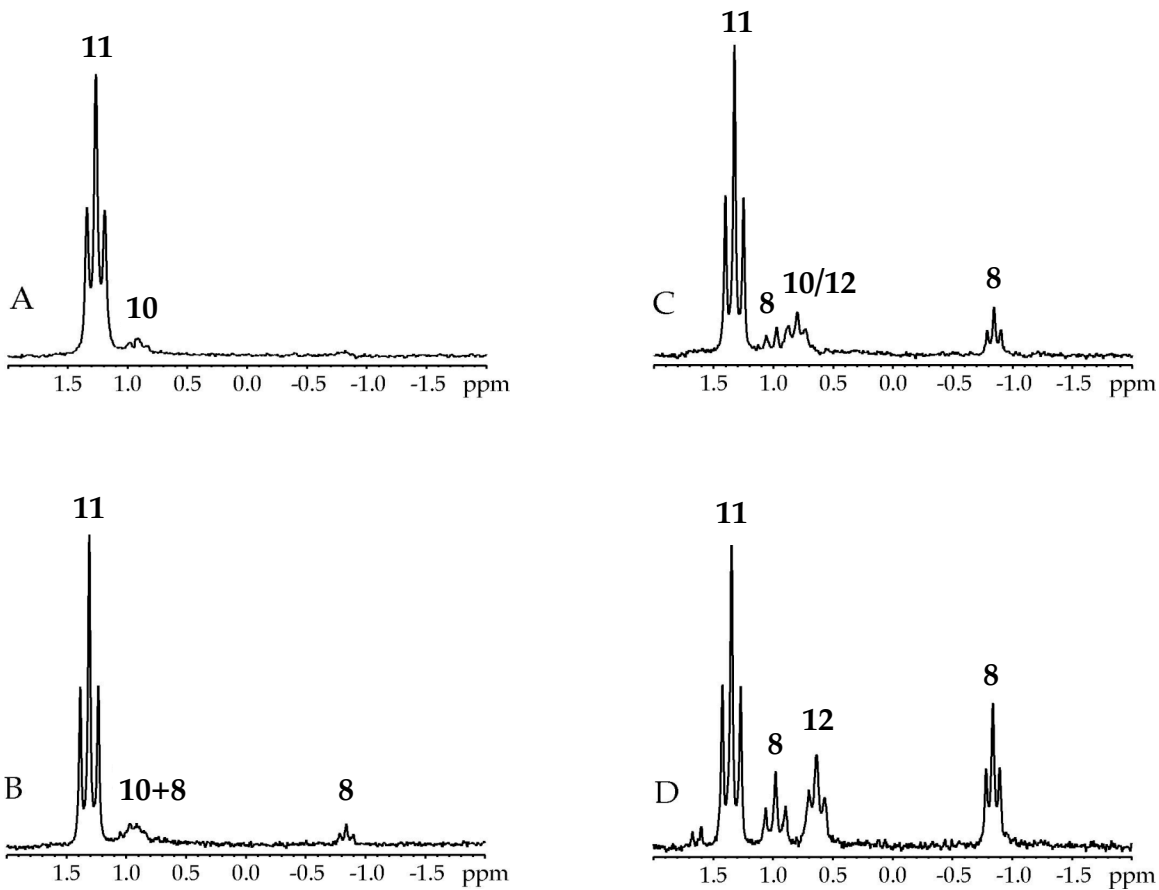
VIII. ${}^{15}\text{N}$ NMR spectra of 0.10 M $[{}^6\text{Li}, {}^{15}\text{N}]\mathbf{3}$ in *n*-BuOMe recorded at -90 °C: (A) ${}^6\text{Li}$ coupled; (B) ${}^6\text{Li}$ decoupled.



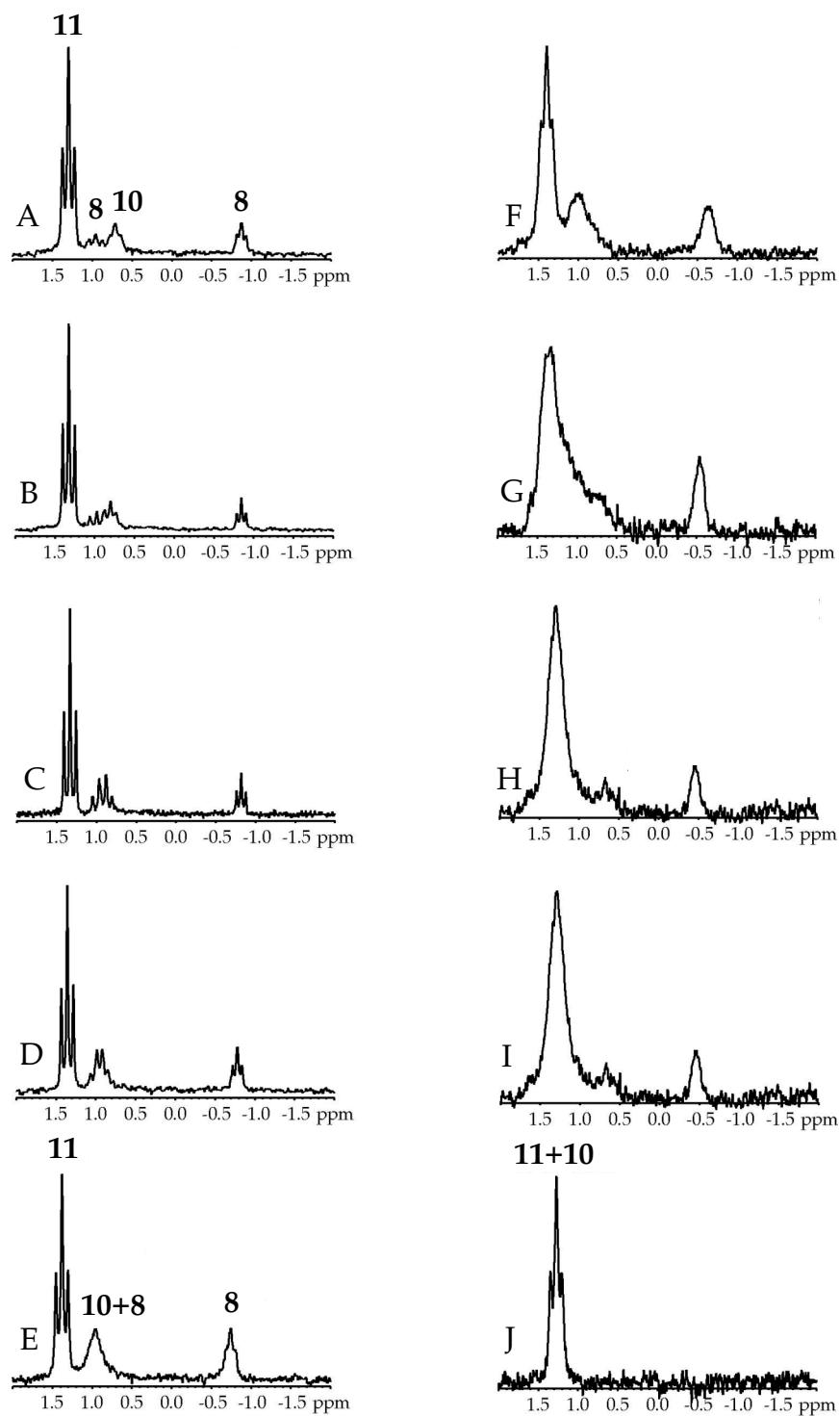
IX. ${}^6\text{Li}$ NMR spectra of 0.10 M $[{}^6\text{Li}, {}^{15}\text{N}]\mathbf{3}$ in *n*-BuOMe recorded at: (A) $-90\text{ }^\circ\text{C}$; (B) $-70\text{ }^\circ\text{C}$; (C) $-60\text{ }^\circ\text{C}$; (D) $-50\text{ }^\circ\text{C}$; (E) $-40\text{ }^\circ\text{C}$; (F) $-20\text{ }^\circ\text{C}$; (G) $0\text{ }^\circ\text{C}$.



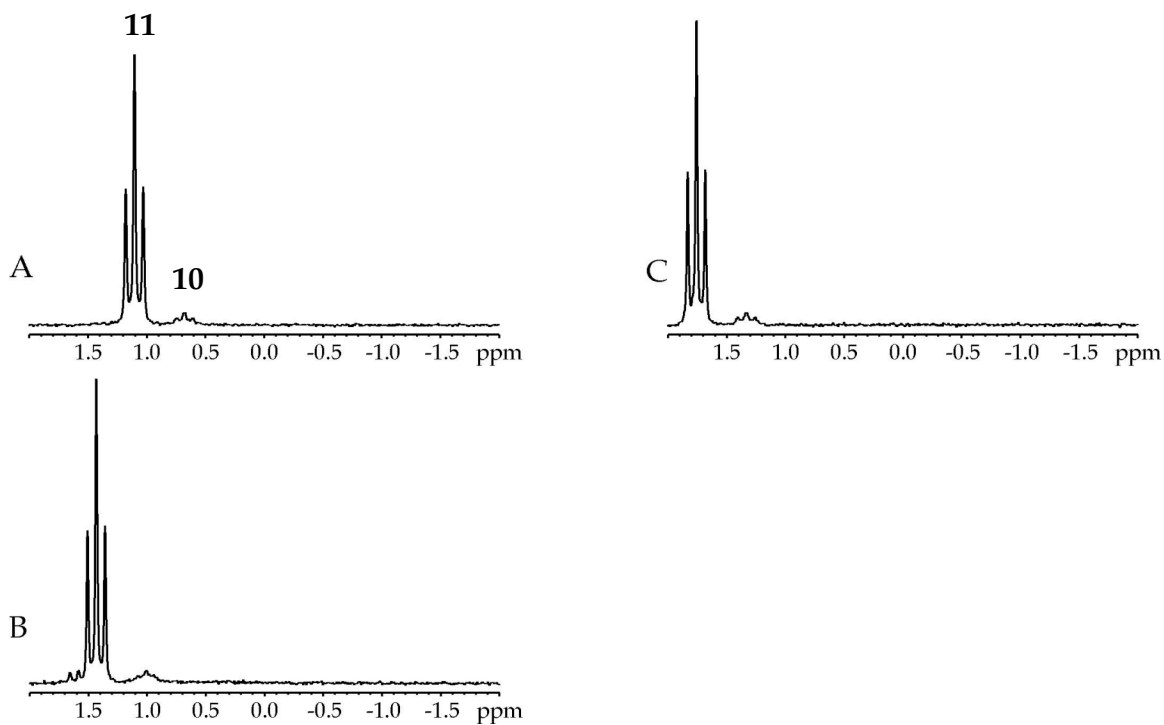
IX. (Continued) ${}^6\text{Li}$ NMR spectra of 0.10 M $[{}^6\text{Li}, {}^{15}\text{N}]\mathbf{3}$ in 4.0 M *n*-BuOMe/toluene recorded at: (A) -90 °C; (B) -100 °C; (C) -110 °C; (D) -120 °C; (E) -130 °C.



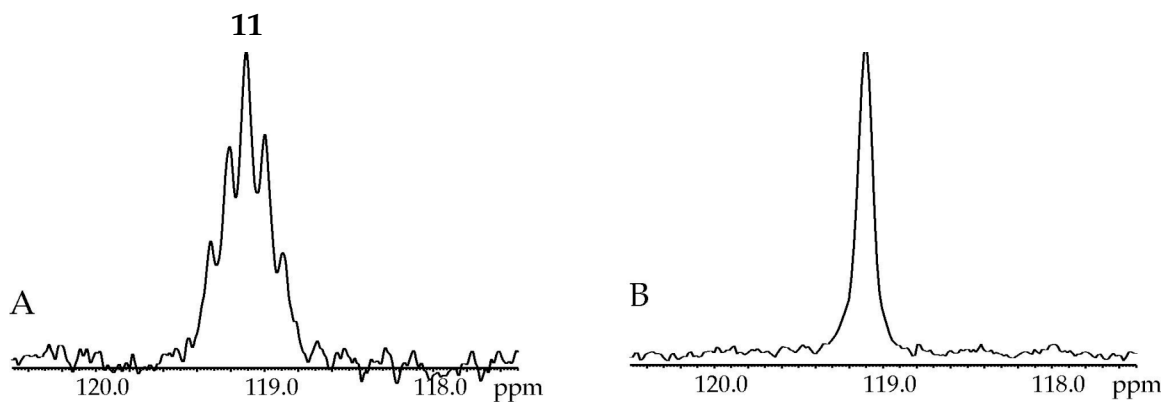
X. ${}^6\text{Li}$ NMR spectra of 0.10 M $[{}^6\text{Li}, {}^{15}\text{N}]\mathbf{3}$ in 2.0 M *n*-BuOMe/THP/toluene recorded at $-90\text{ }^\circ\text{C}$: (A) 0.00 M THP; (B) 0.10 M THP; (C) 0.20 M THP; (D) 0.50 M THP.



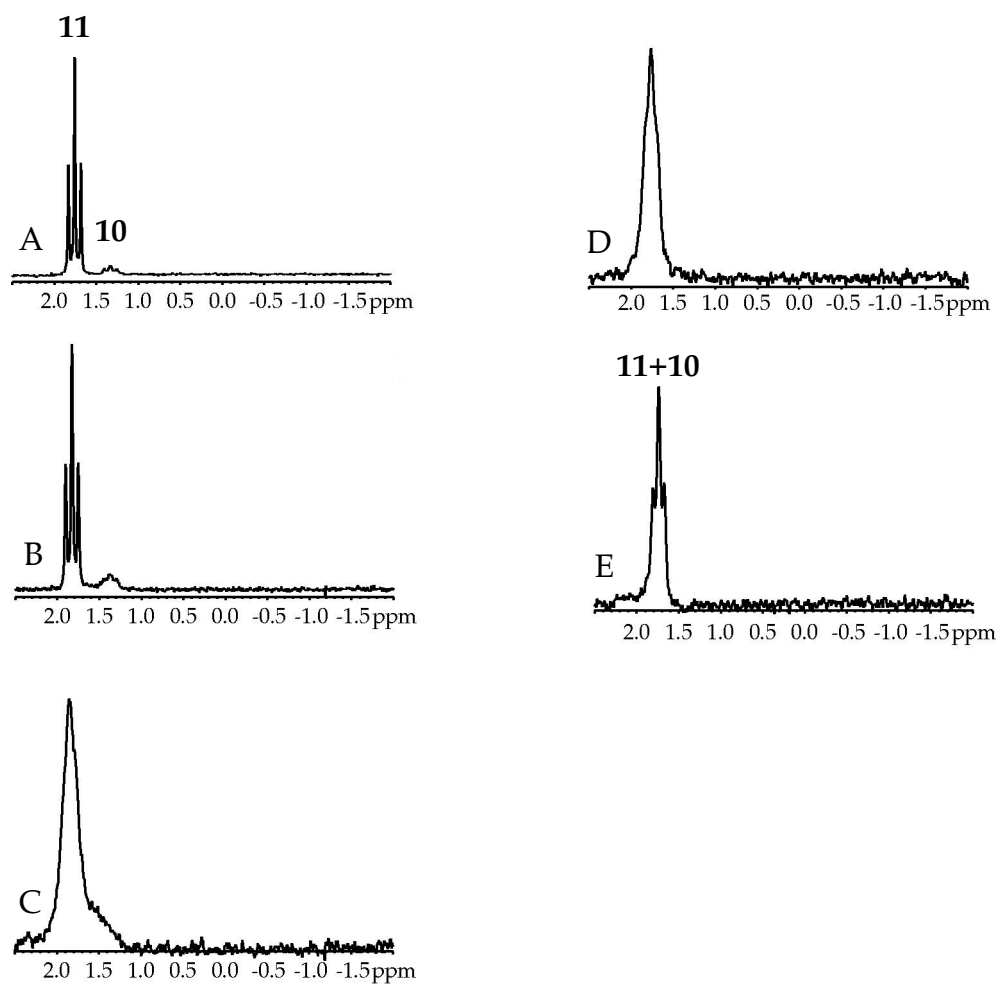
XI. ${}^6\text{Li}$ NMR spectra of 0.10 M $[{}^6\text{Li}, {}^{15}\text{N}]\mathbf{3}$ in 2.0 M *n*-BuOMe/0.20 M THP/toluene recorded at: (A) -100 °C; (B) -90 °C; (C) -80 °C; (D) -70 °C; (E) -60 °C; (F) -50 °C; (G) -40 °C; (H) -30 °C; (I) -20 °C; (J) 0 °C.



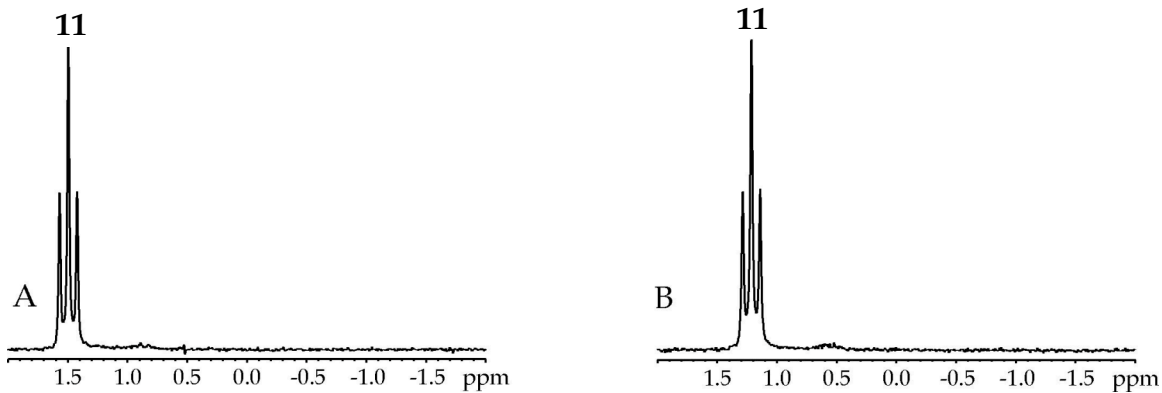
XII. ${}^6\text{Li}$ NMR spectra of 0.10 M $[{}^6\text{Li}, {}^{15}\text{N}]\mathbf{3}$ in Et_2O /toluene recorded at $-90\text{ }^\circ\text{C}$: (A) 2.3 M Et_2O ; (B) 4.7 M Et_2O ; (C) 9.4 M Et_2O .



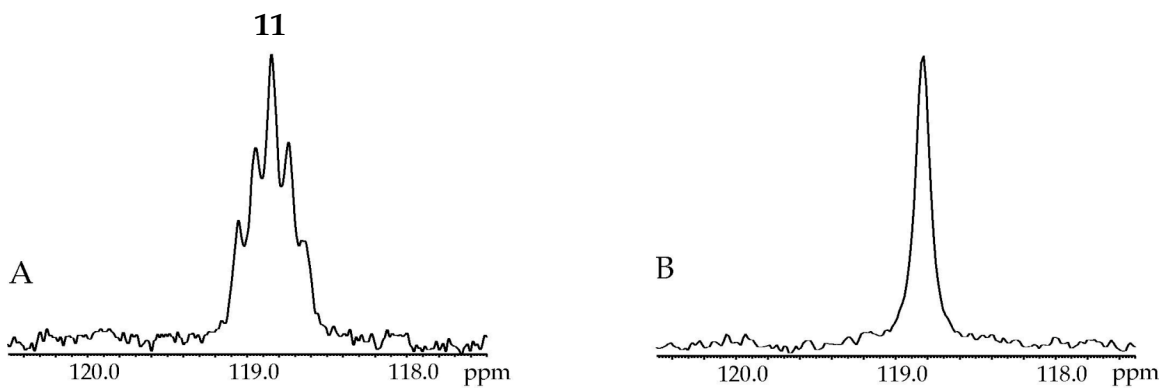
XIII. ${}^{15}\text{N}$ NMR spectra of 0.10 M $[{}^6\text{Li}, {}^{15}\text{N}]\mathbf{3}$ in Et_2O recorded at $-90\text{ }^\circ\text{C}$: (A) ${}^6\text{Li}$ coupled; (B) ${}^6\text{Li}$ decoupled.



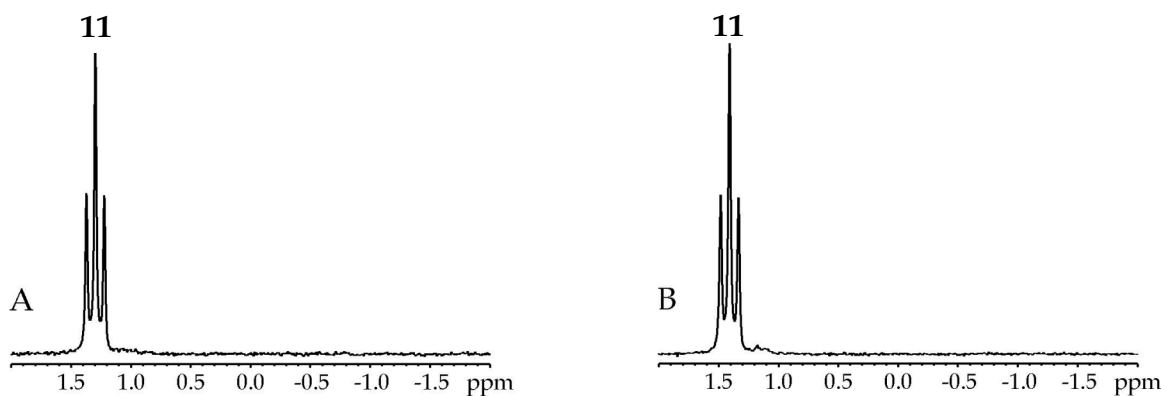
XIV. ${}^6\text{Li}$ NMR spectra of 0.10 M $[{}^6\text{Li}, {}^{15}\text{N}]\mathbf{3}$ in Et_2O recorded at: (A) -90 °C; (B) -75 °C; (C) -50 °C; (D) -30 °C; (E) 0 °C.



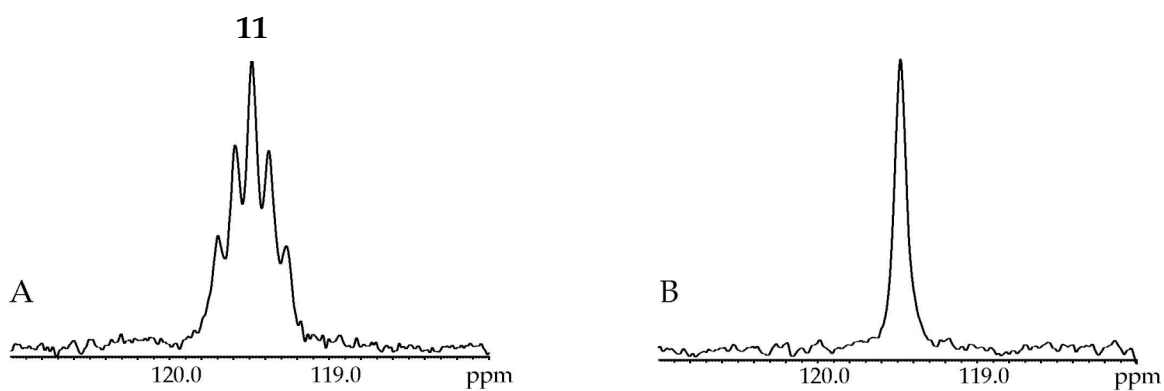
XV. ${}^6\text{Li}$ NMR spectra of 0.10 M $[{}^6\text{Li}, {}^{15}\text{N}]\mathbf{3}$ in *t*-BuOMe/toluene recorded at $-90\text{ }^\circ\text{C}$: (A) 2.0 M *t*-BuOMe; (B) 8.1 M *t*-BuOMe.



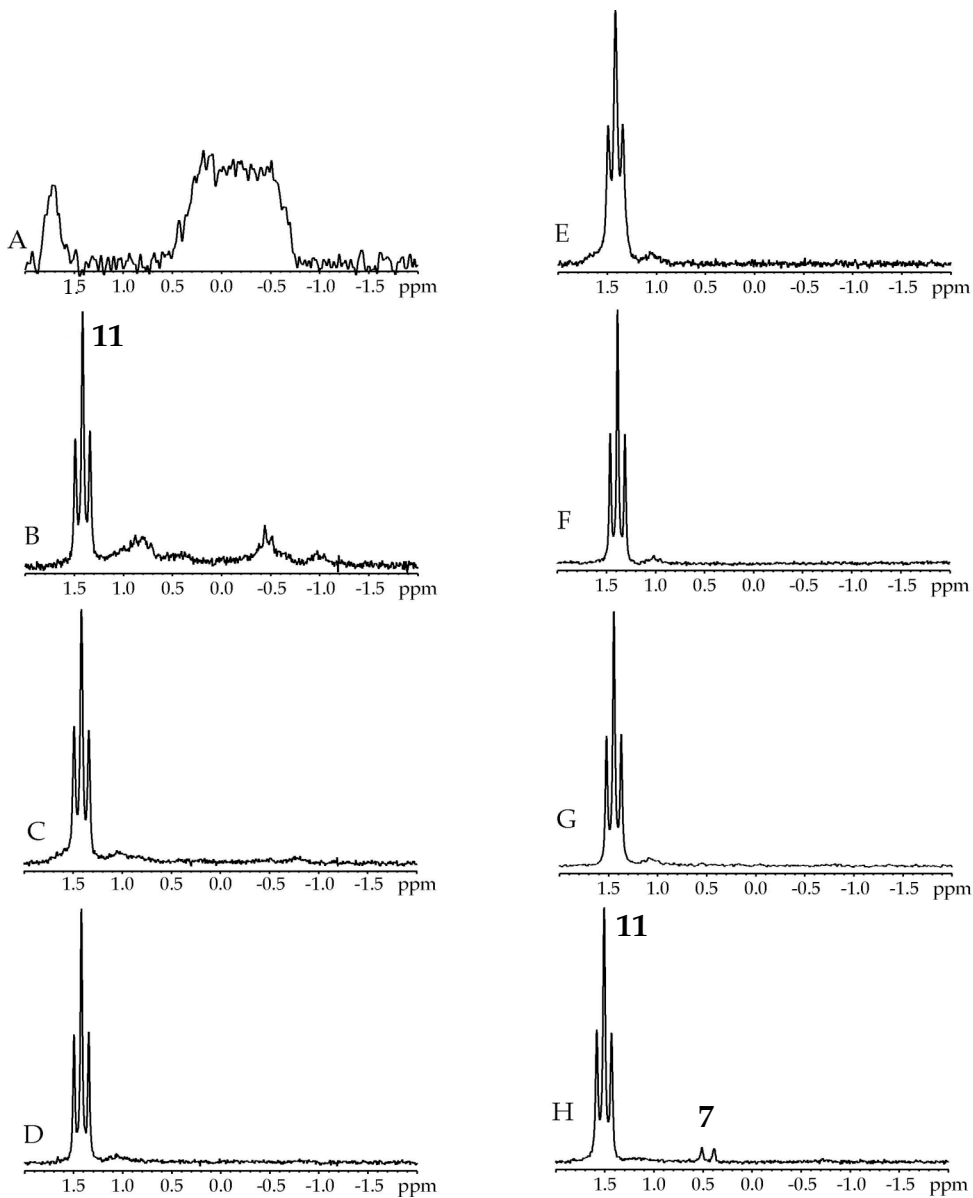
XVI. ${}^{15}\text{N}$ NMR spectra of 0.10 M $[{}^6\text{Li}, {}^{15}\text{N}]\mathbf{3}$ in *t*-BuOMe recorded at $-90\text{ }^\circ\text{C}$: (A) ${}^6\text{Li}$ coupled; (B) ${}^6\text{Li}$ decoupled.



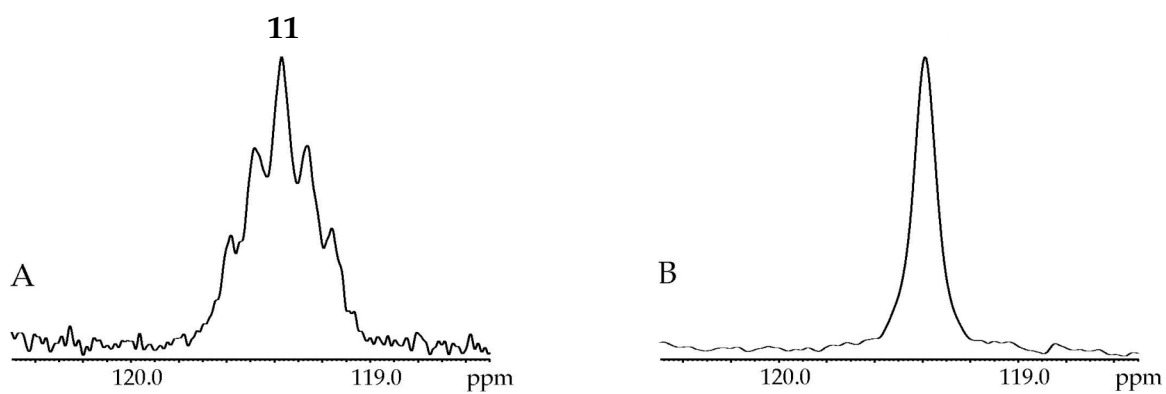
XVII. ${}^6\text{Li}$ NMR spectra of 0.10 M $[{}^6\text{Li}, {}^{15}\text{N}]\mathbf{3}$ in 2,2-Me₂THF / toluene recorded at -90 °C: (A) 2.1 M 2,2-Me₂THF; (B) 8.4 M 2,2-Me₂THF.



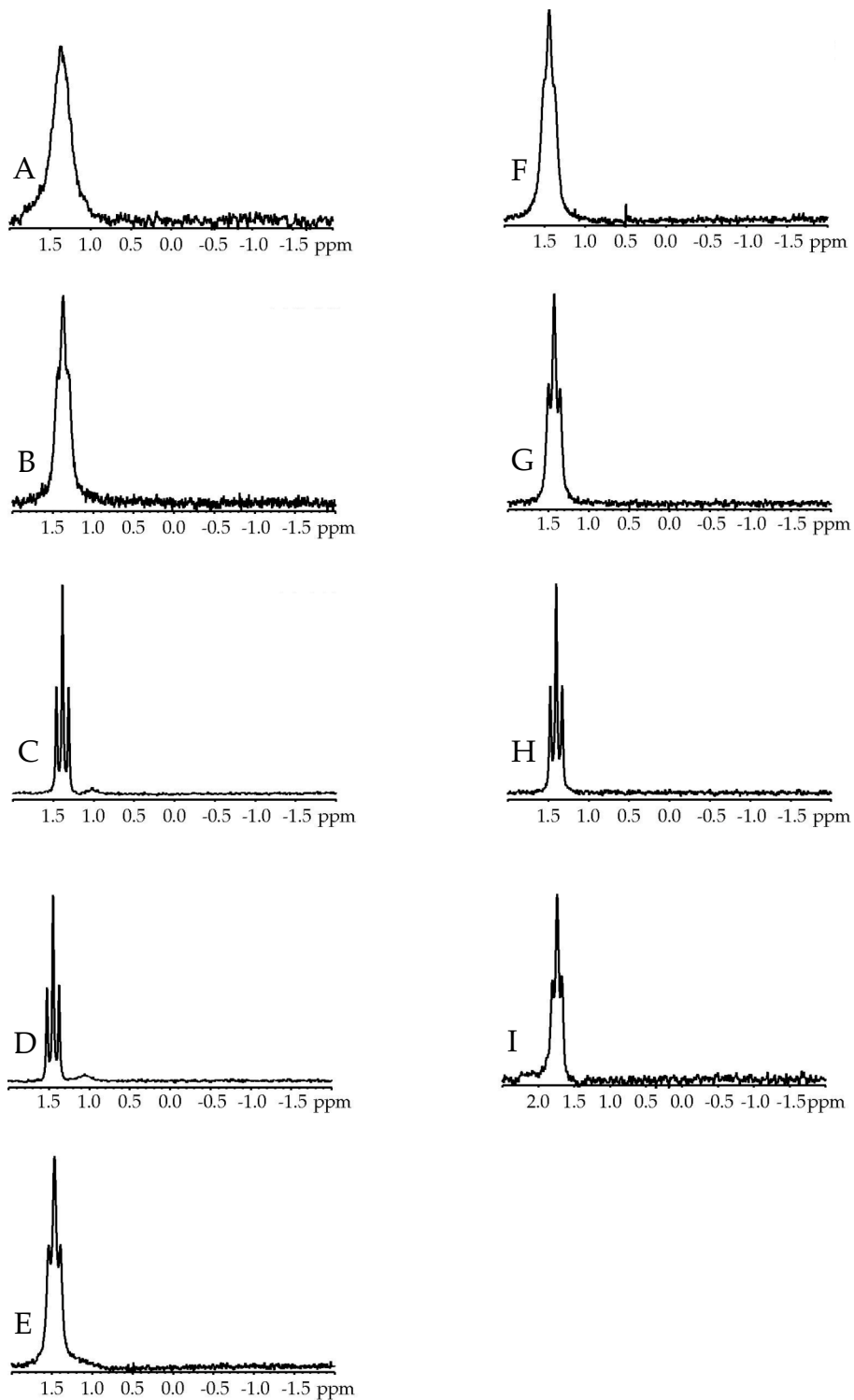
XVIII. ${}^{15}\text{N}$ NMR spectra of 0.10 M $[{}^6\text{Li}, {}^{15}\text{N}]\mathbf{3}$ in 2,2-Me₂THF recorded at -90 °C: (A) ${}^6\text{Li}$ coupled; (B) ${}^6\text{Li}$ decoupled.



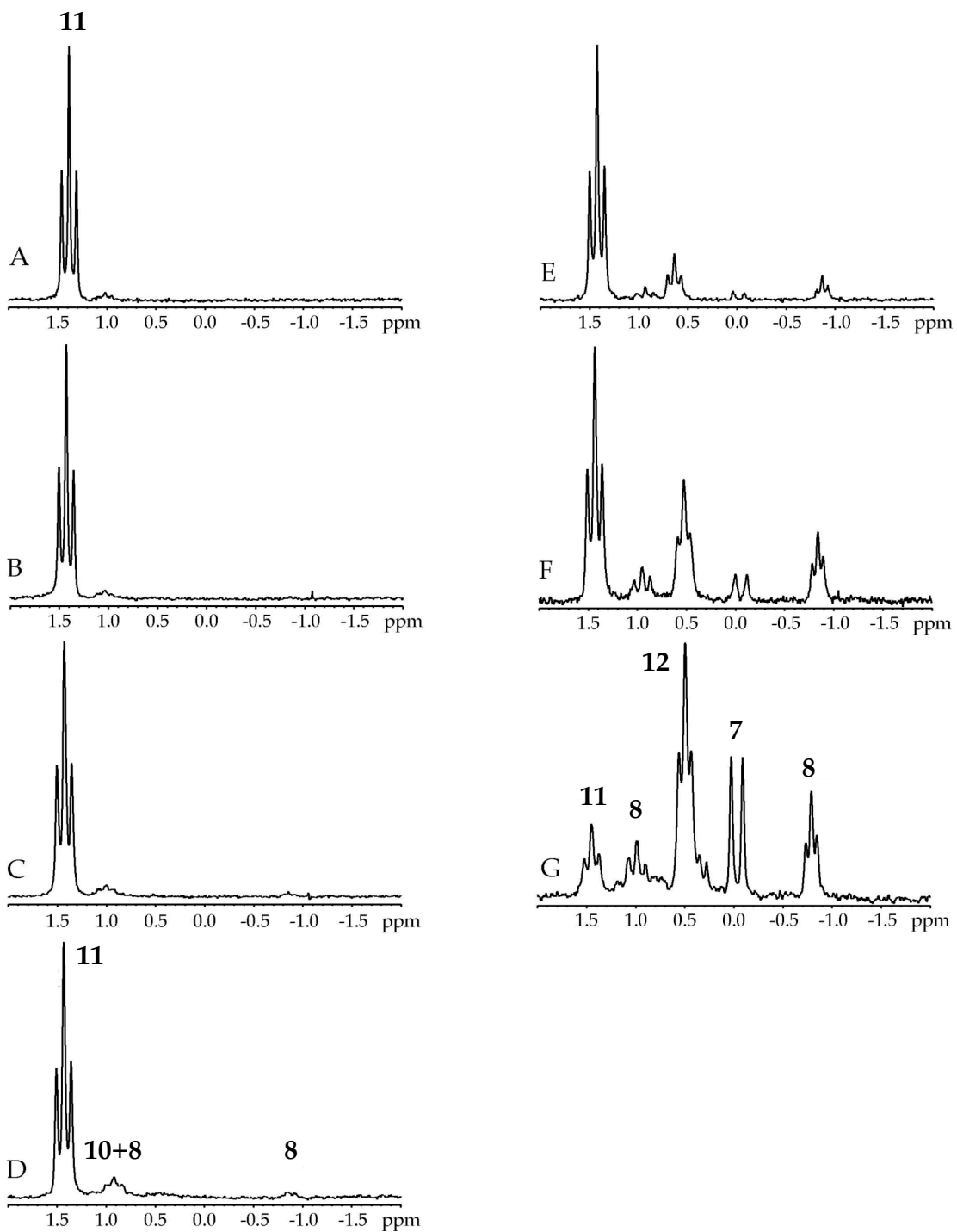
XIX. (A) ${}^6\text{Li}$ NMR spectra of 0.10 M $[{}^6\text{Li}, {}^{15}\text{N}]\mathbf{3}$ in toluene recorded at $-60\text{ }^\circ\text{C}$. ${}^6\text{Li}$ NMR spectra of 0.10 M $[{}^6\text{Li}, {}^{15}\text{N}]\mathbf{3}$ in 2-MeTHF/toluene recorded at $-90\text{ }^\circ\text{C}$: (B) 0.05 M 2-MeTHF; (C) 0.075 M 2-MeTHF; (D) 0.10 M 2-MeTHF; (E) 0.20 M 2-MeTHF; (F) 2.40 M 2-MeTHF; (G) 4.90 M 2-MeTHF; (H) 9.90 M 2-MeTHF.



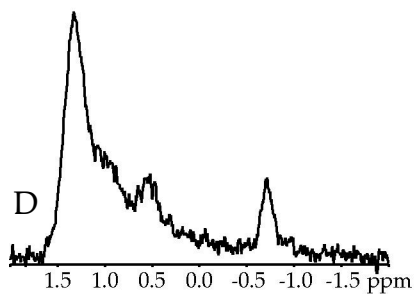
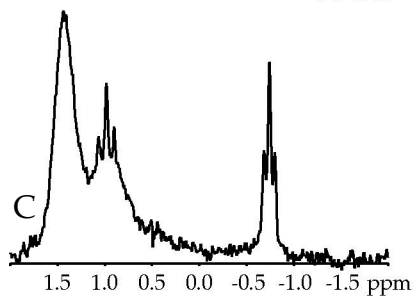
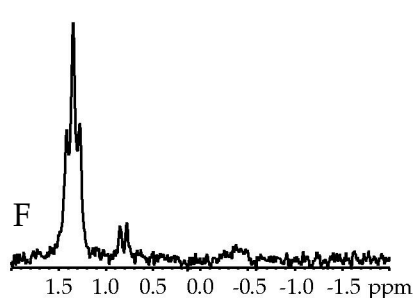
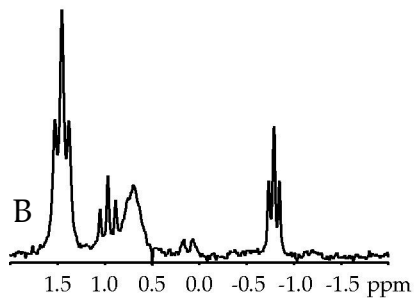
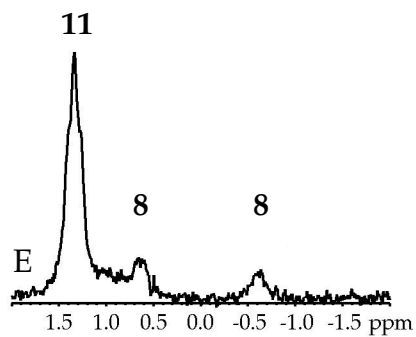
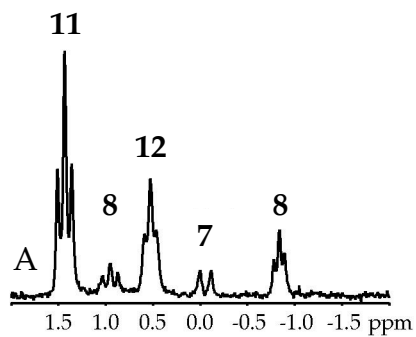
XX. ^{15}N NMR spectra of 0.10 M [$^6\text{Li}, ^{15}\text{N}$]3 in 2-MeTHF recorded at $-90\text{ }^\circ\text{C}$: (A) ^6Li coupled; (B) ^6Li decoupled.



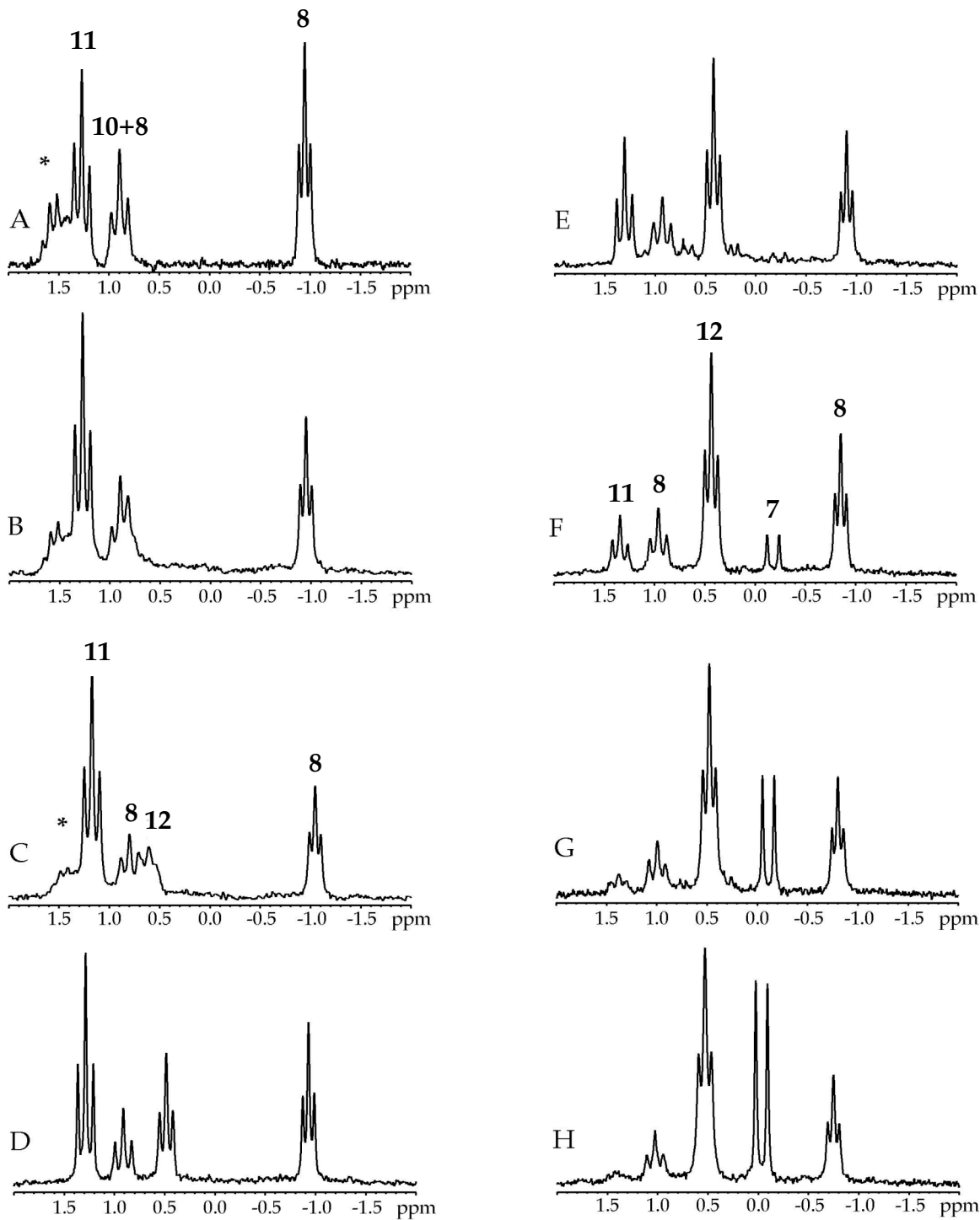
XXI. ${}^6\text{Li}$ NMR spectra of 0.10 M $[{}^6\text{Li}, {}^{15}\text{N}]\mathbf{3}$ in 2.4 M 2-MeTHF/toluene recorded at: (A) $-115\text{ }^\circ\text{C}$; (B) $-110\text{ }^\circ\text{C}$; (C) $-90\text{ }^\circ\text{C}$; (D) $-75\text{ }^\circ\text{C}$; (E) $-60\text{ }^\circ\text{C}$; (F) $-50\text{ }^\circ\text{C}$; (G) $-40\text{ }^\circ\text{C}$; (H) $-20\text{ }^\circ\text{C}$; (I) $0\text{ }^\circ\text{C}$.



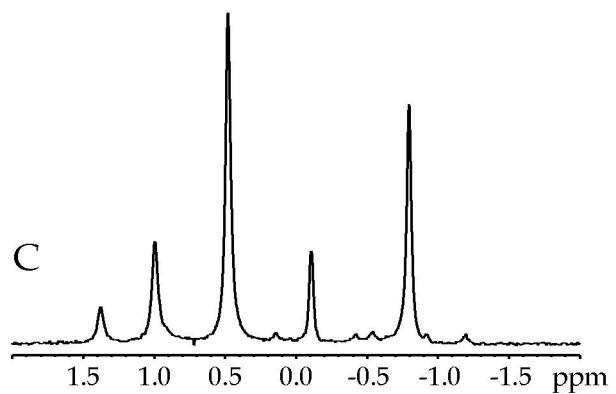
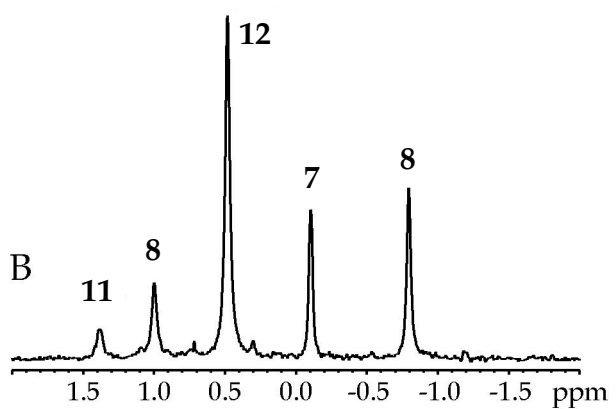
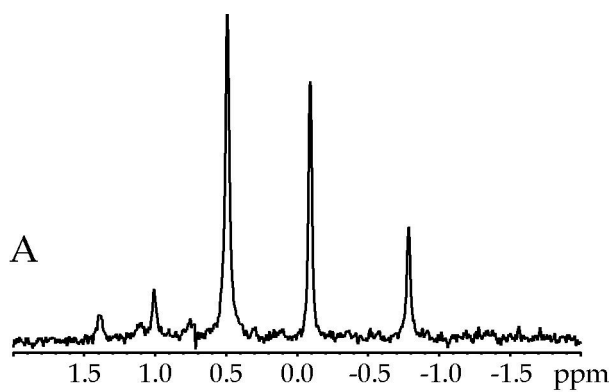
XXII. ${}^6\text{Li}$ NMR spectra of 0.10 M $[{}^6\text{Li}, {}^{15}\text{N}]\mathbf{3}$ in 2.0 M 2-MeTHF/THP/toluene recorded at $-90\text{ }^\circ\text{C}$: (A) 0.00 M THP; (B) 0.10 M THP; (C) 0.20 M THP; (D) 0.50 M THP; (E) 1.0 M THP; (F) 2.0 M THP; (G) 4.0 M THP.



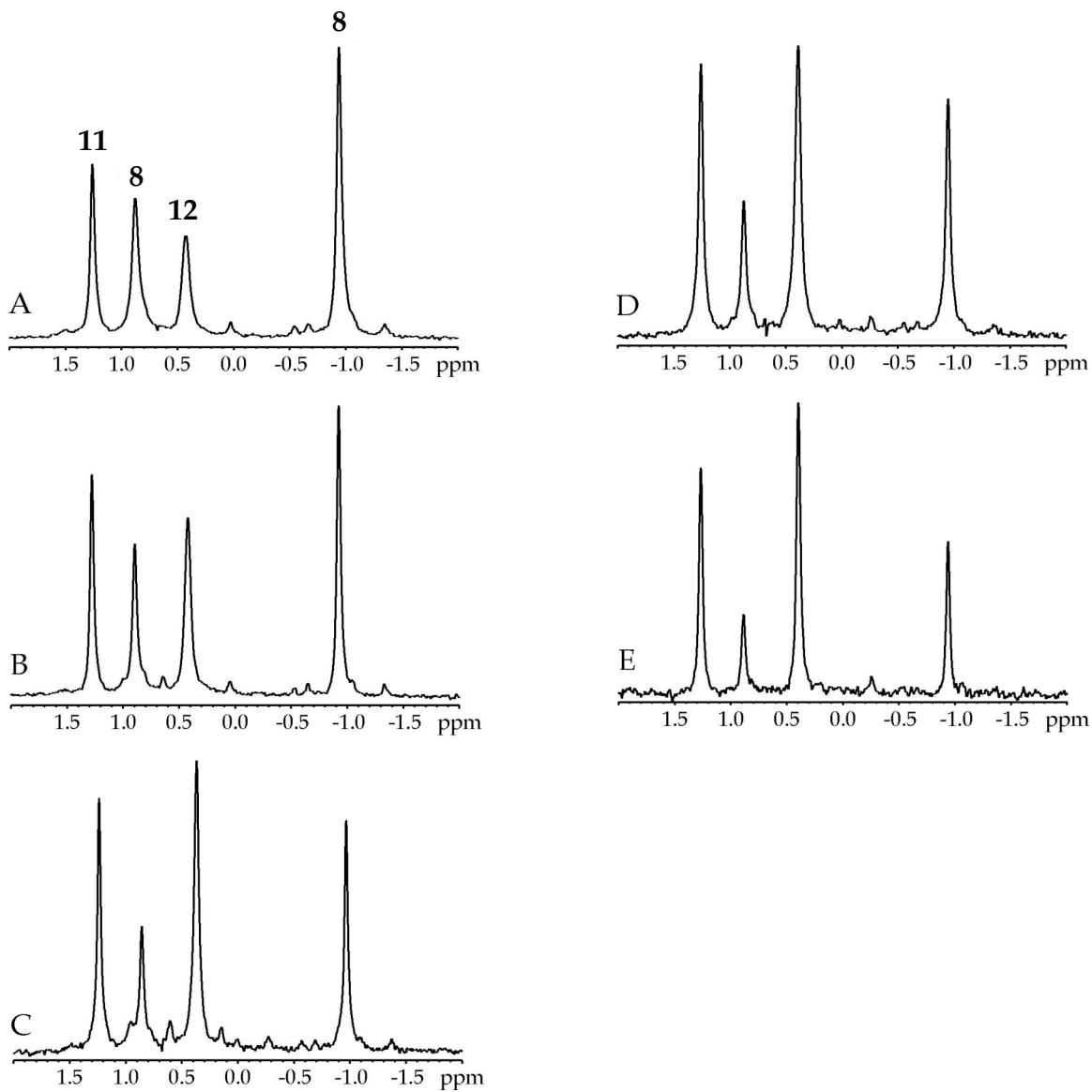
XXIII. ${}^6\text{Li}$ NMR spectra of 0.10 M $[{}^6\text{Li}, {}^{15}\text{N}]\mathbf{3}$ in 2.0 M 2-MeTHF/2.0 M THP/toluene recorded at: (A) $-90\text{ }^\circ\text{C}$; (B) $-75\text{ }^\circ\text{C}$; (C) $-60\text{ }^\circ\text{C}$; (D) $-50\text{ }^\circ\text{C}$; (E) $-40\text{ }^\circ\text{C}$; (F) $-20\text{ }^\circ\text{C}$.



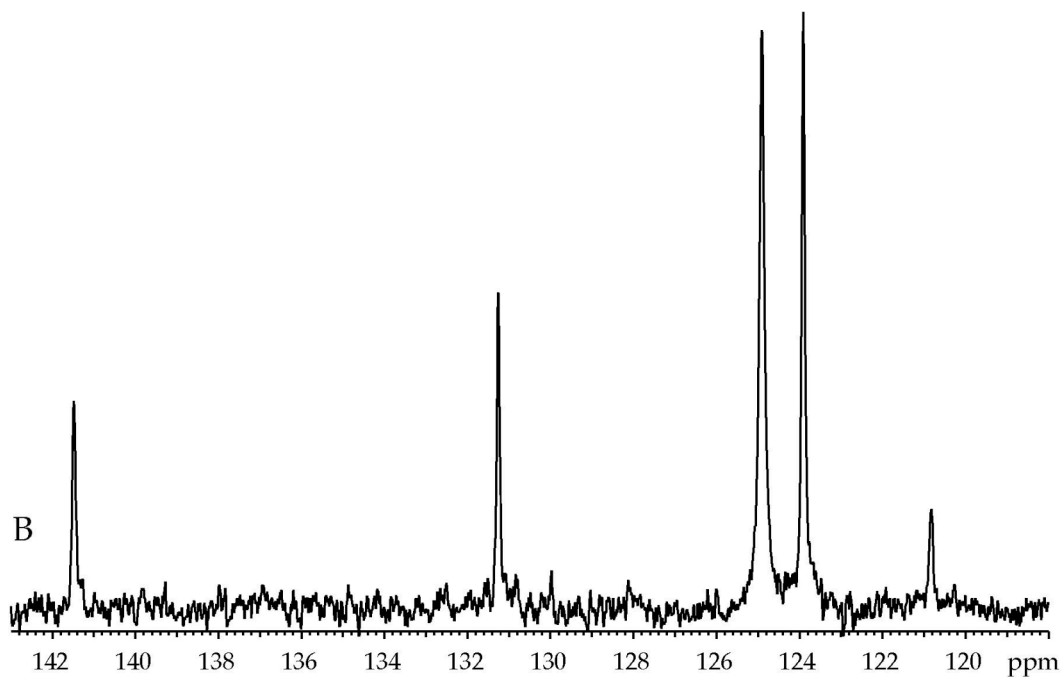
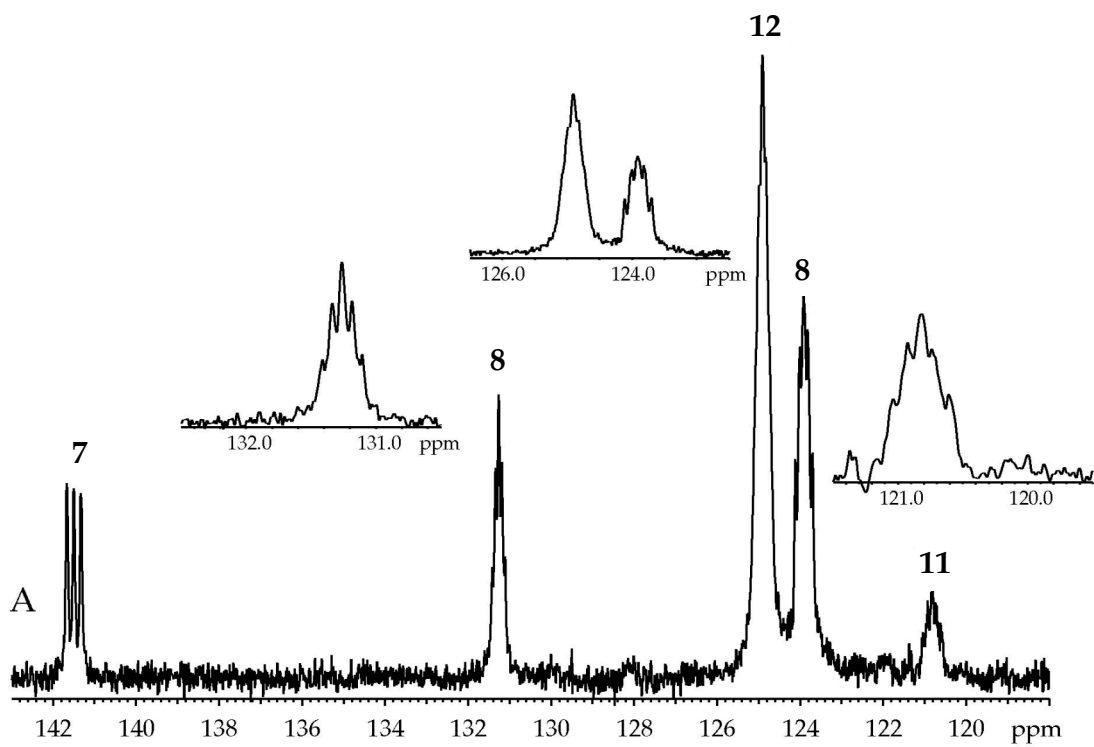
XXIV. ${}^6\text{Li}$ NMR spectra of 0.10 M $[{}^6\text{Li}, {}^{15}\text{N}]\mathbf{3}$ in THP/toluene recorded at $-90\text{ }^\circ\text{C}$: (A) 0.075 M; (B) 0.10 M THP; (C) 0.20 M THP; (D) 0.80 M THP; (E) 1.60 M THP; (F) 3.30 M THP; (G) 5.0 M THP; (H) 6.70 M THP. * Unassigned.



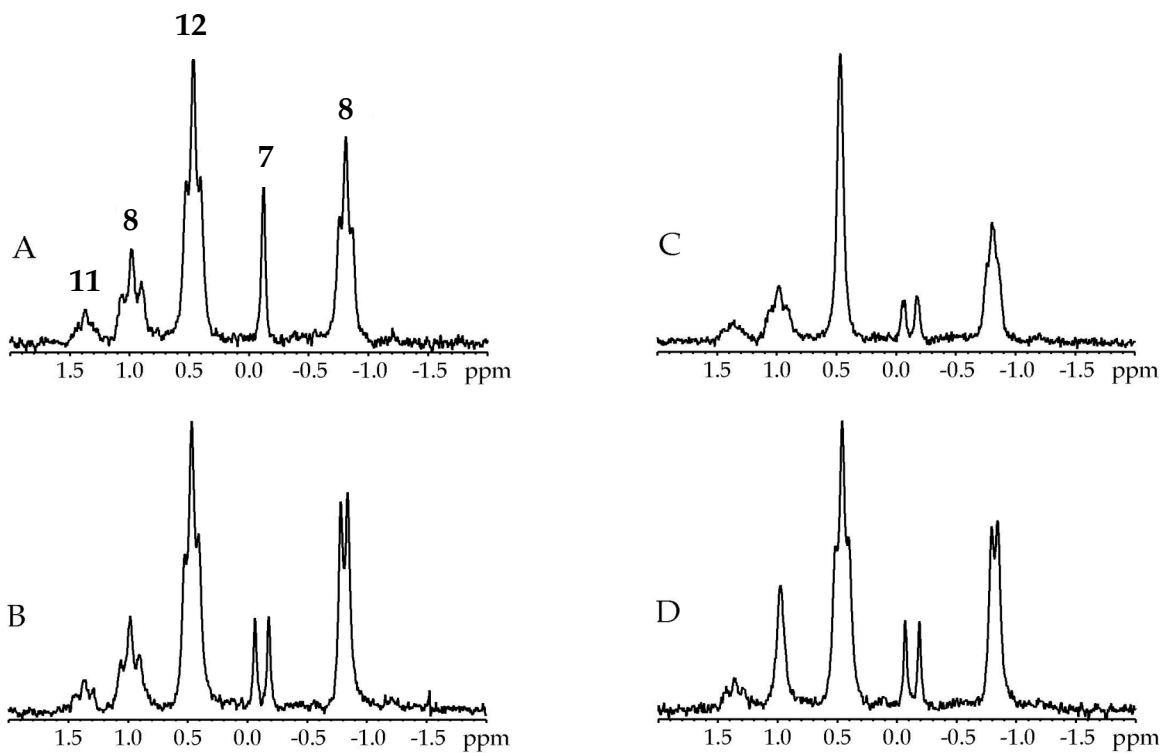
XXV. ${}^6\text{Li}\{^{15}\text{N}\}$ NMR spectra of $[{}^6\text{Li},^{15}\text{N}]\mathbf{3}$ in 5.0 M THP/toluene recorded at -90°C : (A) 0.030 M $[{}^6\text{Li},^{15}\text{N}]\mathbf{3}$; (B) 0.10 M $[{}^6\text{Li},^{15}\text{N}]\mathbf{3}$; (C) 0.20 M $[{}^6\text{Li},^{15}\text{N}]\mathbf{3}$.



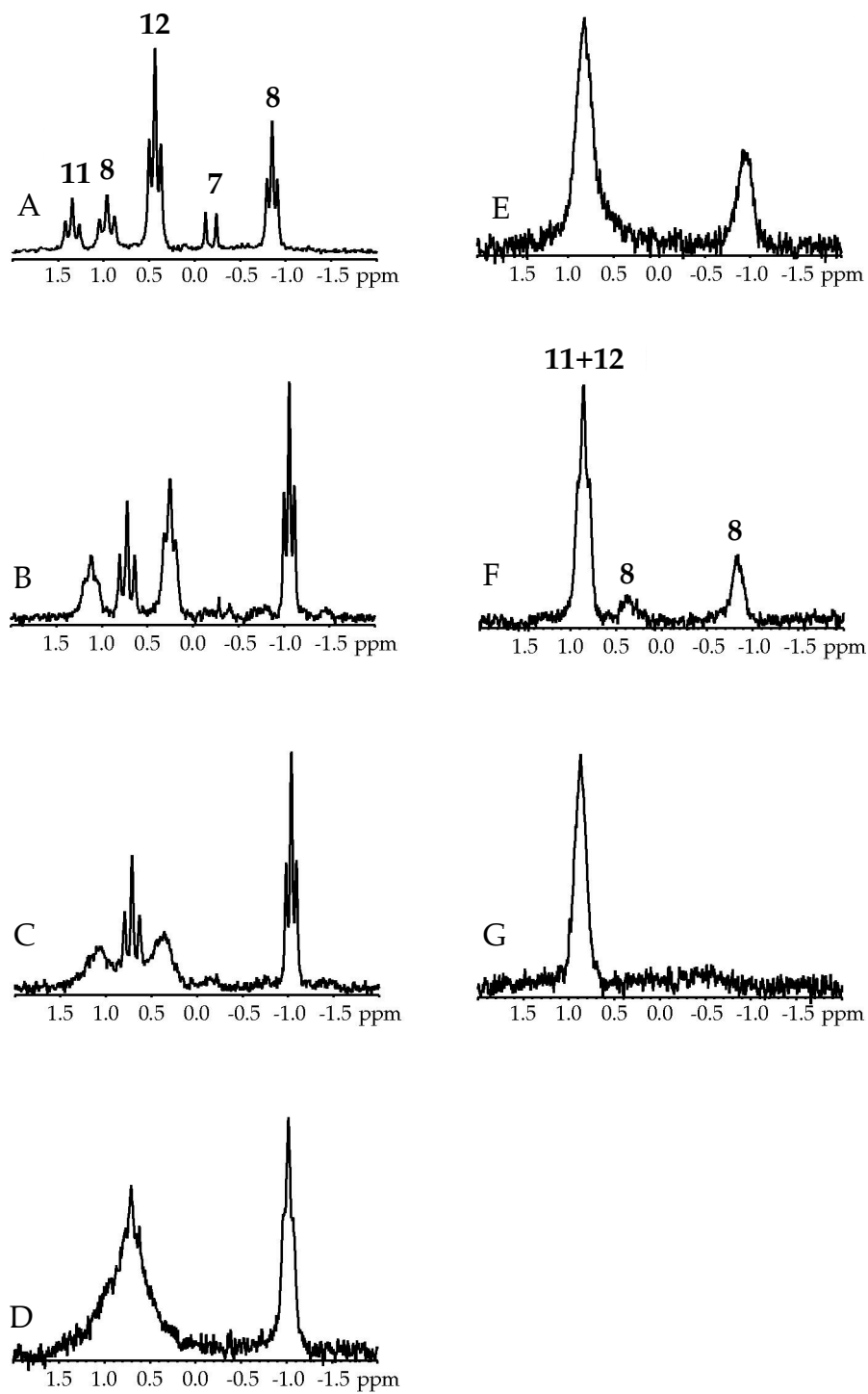
XXVI. ${}^6\text{Li}\{^{15}\text{N}\}$ NMR spectra of $[{}^6\text{Li}, {}^{15}\text{N}]\mathbf{3}$ in 1.6 M THP/toluene recorded at -90 $^{\circ}\text{C}$: (A) 0.40 M $[{}^6\text{Li}, {}^{15}\text{N}]\mathbf{3}$; (B) 0.20 M $[{}^6\text{Li}, {}^{15}\text{N}]\mathbf{3}$; (C) 0.10 M $[{}^6\text{Li}, {}^{15}\text{N}]\mathbf{3}$; (D) 0.050 M $[{}^6\text{Li}, {}^{15}\text{N}]\mathbf{3}$; (E) 0.025 M $[{}^6\text{Li}, {}^{15}\text{N}]\mathbf{3}$.



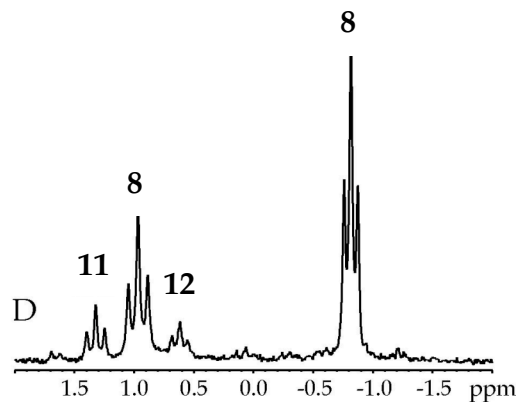
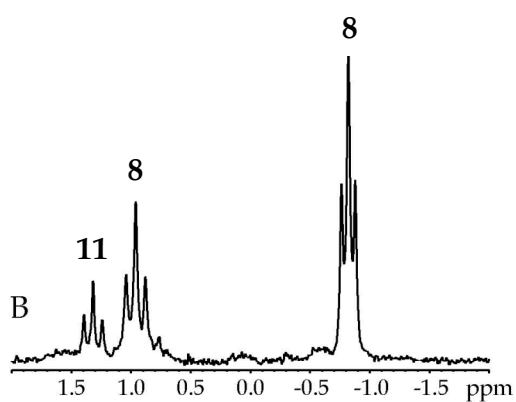
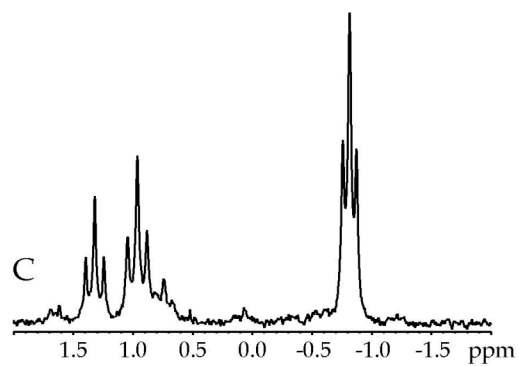
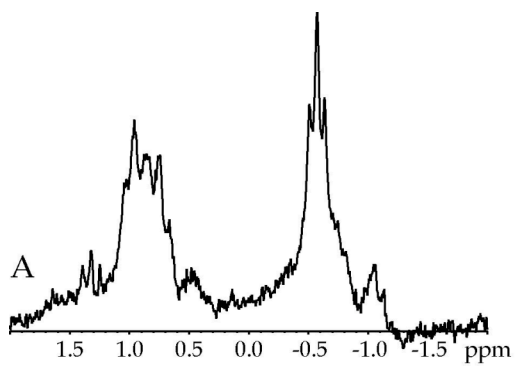
XXVII. ^{15}N NMR spectra of $0.20\text{ M } [^6\text{Li}, ^{15}\text{N}]3$ in 5.0 M THP/toluene recorded at -90°C : (A) ^6Li coupled; (B) ^6Li decoupled.



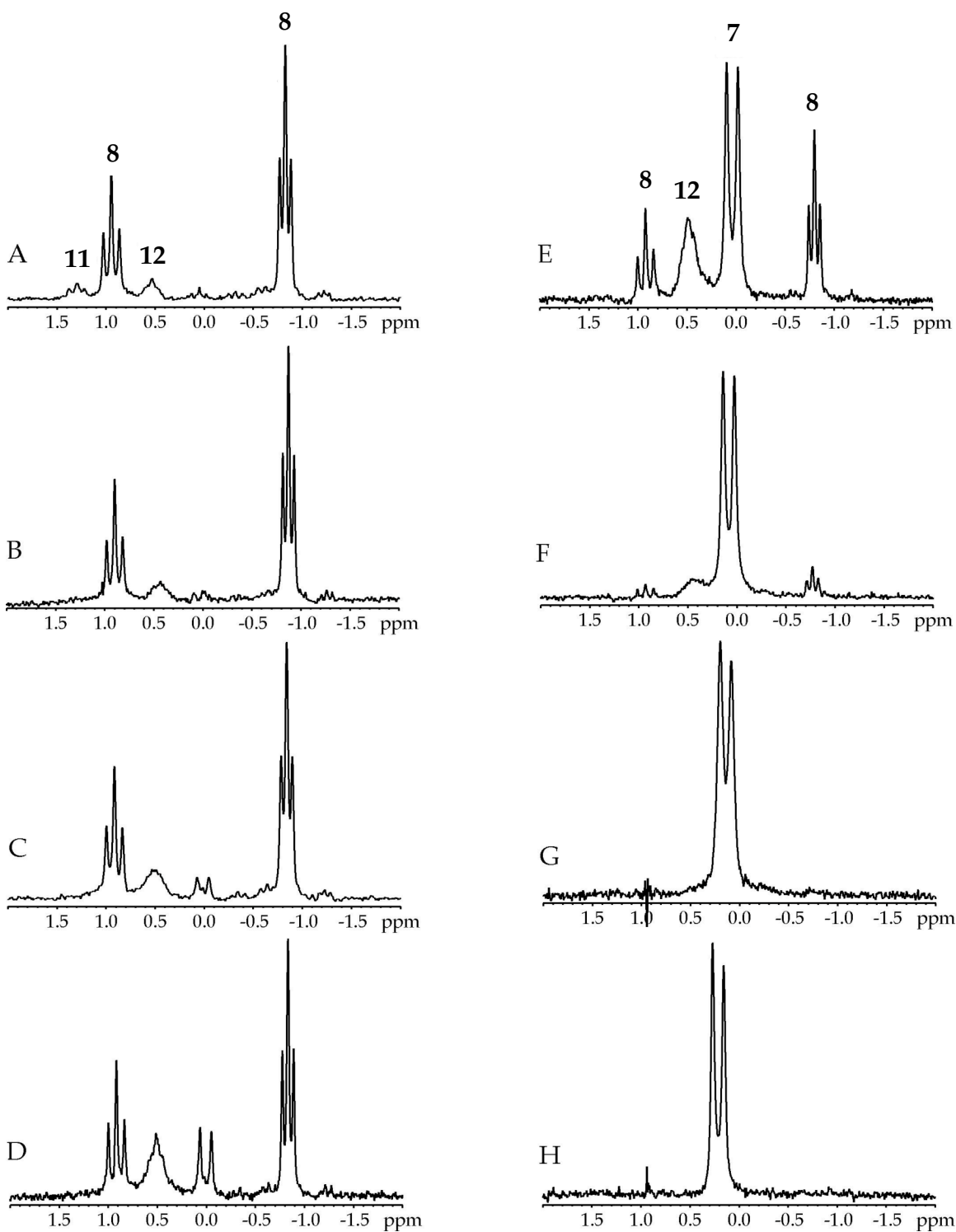
XXVIII. Selective ${}^{15}\text{N}$ decoupled ${}^6\text{Li}$ NMR spectra of 0.20 M $[{}^6\text{Li}, {}^{15}\text{N}]\mathbf{3}$ in 5.0 M THP/toluene recorded at $-90\text{ }^\circ\text{C}$: (A) 142 ppm; (B) 131 ppm; (C) 125 ppm; (D) 124 ppm.



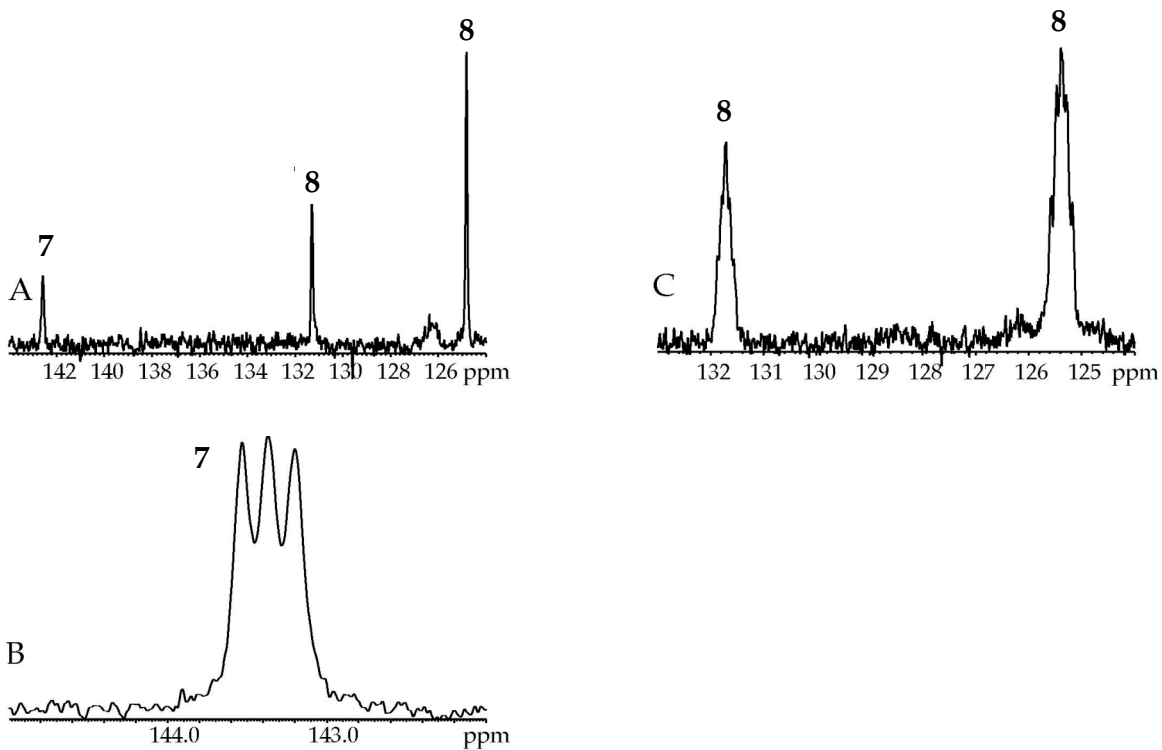
XXIX. ${}^6\text{Li}$ NMR spectra of 0.10 M [${}^6\text{Li}, {}^{15}\text{N}$]3 in 5.0 M THP/toluene recorded at: (A) $-90\text{ }^\circ\text{C}$; (B) $-75\text{ }^\circ\text{C}$; (C) $-60\text{ }^\circ\text{C}$; (D) $-50\text{ }^\circ\text{C}$; (E) $-35\text{ }^\circ\text{C}$; (F) $-20\text{ }^\circ\text{C}$; (G) $0\text{ }^\circ\text{C}$.



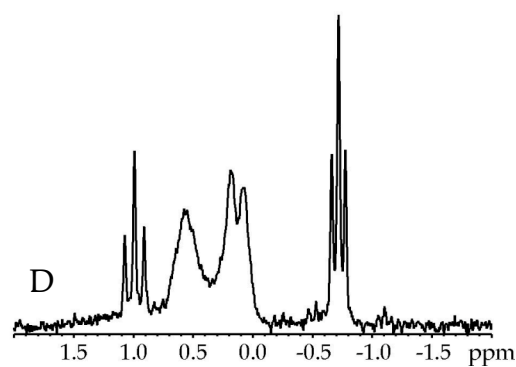
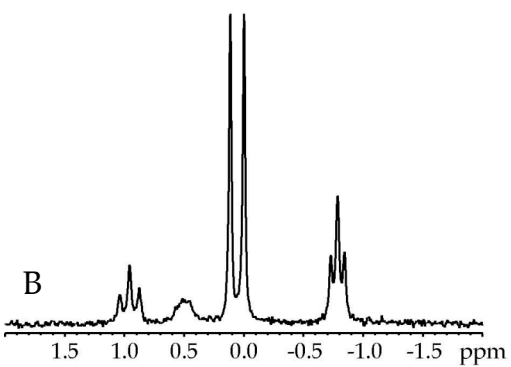
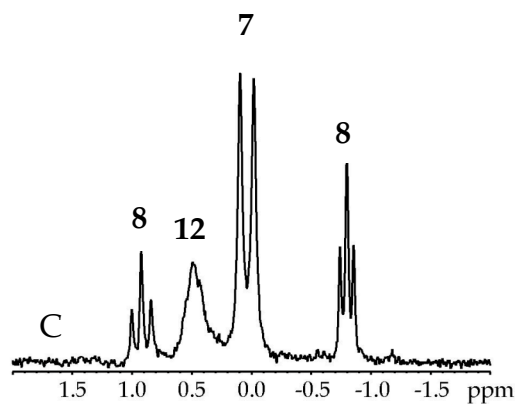
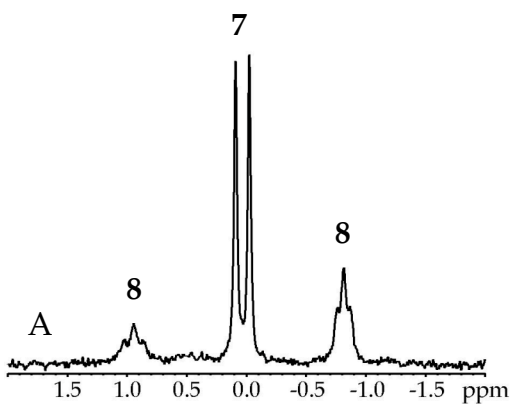
XXX. ${}^6\text{Li}$ NMR spectra of 0.10 M $[{}^6\text{Li}, {}^{15}\text{N}]\mathbf{3}$ in THF/toluene recorded at $-90\text{ }^\circ\text{C}$:
 (A) 0.050 M THF; (B) 0.075 M THF; (C) 0.10 M THF; (D) 0.20 M THF.



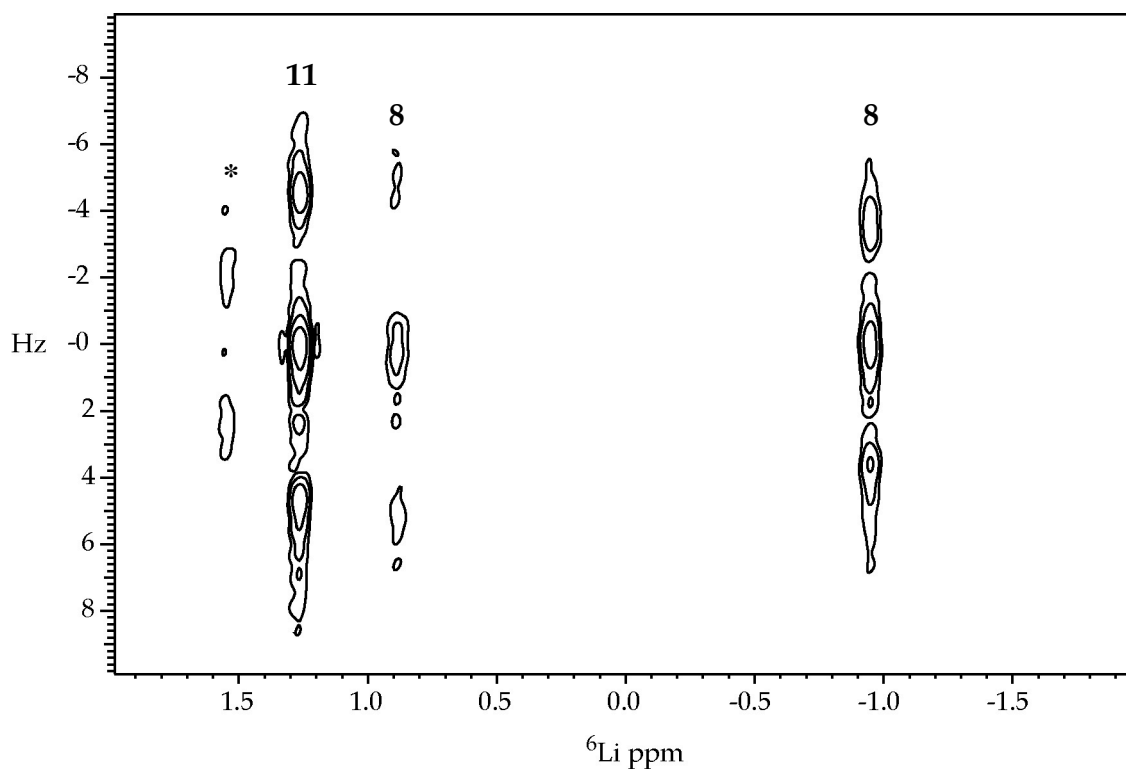
XXXI. ${}^6\text{Li}$ NMR spectra of 0.10 M [${}^6\text{Li}, {}^{15}\text{N}$]**3** in THF/toluene recorded at $-90\text{ }^\circ\text{C}$: (A) 0.50 M THF; (B) 1.0 M THF; (C) 2.0 M THF; (D) 3.0 M THF; (E) 5.0 M THF; (F) 7.0 M THF; (G) 9.0 M THF.



XXXII. ^{15}N NMR spectra of 0.10 M $[^6\text{Li}, ^{15}\text{N}]\mathbf{3}$ in THF/toluene recorded at $-90\text{ }^\circ\text{C}$: (A) 2.0 M THF, ^6Li decoupled; (B) 9.0 M THF, ^6Li coupled; (C) 0.50 M THF, ^6Li coupled.

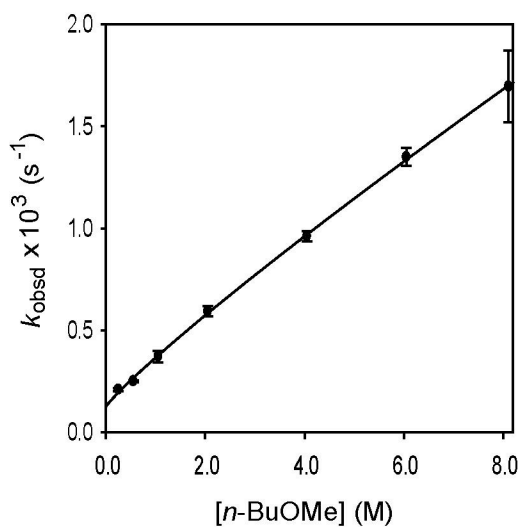


XXXIII. ${}^6\text{Li}$ NMR spectra of 0.10 M $[{}^6\text{Li}, {}^{15}\text{N}]\mathbf{3}$ in 5.0 M THF/toluene recorded at: (A) $-110\text{ }^\circ\text{C}$; (B) $-100\text{ }^\circ\text{C}$; (C) $-90\text{ }^\circ\text{C}$; (D) $-80\text{ }^\circ\text{C}$.



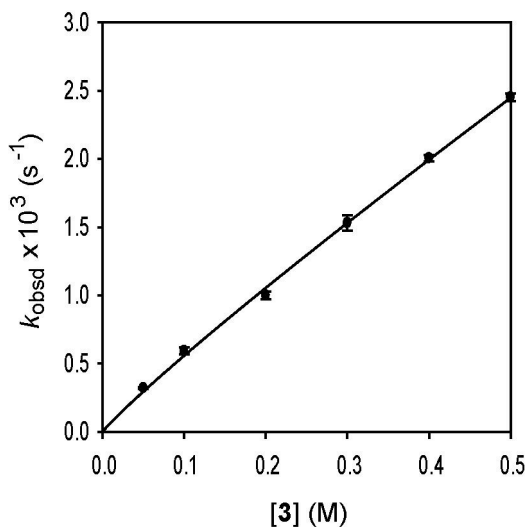
XXXIV. $J(^6\text{Li}, ^{15}\text{N})$ -resolved NMR spectrum of 0.10 M $[^6\text{Li}, ^{15}\text{N}]\mathbf{3}$ in 0.075 M THP/toluene recorded at $-90\text{ }^\circ\text{C}$. * Unassigned.

Part 3: Rate Studies



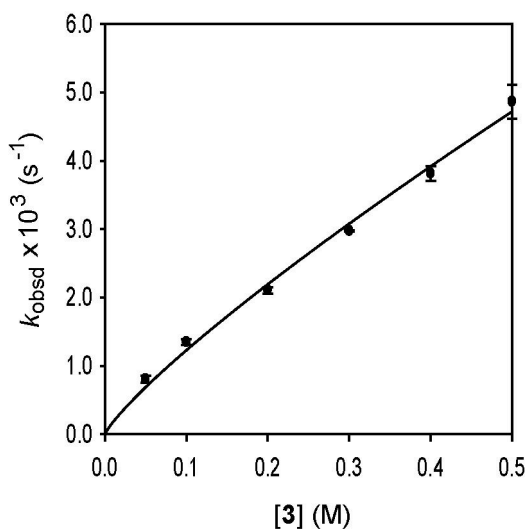
XXXV. Plot of k_{obsd} vs $[n\text{-BuOMe}]$ in toluene cosolvent for the alkylation of **3** (0.10 M) with $n\text{-C}_7\text{H}_{15}\text{I}$ (0.005 M) at 0 °C. The curve depicts an unweighted least-squares fit to $k_{\text{obsd}} = a + b[n\text{-BuOMe}]^c$ ($a = 0.13 \pm 0.05$, $b = 0.24 \pm 0.05$, $c = 0.90 \pm 0.09$).

$[n\text{-BuOMe}]$ (M)	$k_{\text{obsd}1} \times 10^3$ (s^{-1})	$k_{\text{obsd}2} \times 10^3$ (s^{-1})	$k_{\text{obsd}av} \times 10^3$ (s^{-1})
0.25	$0.214 \pm 6\text{E-}3$	$0.204 \pm 3\text{E-}3$	$0.209 \pm 7\text{E-}3$
0.55	$0.254 \pm 5\text{E-}3$	$0.247 \pm 5\text{E-}3$	$0.251 \pm 5\text{E-}3$
1.05	$0.352 \pm 9\text{E-}3$	$0.392 \pm 6\text{E-}3$	$0.372 \pm 3\text{E-}2$
2.05	$0.57 \pm 2\text{E-}2$	$0.61 \pm 2\text{E-}2$	$0.59 \pm 3\text{E-}2$
4.05	$0.94 \pm 2\text{E-}2$	$0.98 \pm 1\text{E-}2$	$0.96 \pm 3\text{E-}2$
6.05	$1.33 \pm 3\text{E-}2$	$1.38 \pm 3\text{E-}2$	$1.35 \pm 3\text{E-}2$
8.05	$1.57 \pm 3\text{E-}2$	$1.82 \pm 2\text{E-}3$	$1.69 \pm 2\text{E-}1$



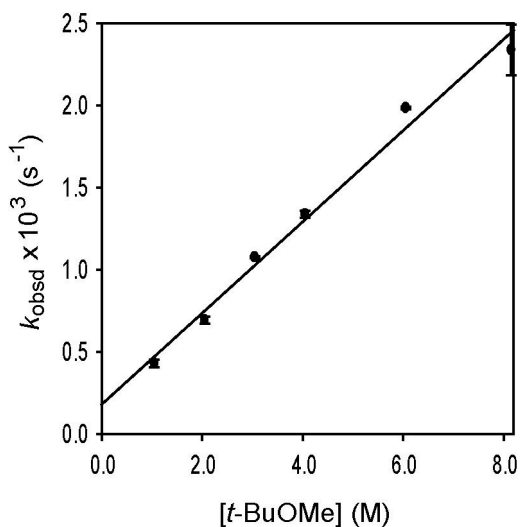
XXXVI. Plot of k_{obsd} vs $[3]$ in 2.10 M *n*-BuOMe and toluene cosolvent for the alkylation of **3** with *n*-C₇H₁₅I (0.005 M) at 0 °C. The curve depicts an unweighted least-squares fit to $k_{\text{obsd}} = a[3]^b$ ($a = 4.6 \pm 0.1$, $b = 0.92 \pm 0.02$).

$[3]$ (M)	$k_{\text{obsd}1} \times 10^3$ (s ⁻¹)	$k_{\text{obsd}2} \times 10^3$ (s ⁻¹)	$k_{\text{obsd}av} \times 10^3$ (s ⁻¹)
0.050	$0.315 \pm 4\text{E-}3$	$0.327 \pm 9\text{E-}3$	$0.321 \pm 8\text{E-}3$
0.10	$0.57 \pm 2\text{E-}2$	$0.61 \pm 2\text{E-}2$	$0.59 \pm 3\text{E-}2$
0.20	$0.98 \pm 4\text{E-}2$	$1.02 \pm 2\text{E-}2$	$1.00 \pm 3\text{E-}2$
0.30	$1.49 \pm 4\text{E-}3$	$1.57 \pm 2\text{E-}2$	$1.53 \pm 6\text{E-}2$
0.40	$2.02 \pm 4\text{E-}2$	$1.99 \pm 2\text{E-}2$	$2.00 \pm 2\text{E-}2$
0.50	$2.4 \pm 1\text{E-}1$	$2.47 \pm 5\text{E-}2$	$2.45 \pm 6\text{E-}2$



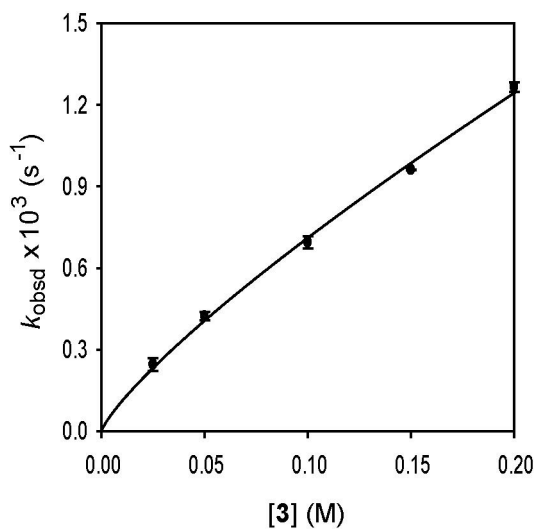
XXXVII. Plot of k_{obsd} vs [3] in 6.10 M *n*-BuOMe and toluene cosolvent for the alkylation of 3 with *n*-C₇H₁₅I (0.005 M) at 0 °C. The curve depicts an unweighted least-squares fit to $k_{\text{obsd}} = a[\mathbf{3}]^b$ ($a = 8.4 \pm 0.3$, $b = 0.84 \pm 0.04$).

[3] (M)	$k_{\text{obsd}1} \times 10^3$ (s ⁻¹)	$k_{\text{obsd}2} \times 10^3$ (s ⁻¹)	$k_{\text{obsd}av} \times 10^3$ (s ⁻¹)
0.050	0.77 ± 2E-2	0.84 ± 1E-2	0.80 ± 5E-2
0.10	1.38 ± 3E-2	1.32 ± 2E-2	1.35 ± 4E-2
0.20	2.14 ± 3E-2	2.07 ± 2E-2	2.11 ± 5E-2
0.30	2.97 ± 5E-2	2.98 ± 1E-2	2.98 ± 1E-2
0.40	3.9 ± 2E-1	3.74 ± 9E-2	3.8 ± 1E-1
0.50	5.04 ± 7E-2	4.69 ± 5E-2	4.9 ± 2E-1



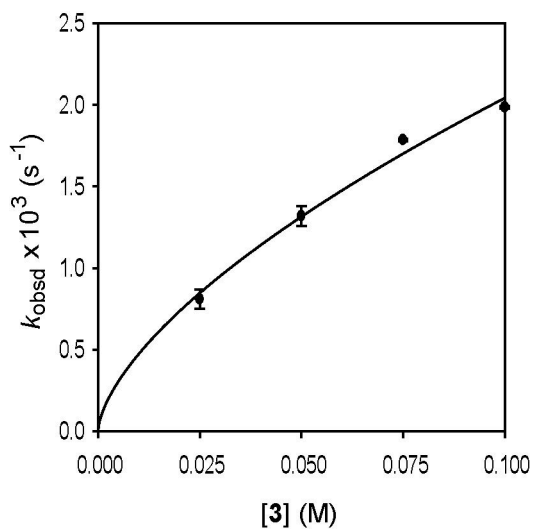
XXXVIII. Plot of k_{obsd} vs $[t\text{-BuOMe}]$ in toluene cosolvent for the alkylation of **3** (0.10 M) with $n\text{-C}_7\text{H}_{15}\text{I}$ (0.005 M) at 0 °C. The curve depicts an unweighted least-squares fit to $k_{\text{obsd}} = a + b[t\text{-BuOMe}]$ ($a = 0.18 \pm 0.06$, $b = 0.28 \pm 0.01$).

$[t\text{-BuOMe}]$ (M)	$k_{\text{obsd}1} \times 10^3$ (s^{-1})	$k_{\text{obsd}2} \times 10^3$ (s^{-1})	$k_{\text{obsd}av} \times 10^3$ (s^{-1})
1.05	$0.45 \pm 2\text{E-}2$	$0.413 \pm 4\text{E-}3$	$0.44 \pm 3\text{E-}2$
2.05	$0.711 \pm 6\text{E-}3$	$0.68 \pm 1\text{E-}2$	$0.69 \pm 2\text{E-}2$
3.05	$1.07 \pm 2\text{E-}2$	$1.08 \pm 2\text{E-}2$	$1.08 \pm 1\text{E-}2$
4.05	$1.36 \pm 2\text{E-}2$	$1.325 \pm 8\text{E-}3$	$1.34 \pm 2\text{E-}2$
6.05	$1.99 \pm 5\text{E-}2$	$1.98 \pm 2\text{E-}2$	$1.99 \pm 1\text{E-}2$
8.05	$2.22 \pm 1\text{E-}2$	$2.45 \pm 2\text{E-}2$	$2.34 \pm 2\text{E-}1$



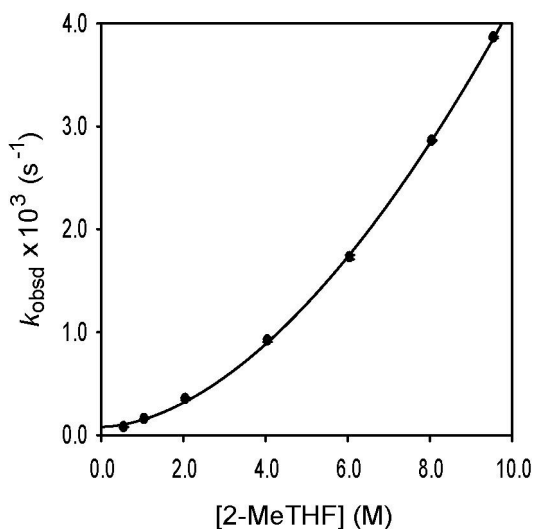
XXXIX. Plot of k_{obsd} vs $[3]$ in 2.10 M *t*-BuOMe and toluene cosolvent for the alkylation of **3** with *n*-C₇H₁₅I (0.005 M) at 0 °C. The curve depicts an unweighted least-squares fit to $k_{\text{obsd}} = a[3]^b$ ($a = 4.5 \pm 0.2$, $b = 0.81 \pm 0.02$).

$[3]$ (M)	$k_{\text{obsd}1} \times 10^3$ (s ⁻¹)	$k_{\text{obsd}2} \times 10^3$ (s ⁻¹)	$k_{\text{obsd}av} \times 10^3$ (s ⁻¹)
0.025	$0.262 \pm 6\text{E-}3$	$0.228 \pm 5\text{E-}3$	$0.24 \pm 2\text{E-}2$
0.05	$0.412 \pm 5\text{E-}3$	$0.433 \pm 3\text{E-}3$	$0.42 \pm 1\text{E-}2$
0.10	$0.711 \pm 6\text{E-}3$	$0.68 \pm 1\text{E-}2$	$0.69 \pm 2\text{E-}2$
0.15	$0.96 \pm 2\text{E-}2$	$0.96 \pm 1\text{E-}2$	$0.96 \pm 1\text{E-}2$
0.20	$1.28 \pm 2\text{E-}2$	$1.25 \pm 1\text{E-}2$	$1.26 \pm 2\text{E-}2$



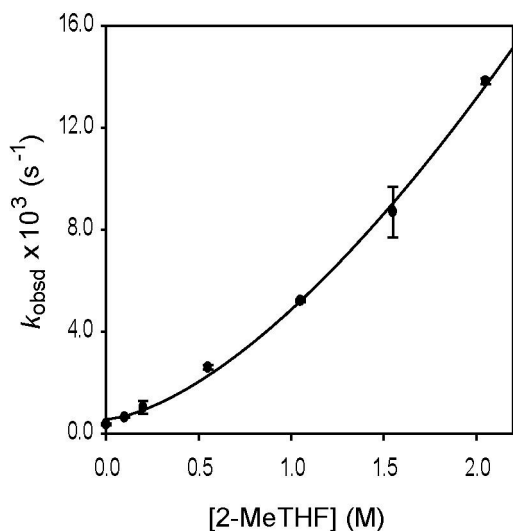
XL. Plot of k_{obsd} vs [3] in 6.10 M *t*-BuOMe and toluene cosolvent for the alkylation of 3 with *n*-C₇H₁₅I (0.005 M) at 0 °C. The curve depicts an unweighted least-squares fit to $k_{\text{obsd}} = a[\mathbf{3}]^b$ ($a = 9 \pm 1$, $b = 0.64 \pm 0.04$).

[3] (M)	$k_{\text{obsd}1} \times 10^3$ (s ⁻¹)	$k_{\text{obsd}2} \times 10^3$ (s ⁻¹)	$k_{\text{obsd}av} \times 10^3$ (s ⁻¹)
0.025	0.77 ± 2E-2	0.85 ± 1E-2	0.81 ± 6E-2
0.05	1.28 ± 1E-2	1.36 ± 2E-2	1.32 ± 6E-2
0.075	1.78 ± 1E-2	1.79 ± 2E-2	1.78 ± 1E-2
0.10	1.99 ± 5E-2	1.98 ± 2E-2	1.99 ± 1E-2



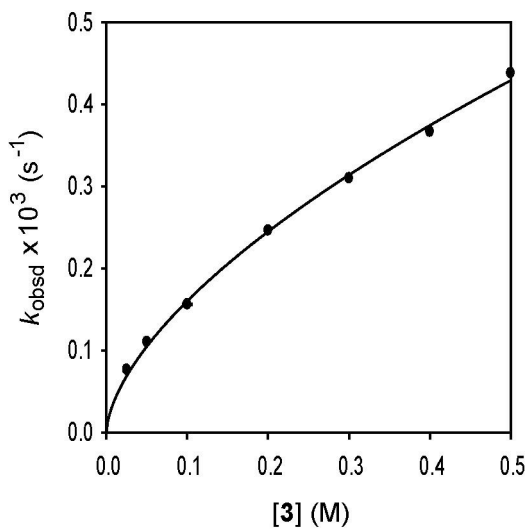
XLI. Plot of k_{obsd} vs [2-MeTHF] in toluene cosolvent for the alkylation of **3** (0.10 M) with $n\text{-C}_8\text{H}_{17}\text{Br}$ (0.005 M) at 0 °C. The curve depicts an unweighted least-squares fit to $k_{\text{obsd}} = a + b[2\text{-MeTHF}]^c$ ($a = 0.08 \pm 0.01$, $b = 0.068 \pm 0.003$, $c = 1.78 \pm 0.02$).

[2-MeTHF] (M)	$k_{\text{obsd}1} \times 10^3$ (s ⁻¹)	$k_{\text{obsd}2} \times 10^3$ (s ⁻¹)	$k_{\text{obsd}av} \times 10^3$ (s ⁻¹)
0.55	$0.0759 \pm 5\text{E-}4$	$0.0788 \pm 3\text{E-}4$	$0.077 \pm 2\text{E-}3$
1.05	$0.157 \pm 1\text{E-}3$	$0.156 \pm 1\text{E-}3$	$0.156 \pm 1\text{E-}3$
2.05	$0.342 \pm 2\text{E-}3$	$0.358 \pm 2\text{E-}3$	$0.35 \pm 1\text{E-}2$
4.05	$0.909 \pm 1\text{E-}3$	$0.929 \pm 6\text{E-}3$	$0.92 \pm 1\text{E-}2$
6.05	$1.71 \pm 3\text{E-}2$	$1.744 \pm 6\text{E-}3$	$1.73 \pm 2\text{E-}2$
8.05	$2.864 \pm 7\text{E-}3$	$2.857 \pm 7\text{E-}3$	$2.861 \pm 5\text{E-}3$
9.55	$3.87 \pm 4\text{E-}2$	$3.86 \pm 2\text{E-}2$	$3.86 \pm 1\text{E-}2$



XLII. Plot of k_{obsd} vs [2-MeTHF] in toluene cosolvent for the alkylation of **3** (0.10 M) with $n\text{-C}_7\text{H}_{15}\text{I}$ (0.005 M) at 0 °C. The curve depicts an unweighted least-squares fit to $k_{\text{obsd}} = a + b[\text{2-MeTHF}]^c$ ($a = 0.6 \pm 0.2$, $b = 4.0 \pm 0.3$, $c = 1.5 \pm 0.1$).

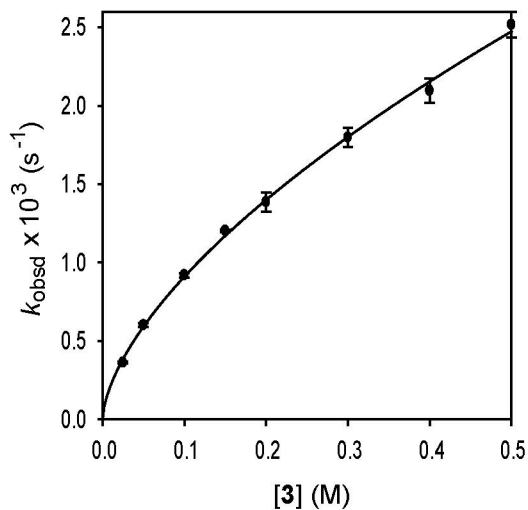
[2-MeTHF] (M)	$k_{\text{obsd}1} \times 10^3 \text{ (s}^{-1}\text{)}$	$k_{\text{obsd}2} \times 10^3 \text{ (s}^{-1}\text{)}$	$k_{\text{obsd}av} \times 10^3 \text{ (s}^{-1}\text{)}$
0.00	$0.341 \pm 5\text{E-}3$	$0.395 \pm 7\text{E-}3$	$0.37 \pm 4\text{E-}2$
0.10	$0.65 \pm 2\text{E-}2$	$0.626 \pm 7\text{E-}3$	$0.64 \pm 2\text{E-}2$
0.20	$0.844 \pm 5\text{E-}3$	$1.21 \pm 2\text{E-}2$	$1.0 \pm 3\text{E-}1$
0.55	$2.66 \pm 1\text{E-}2$	$2.533 \pm 9\text{E-}3$	$2.60 \pm 9\text{E-}2$
1.05	$5.2 \pm 1\text{E-}1$	$5.25 \pm 3\text{E-}2$	$5.22 \pm 3\text{E-}2$
1.55	$8.00 \pm 8\text{E-}2$	$9.40 \pm 6\text{E-}2$	$8.70 \pm 6\text{E-}2$
2.05	$13.9 \pm 4\text{E-}1$	$13.7 \pm 1\text{E-}1$	$13.8 \pm 1\text{E-}1$



XLIII. Plot of k_{obsd} vs [3] in 1.10 M 2-MeTHF and toluene cosolvent for the alkylation of **3** with $n\text{-C}_8\text{H}_{17}\text{Br}$ (0.005 M) at 0 °C. The curve depicts an unweighted least-squares fit to $k_{\text{obsd}} = a[\mathbf{3}]^b$ ($a = 0.66 \pm 0.01$, $b = 0.61 \pm 0.02$).

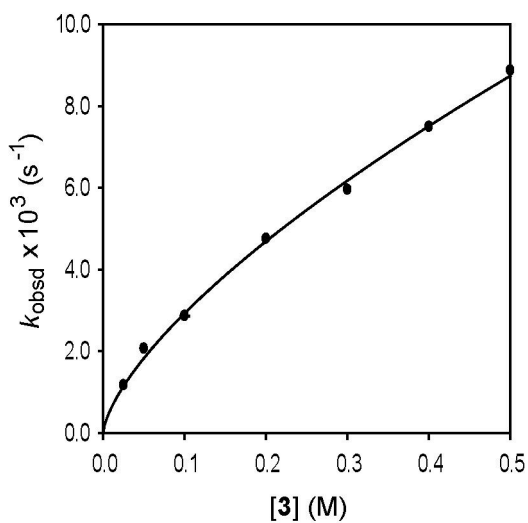
[3] (M)	$k_{\text{obsd}} \times 10^3$ (s ⁻¹)
0.025	0.076 ± 1E-3
0.05	0.110 ± 1E-3
0.10	0.156 ± 1E-3 ^a
0.20	0.246 ± 2E-3
0.30	0.310 ± 6E-3
0.40	0.367 ± 3E-1
0.50	0.44 ± 2E-2

^aAverage of two measurements.



XLIV. Plot of k_{obsd} vs $[3]$ in 4.10 M 2-MeTHF and toluene cosolvent for the alkylation of **3** with $n\text{-C}_8\text{H}_{17}\text{Br}$ (0.005 M) at 0 °C. The curve depicts an unweighted least-squares fit to $k_{\text{obsd}} = a[3]^b$ ($a = 3.8 \pm 0.1$, $b = 0.62 \pm 0.01$).

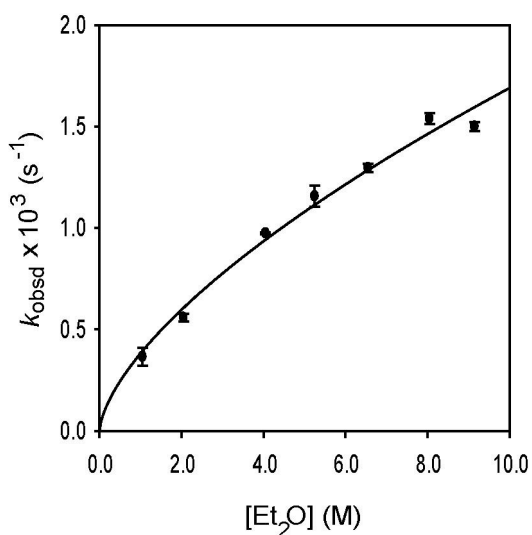
$[3]$ (M)	$k_{\text{obsd}1} \times 10^3$ (s ⁻¹)	$k_{\text{obsd}2} \times 10^3$ (s ⁻¹)	$k_{\text{obsd}av} \times 10^3$ (s ⁻¹)
0.025	$0.368 \pm 4\text{E-}3$	$0.357 \pm 5\text{E-}3$	$0.363 \pm 8\text{E-}3$
0.05	$0.610 \pm 3\text{E-}3$	$0.591 \pm 3\text{E-}3$	$0.60 \pm 1\text{E-}2$
0.10	$0.909 \pm 1\text{E-}3$	$0.929 \pm 6\text{E-}3$	$0.92 \pm 1\text{E-}2$
0.15	$1.20 \pm 1\text{E-}2$	$1.21 \pm 1\text{E-}2$	$1.20 \pm 1\text{E-}2$
0.20	$1.34 \pm 2\text{E-}2$	$1.43 \pm 1\text{E-}2$	$1.39 \pm 6\text{E-}2$
0.30	$1.84 \pm 3\text{E-}2$	$1.75 \pm 2\text{E-}2$	$1.80 \pm 6\text{E-}2$
0.40	$2.0 \pm 1\text{E-}1$	$2.15 \pm 3\text{E-}2$	$2.10 \pm 1\text{E-}1$
0.50	$2.57 \pm 1\text{E-}2$	$2.46 \pm 5\text{E-}2$	$2.52 \pm 8\text{E-}2$



XLV. Plot of k_{obsd} vs [3] in 8.10 M 2-MeTHF and toluene cosolvent for the alkylation of **3** with $n\text{-C}_8\text{H}_{17}\text{Br}$ (0.005 M) at 0 °C. The curve depicts an unweighted least-squares fit to $k_{\text{obsd}} = a[\mathbf{3}]^b$ ($a = 14.0 \pm 0.3$, $b = 0.68 \pm 0.02$).

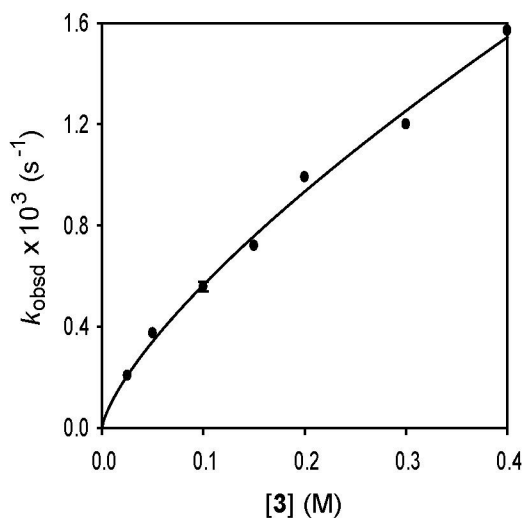
[3] (M)	$k_{\text{obsd}} \times 10^3$ (s ⁻¹)
0.025	1.17 ± 2E-2
0.05	2.061 ± 9E-3
0.10	2.861 ± 5E-3 ^a
0.20	4.75 ± 4E-2
0.30	5.95 ± 9E-2
0.40	7.49 ± 5E-2
0.50	8.9 ± 1E-1

^aAverage of two measurements.



XLVI. Plot of k_{obsd} vs $[\text{Et}_2\text{O}]$ in toluene cosolvent for the alkylation of **3** (0.10 M) with $n\text{-C}_7\text{H}_{15}\text{I}$ (0.005 M) at 0 °C. The curve depicts an unweighted least-squares fit to $k_{\text{obsd}} = a[\text{Et}_2\text{O}]^b$ ($a = 0.38 \pm 0.03$, $b = 0.65 \pm 0.03$).

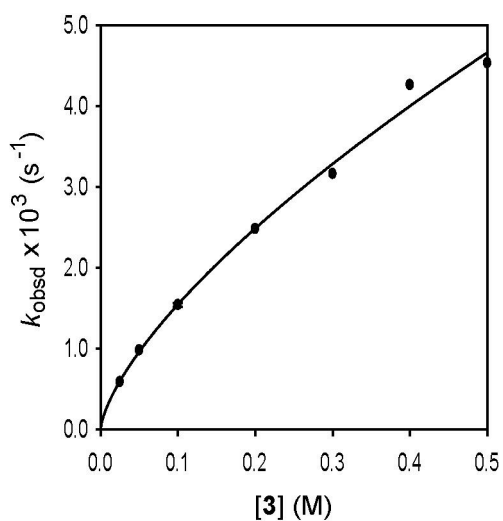
$[\text{Et}_2\text{O}]$ (M)	$k_{\text{obsd}1} \times 10^3$ (s ⁻¹)	$k_{\text{obsd}2} \times 10^3$ (s ⁻¹)	$k_{\text{obsd}av} \times 10^3$ (s ⁻¹)
1.05	$0.333 \pm 5\text{E-}3$	$0.397 \pm 4\text{E-}3$	$0.365 \pm 4\text{E-}2$
2.05	$0.57 \pm 1\text{E-}2$	$0.554 \pm 5\text{E-}3$	$0.563 \pm 1\text{E-}2$
4.05	$0.97 \pm 2\text{E-}2$	$0.977 \pm 9\text{E-}3$	$0.974 \pm 5\text{E-}3$
5.25	$1.19 \pm 2\text{E-}2$	$1.12 \pm 2\text{E-}2$	$1.157 \pm 5\text{E-}3$
6.55	$1.28 \pm 2\text{E-}2$	$1.31 \pm 3\text{E-}2$	$1.30 \pm 2\text{E-}2$
8.05	$1.52 \pm 4\text{E-}2$	$1.56 \pm 2\text{E-}2$	$1.54 \pm 3\text{E-}2$
9.15	$1.51 \pm 2\text{E-}2$	$1.48 \pm 2\text{E-}2$	$1.50 \pm 2\text{E-}2$



XLVII. Plot of k_{obsd} vs $[3]$ in 2.10 M Et₂O and toluene cosolvent for the alkylation of **3** with *n*-C₇H₁₅I (0.005 M) at 0 °C. The curve depicts an unweighted least-squares fit to $k_{\text{obsd}} = a[3]^b$ ($a = 3.0 \pm 0.1$, $b = 0.73 \pm 0.03$).

$[3]$ (M)	$k_{\text{obsd}} \times 10^3$ (s ⁻¹)
0.025	$0.206 \pm 3\text{E-}3$
0.05	$0.374 \pm 7\text{E-}3$
0.10	$0.563 \pm 1\text{E-}2^a$
0.15	$0.72 \pm 1\text{E-}2$
0.20	$0.99 \pm 1\text{E-}2$
0.30	$1.20 \pm 3\text{E-}2$
0.40	$1.57 \pm 5\text{E-}2$

^a Average of two measurements.



XLVIII. Plot of k_{obsd} vs [3] in 8.10 M Et₂O and toluene cosolvent for the alkylation of 3 with *n*-C₇H₁₅I (0.005 M) at 0 °C. The curve depicts an unweighted least-squares fit to $k_{\text{obsd}} = a[\mathbf{3}]^b$ ($a = 7.5 \pm 0.3$, $b = 0.69 \pm 0.03$).

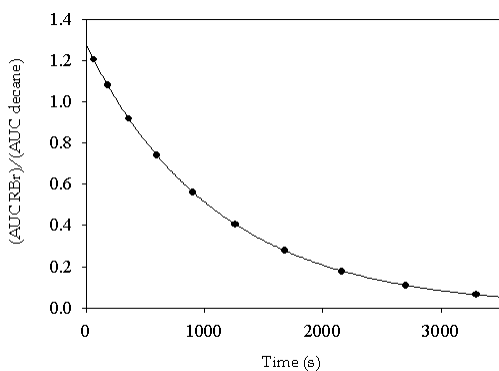
[3] (M)	$k_{\text{obsd}} \times 10^3$ (s ⁻¹)
0.025	0.59 ± 2E-2
0.05	0.98 ± 3E-2
0.10	1.54 ± 3E-2 ^a
0.20	2.48 ± 8E-2
0.30	3.2 ± 1E-1
0.40	4.3 ± 1E-1
0.50	4.53 ± 9E-2

^a Average of two measurements.

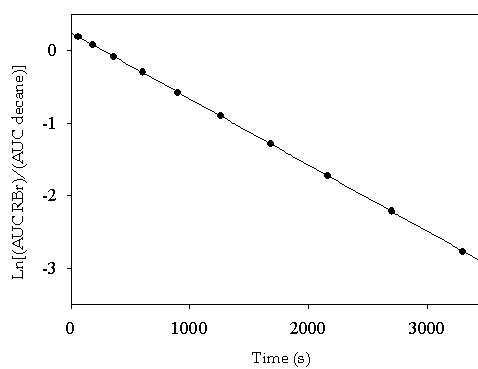
XLIX. Table of data for k_{obsd} in various ethereal solvents (1.10 M) and toluene cosolvent for the alkylation of **3** (0.10 M) with $n\text{-C}_7\text{H}_{15}\text{I}$ (0.005 M) at 0 °C.

Solvent	$k_{\text{obsd}1} \times 10^3 \text{ (s}^{-1}\text{)}$	$k_{\text{obsd}2} \times 10^3 \text{ (s}^{-1}\text{)}$	$k_{\text{obsd}av} \times 10^3 \text{ (s}^{-1}\text{)}$	k_{rel}
Et ₂ O	$0.333 \pm 5\text{E-}3$	$0.397 \pm 4\text{E-}3$	$0.36 \pm 4\text{E-}2$	1.0
<i>n</i> -BuOMe	$0.352 \pm 9\text{E-}3$	$0.392 \pm 6\text{E-}3$	$0.37 \pm 3\text{E-}2$	1.0
<i>t</i> -BuOMe	$0.45 \pm 2\text{E-}2$	$0.41 \pm 4\text{E-}2$	$0.43 \pm 3\text{E-}2$	1.2
THP	$3.42 \pm 8\text{E-}2$	$3.68 \pm 6\text{E-}2$	$3.55 \pm 2\text{E-}1$	10
2-MeTHF	$5.2 \pm 1\text{E-}1$	$5.25 \pm 3\text{E-}2$	$5.22 \pm 4\text{E-}2$	14
THF	$23.3 \pm 4\text{E-}1$	$20.8 \pm 4\text{E-}1$	22 ± 2	61

L. Representative plots of the time-dependent decay of $n\text{-C}_8\text{H}_{17}\text{Br}$ relative to an $n\text{-C}_8\text{H}_{18}$ internal standard (relative area under the curve, AUC).



A



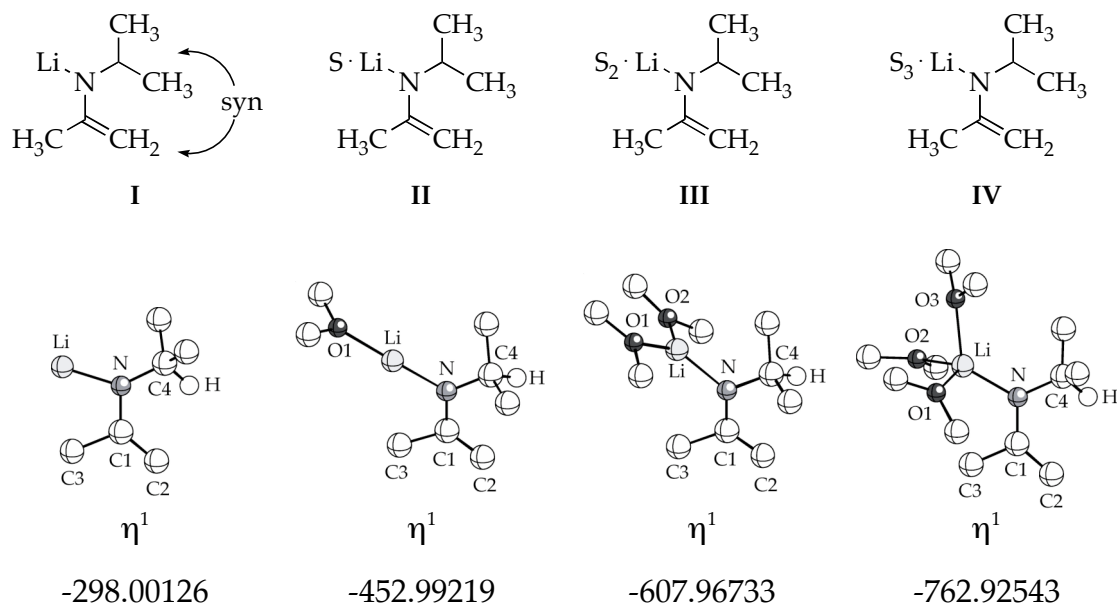
B

(A) Plot of the GC integration of $n\text{-C}_8\text{H}_{17}\text{Br}$ vs time (s) for sequentially quenched samples of a reaction mixture containing **3** (0.1 M), 2-MeTHF (4.10 M), $n\text{-C}_8\text{H}_{17}\text{Br}$ (0.005 M), and toluene cosolvent at 0 °C. The curve depicts a least squares fit to $f(x) = ae^{-bx}$ ($a = 1.273 \pm 0.001$, $b = k_{\text{obsd}} = (0.909 \pm 0.001) \times 10^{-3}$). (B) Plot of the natural logarithm of the data plotted in A vs time (s). The curve depicts a least squares fit to $f(x) = ax + b$ ($a = (-9.128 \pm 0.008) \times 10^{-3}$, $b = 0.24 \pm 0.01$).

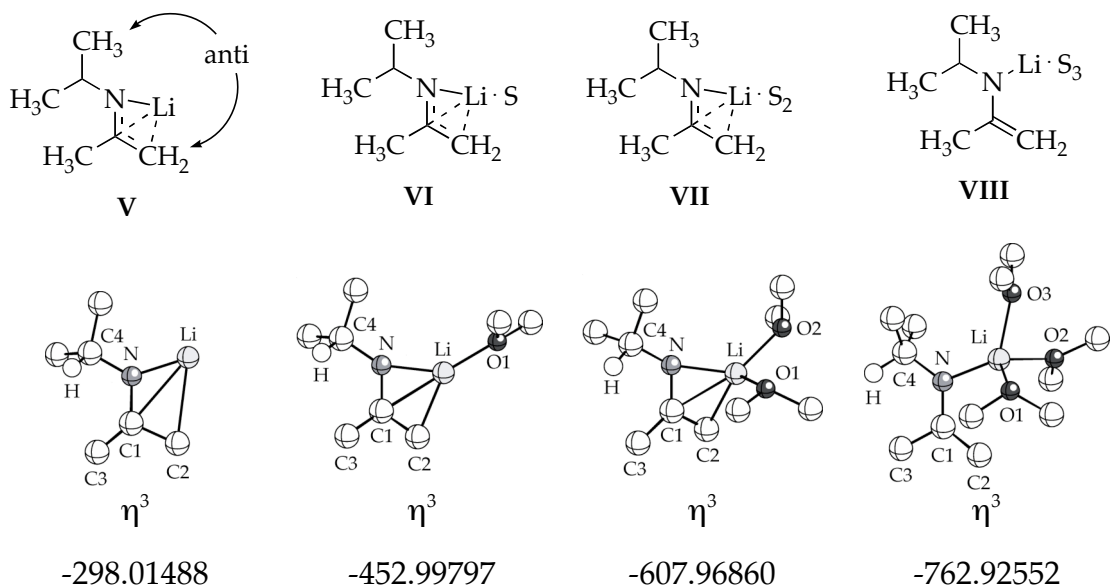
Part 4: DFT Computational Studies

LI. Optimized geometries and free energies (G , Hartrees) of monomers AS_n ^a

A. Syn isomers AS_n . $n = 0-3$, $S = Me_2O$ ($\Delta G = -154.97011$ Hartrees).



B. Anti isomers AS_n .



^a Only selected hydrogens shown for clarity.

LII. Selected bond lengths (Å) and angles (deg) of monomers $\text{AS}_n^{a,b}$

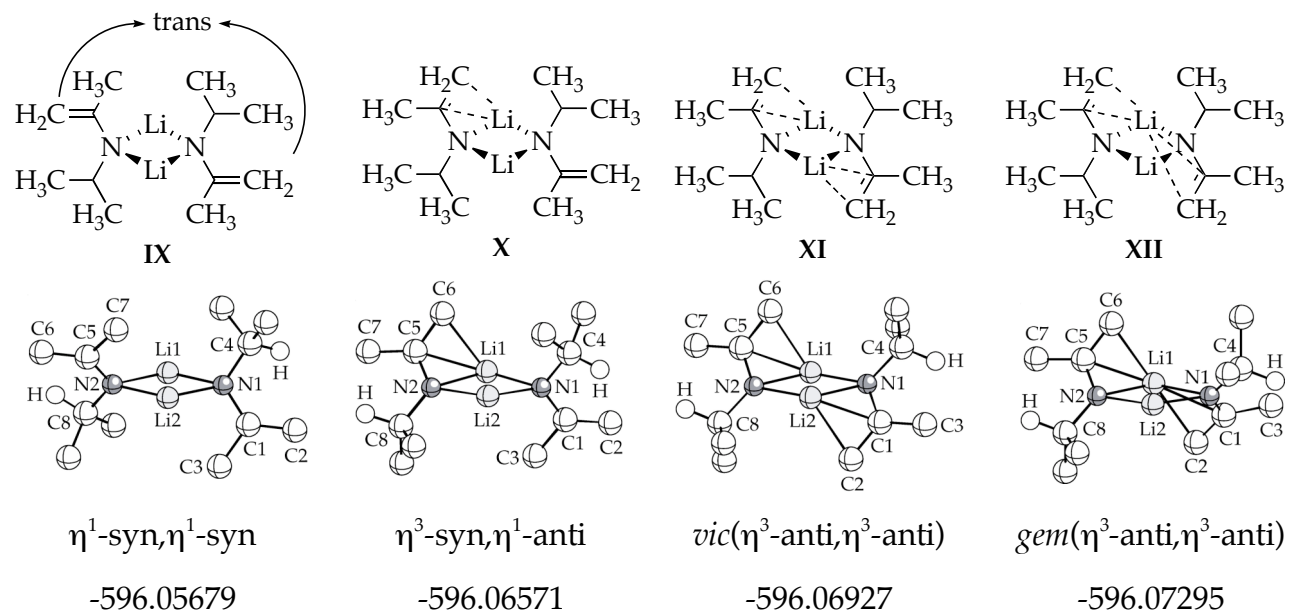
	I	II	III	IV	V	VI	VII	VIII
Li-N ^b	1.80	1.83	1.89	1.95	1.85	1.88	1.92	1.96
Li-C1 ^b	2.60	2.77	2.83	2.86	2.09	2.16	2.25	2.83
Li-C2 ^b	---	---	---	---	2.11	2.15	2.22	3.03
Li-O1	---	1.89	1.95	2.10	---	1.93	2.02	2.09
Li-O2	---	---	1.96	2.07	---	---	1.99	2.07
Li-O3	---	---	---	2.06	---	---	---	2.05
N-C1	1.38	1.37	1.37	1.37	1.35	1.35	1.35	1.37
C1-C2	1.36	1.36	1.36	1.37	1.41	1.40	1.39	1.38
Li-N-C1	109.0	119.1	119.5	117.4	80.9	81.7	83.6	115.4
N-Li-C2	---	---	---	---	73.4	71.5	69.0	52.8
N-C1-C2	129.8	129.2	129.4	129.4	118.6	119.2	119.9	123.5
Li-N-C1-C2	182.9	184.9	206.8	216.6	39.6	41.7	42.2	179.5

^aSee 3D representations in Section LI for atom numbering.

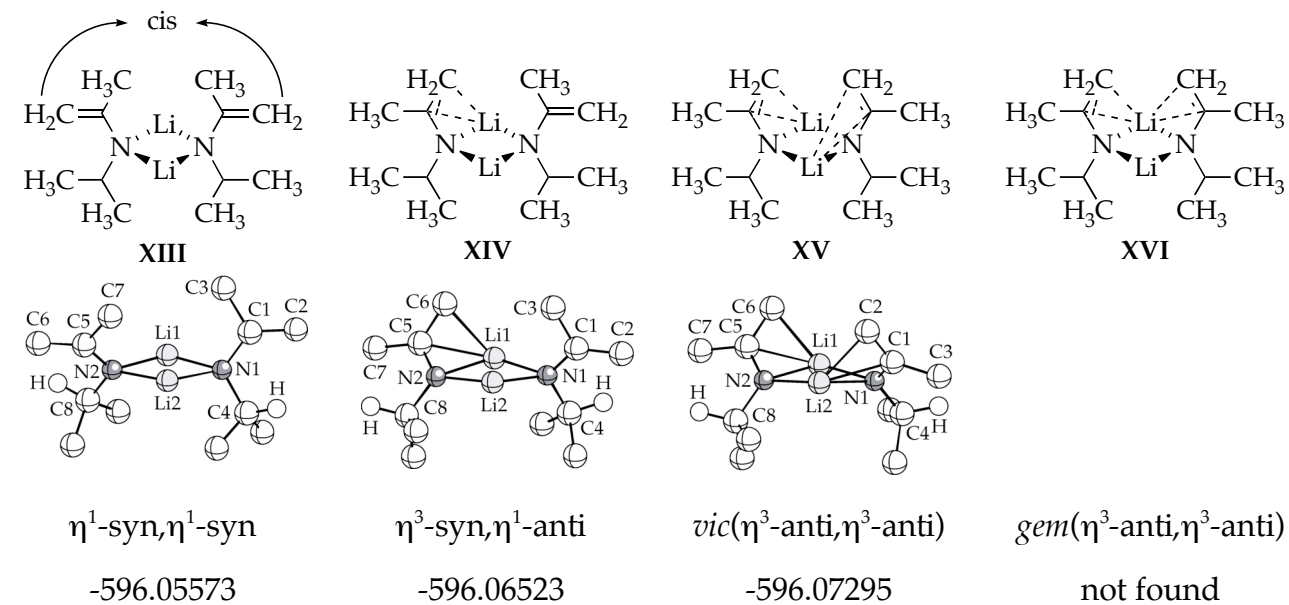
^bN-C1-C2 constitute the azaallylic moiety.

LIII. Optimized geometries and free energies (G , Hartrees) of dimers A_2S_n .^a

A. Unsolvated trans isomers A_2S_n , $n = 0$.



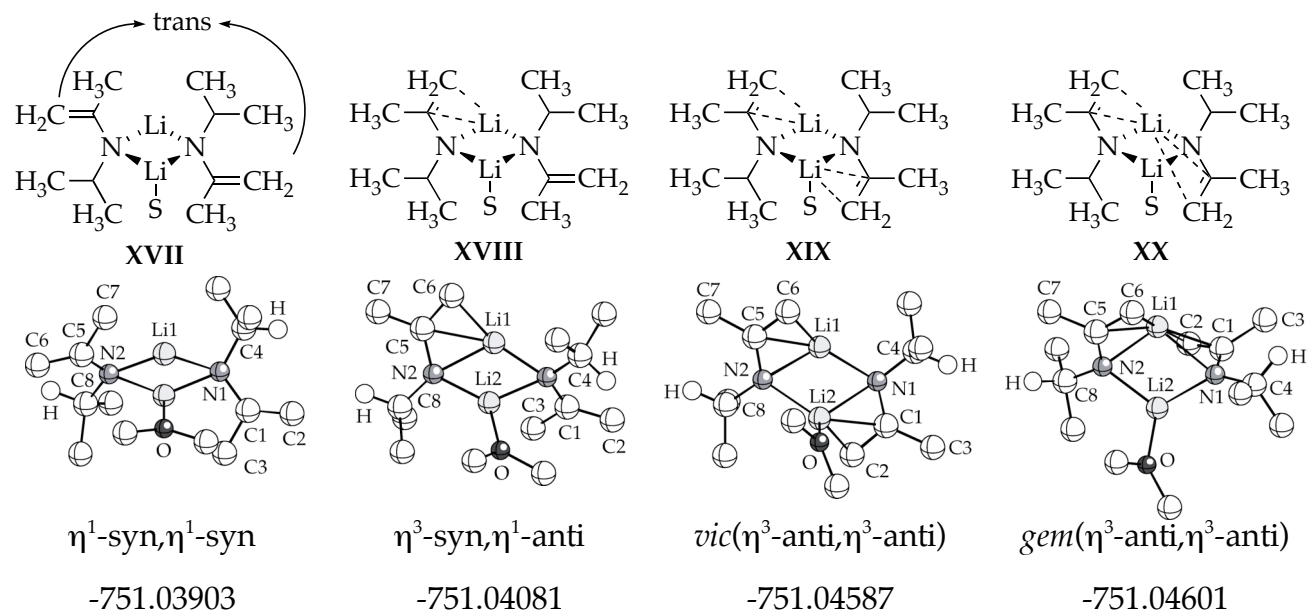
B. Unsolvated cis isomers A_2S_n



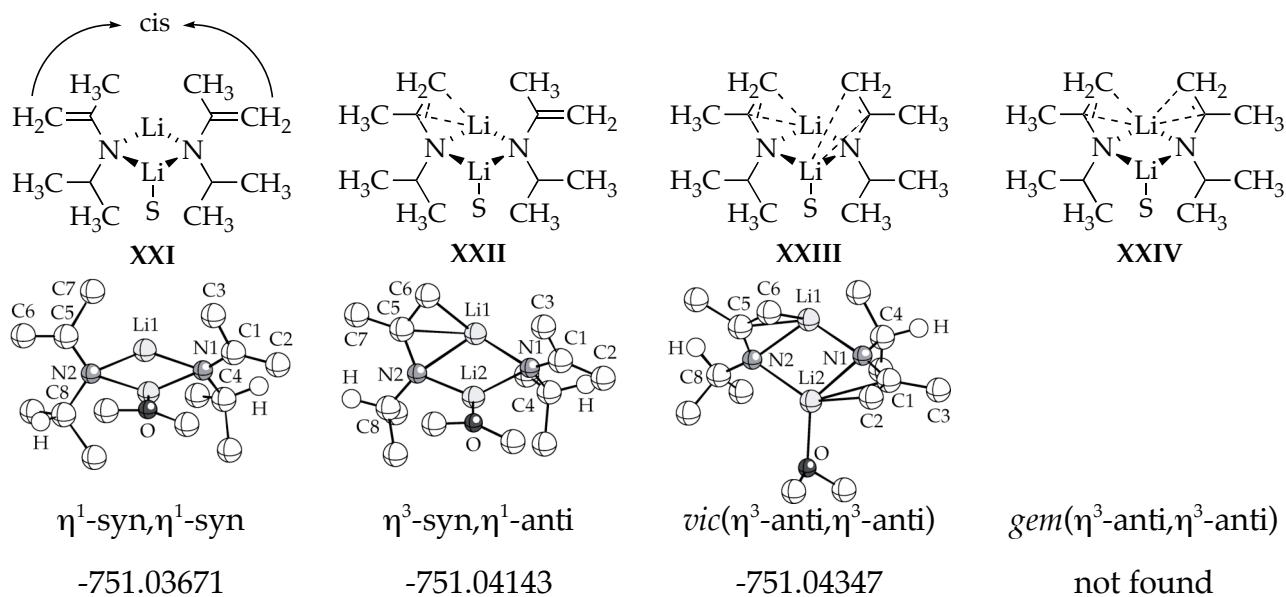
^a Only selected hydrogens shown for clarity.

LIII (Continued).

C. Monosolvated trans isomers A_2S_n , $n = 1$, $S = Me_2O$ ($G = -154.97011$ Hartrees).



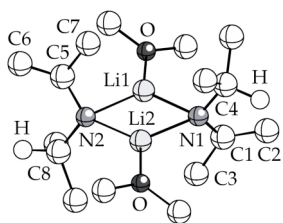
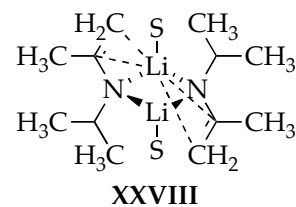
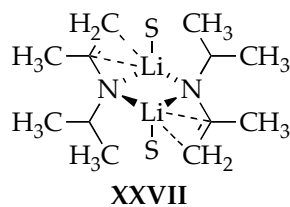
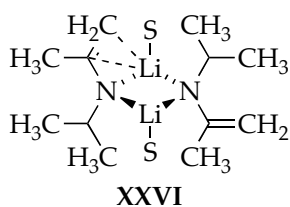
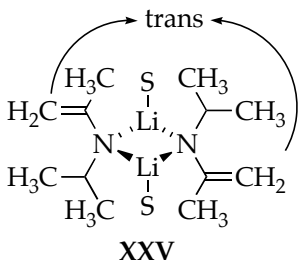
D. Monosolvated cis isomers A_2S_n , $n = 1$, $S = Me_2O$



^aOnly selected hydrogens shown for clarity.

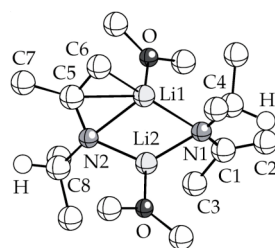
LIII (Continued).

E. Disolvated trans isomers A_2S_n , $n = 2$, $S = Me_2O$ ($G = -154.97011$ Hartrees).



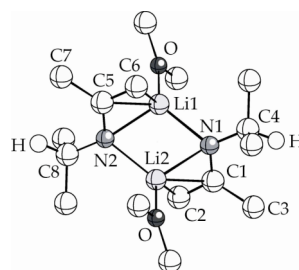
η^1 -syn, η^1 -syn

-906.01273



η^3 -syn, η^1 -anti

-906.01459



vic(η^3 -anti, η^3 -anti)

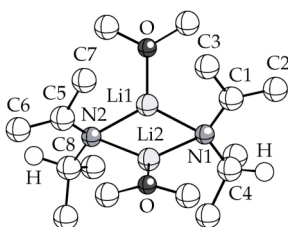
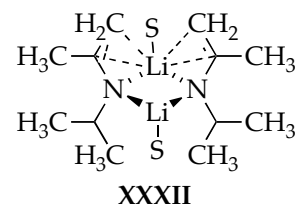
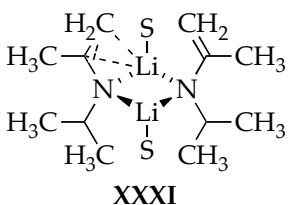
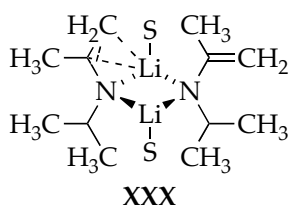
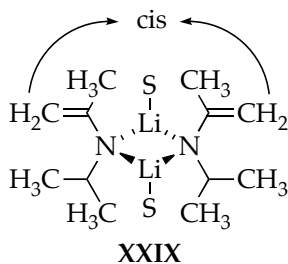
-906.02107



gem(η^3 -anti, η^3 -anti)

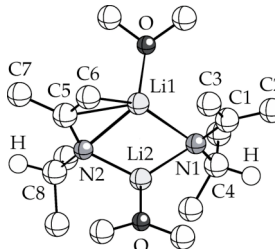
not found

F. Disolvated cis isomers A_2S_n , $n = 2$, $S = Me_2O$



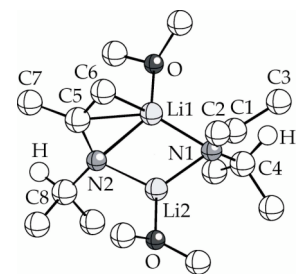
η^1 -syn, η^1 -syn

-906.01500



η^3 -syn, η^1 -anti

-906.01371



η^3 -anti, η^1 -anti^b

-906.01069



gem(η^3 -anti, η^3 -anti)

not found

^a Only selected hydrogens shown for clarity.

^b Li2 and the azaallyl moiety N1-C1-C2 show no evidence of π complexation.

LIV. Selected bond lengths (Å) and angles (deg) calculated for unsolvated dimers \mathbf{A}_2 .^{a, b}

	IX	X	XI	XII	XIII	XIV	XV
Li1-N1 ^b	1.98	1.94	2.07	1.93	1.97	1.96	2.05
Li1-N2 ^b	1.98	1.97	2.01	1.93	1.99	1.95	2.01
Li2-N1 ^b	1.97	2.03	2.01	2.18	1.99	2.01	2.01
Li2-N2 ^b	1.98	2.11	2.07	2.18	1.98	2.17	2.05
Li1-C1 ^b	---	---	2.22	---	---	---	2.23
Li1-C2 ^b	---	---	2.19	---	---	---	2.17
Li2-C1 ^b	---	---	---	2.28	---	---	---
Li2-C2 ^b	---	---	---	2.19	---	---	---
Li2-C5 ^b	---	2.25	2.22	2.28	---	2.26	2.23
Li2-C6 ^b	---	2.16	2.19	2.19	---	2.15	2.16
N1-C1	1.39	1.39	1.37	1.37	1.39	1.39	1.37
N2-C5	1.39	1.37	1.37	1.37	1.40	1.36	1.37
C1-C2	1.36	1.36	1.38	1.38	1.36	1.36	1.39
C5-C6	1.36	1.39	1.38	1.38	1.36	1.39	1.39
Li1-N1-C1-C2	150.0	144.0	46.0	45.0	149.7	136.1	42.1
Li2-N2-C5-C6	136.2	42.5	46.0	6.5	150.4	44.0	42.1

^aSee 3D representations in Section LIII for atom numbering.

^bN1-C1-C2, and N2-C5-C6 constitute the azaallylic moieties.

LIV (Continued). Selected bond lengths (Å) and angles (deg) calculated for monosolvated dimers A_2S .^{a, b}

	XVII	XVIII	XIX	XX	XXI	XXII	XXIII
Li1-N1 ^b	2.08	2.04	2.20	2.02	2.05	2.06	2.05
Li1-N2 ^b	2.06	2.07	2.09	2.02	2.07	2.03	2.11
Li2-N1 ^b	1.95	2.00	1.97	2.05	1.97	1.98	1.98
Li2-N2 ^b	1.94	2.10	2.02	2.20	1.96	2.13	2.03
Li1-C1 ^b	---	---	2.30	---	---	---	2.43
Li1-C2 ^b	---	---	2.24	---	---	---	2.46
Li2-C1 ^b	---	---	---	2.29	---	---	---
Li2-C2 ^b	---	---	---	2.26	---	---	---
Li2-C5 ^b	---	2.23	2.22	2.23	---	2.45	2.18
Li2-C6 ^b	---	2.17	2.23	2.21	---	2.17	2.18
Li1-O	1.92	1.95	1.95	1.97	1.91	1.94	2.00
N1-C1	1.39	1.39	1.35	1.37	1.39	1.39	1.37
N2-C5	1.39	1.37	1.37	1.37	1.39	1.37	1.37
C1-C2	1.36	1.36	1.38	1.38	1.36	1.36	1.37
C5-C6	1.36	1.38	1.39	1.38	1.36	1.39	1.39
Li1-N1-C1-C2	126.3	133.2	47.2	38.5	116.0	117.4	40.3
Li2-N2-C5-C6	159.1	43.9	46.4	51.7	161.1	44.7	45.8

^aSee 3D representations in Section LIII for atom numbering.

^bN1-C1-C2, and N2-C5-C6 constitute the azaallylic moieties.

LIV (Continued). Selected bond lengths (Å) and angles (deg) calculated for disolvated dimers A_2S_2 .^{a, b}

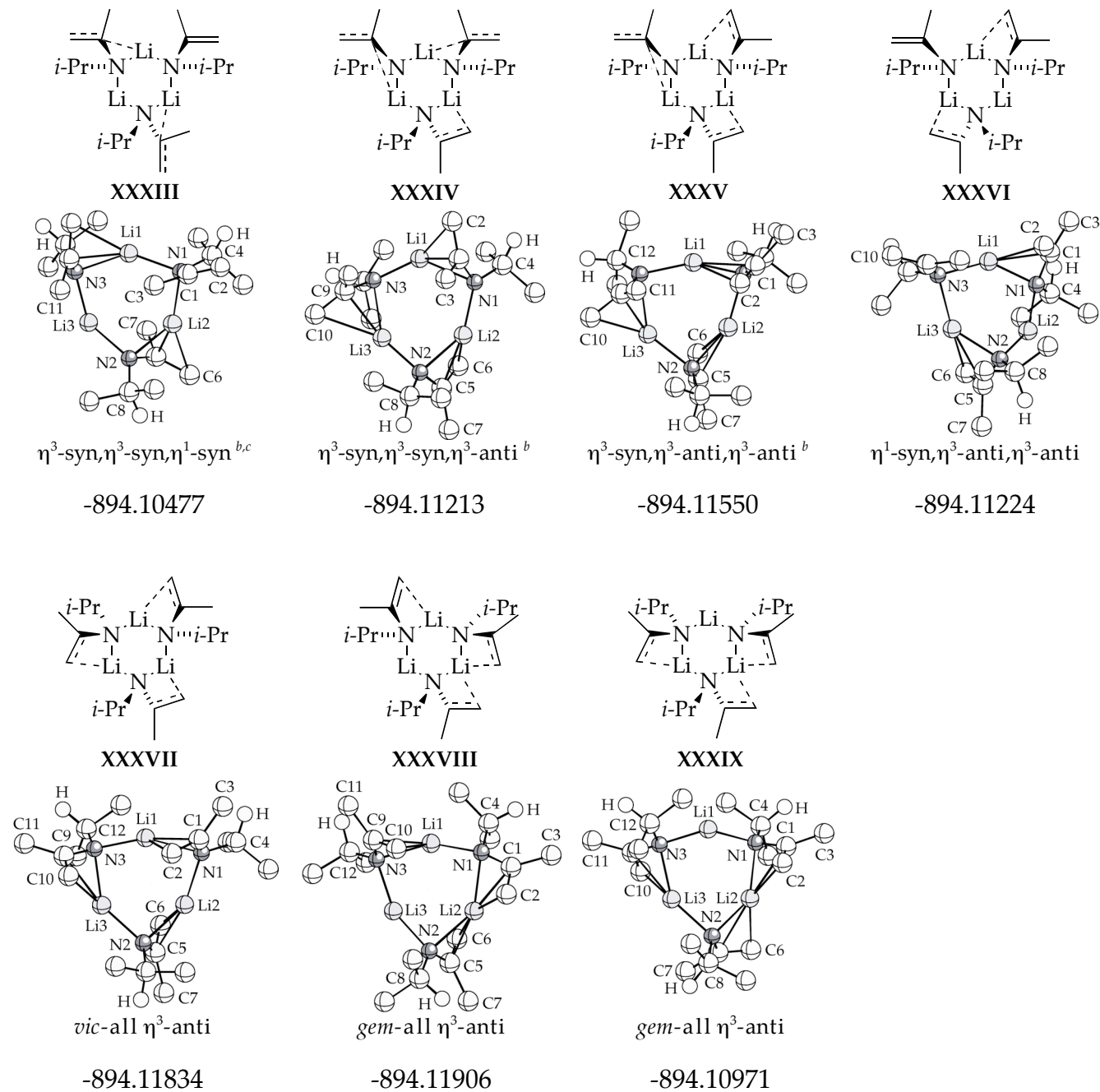
	XXV	XXVI	XXVII	XXIX	XXX	XXXI
Li1-N1 ^b	2.04	2.00	2.12	2.02	2.01	2.10
Li1-N2 ^b	2.03	2.03	2.05	2.07	2.03	2.08
Li2-N1 ^b	2.06	2.13	2.05	2.07	2.10	2.03
Li2-N2 ^b	2.06	2.13	2.12	2.01	2.08	2.01
Li1-C1 ^b	---	---	2.29	---	---	2.30
Li1-C2 ^b	---	---	2.30	---	---	2.32
Li2-C5 ^b	---	2.36	2.29	---	2.30	2.83
Li2-C6 ^b	---	2.33	2.29	---	2.32	2.97
Li1-O	1.95	1.95	1.96	1.93	1.97	1.99
Li2-O	1.92	1.96	1.96	1.93	2.00	1.97
N1-C1	1.39	1.39	1.36	1.39	1.40	1.38
N2-C5	1.39	1.37	1.36	1.39	1.38	1.39
C1-C2	1.36	1.37	1.38	1.36	1.36	1.38
C5-C6	1.36	1.38	1.38	1.36	1.38	1.36
Li1-N1-C1-C2	136.1	162.6	47.7	157.5	154.8	47.6
Li2-N2-C5-C6	150.0	44.1	47.7	156.9	52.9	6.5

^aSee 3D representations in Section LIII for atom numbering.

^bN1-C1- C2, and N2-C5-C6 constitute the azaallylic moieties.

LV. Optimized geometries and free energies (G , Hartrees) of trimers A_3S_n .^a

A. Unsolvated cis,trans isomers A_3S_n . $n = 0$.



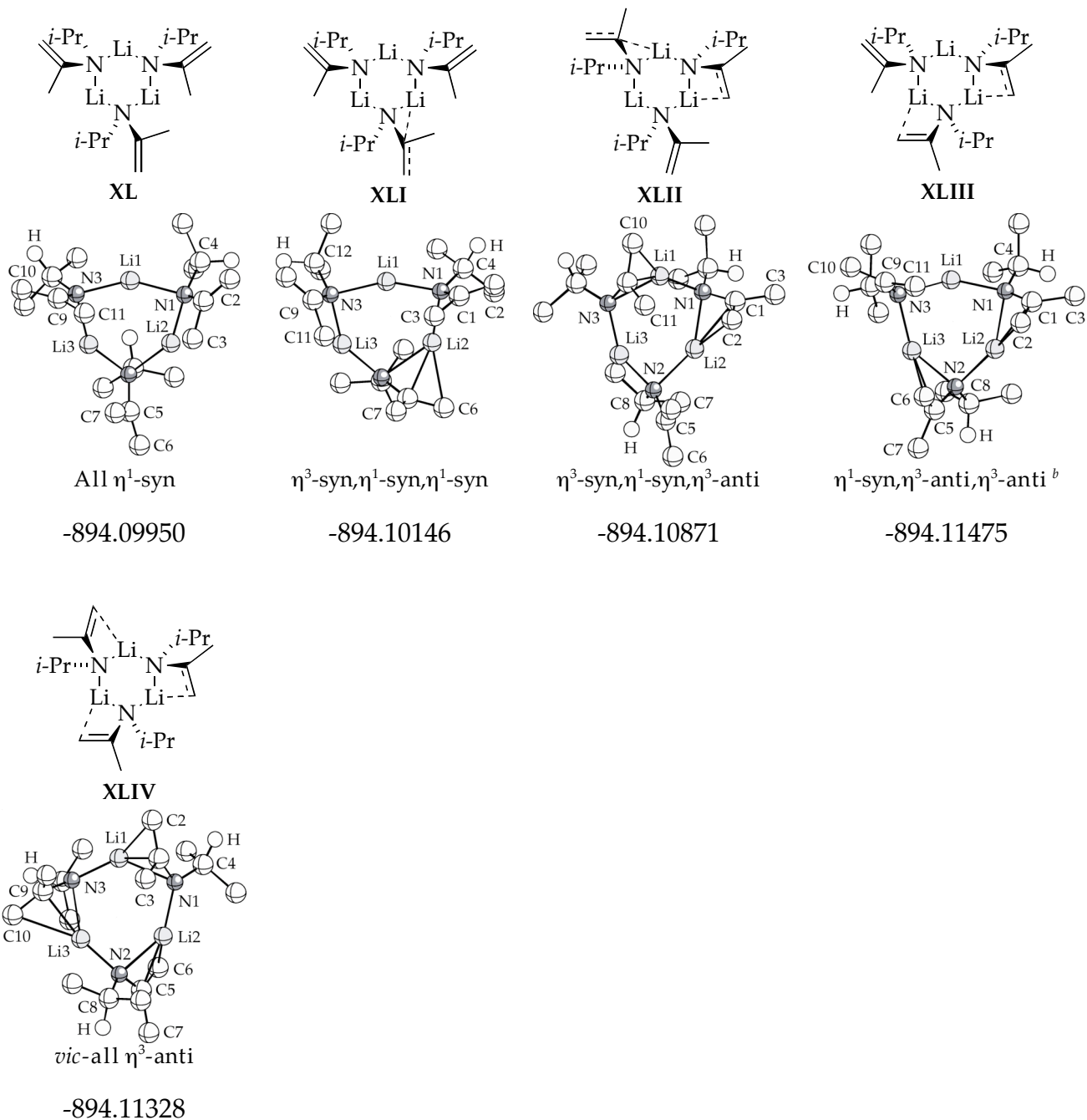
^a Only selected hydrogens shown for clarity.

^b η^1 -Syn azaallyl moieties turned into η^3 -syn upon geometry optimization.

^c All η^3 -syn not found.

LV (Continued).

B. Unsolvated cis,cis isomers A_3S_n , $n = 0$.^a

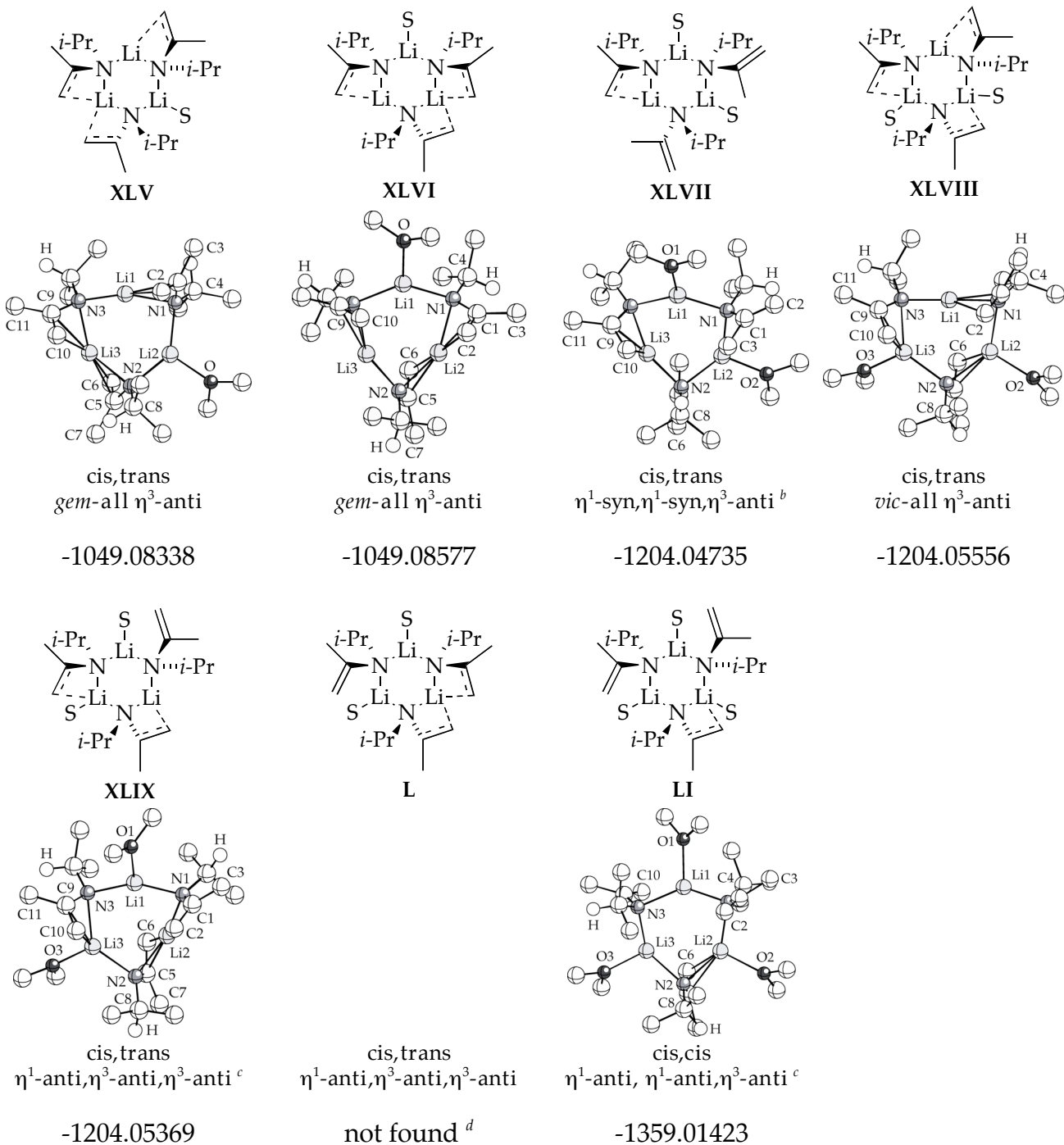


^a Only selected hydrogens shown for clarity.

^b η^3 -Syn isomer not found.

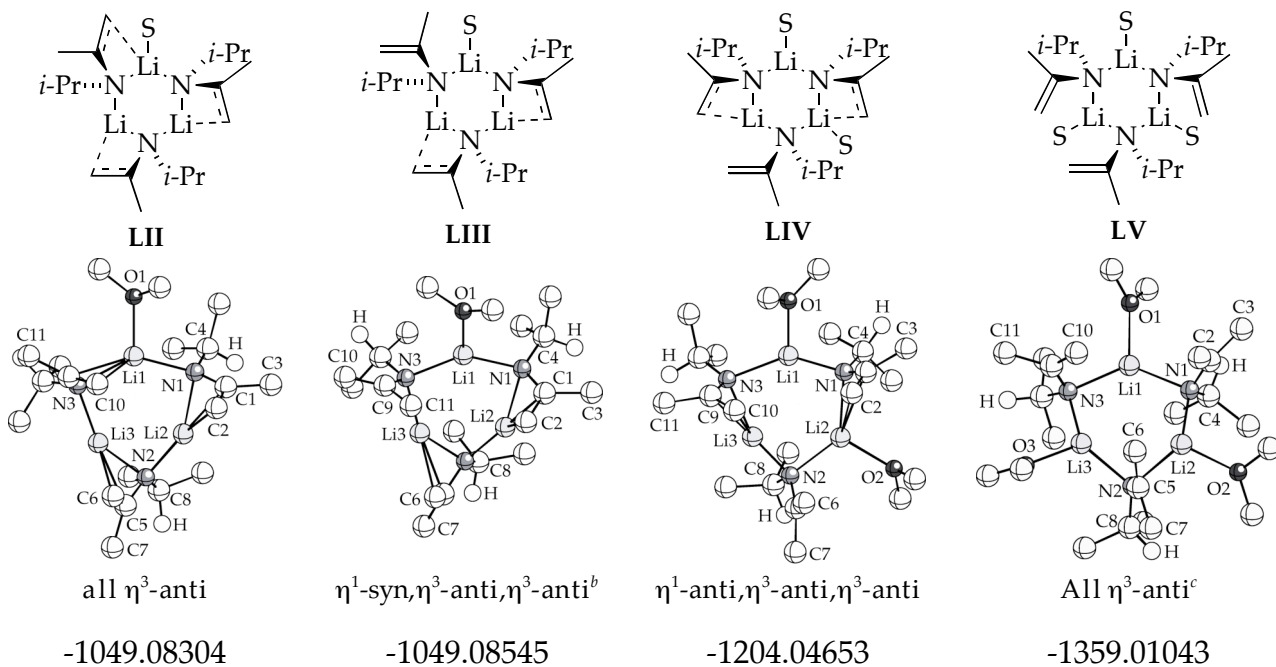
LV (Continued).

C. Solvated cis,trans isomers A_3S_n , $n = 1-3$, $S = Me_2O$ ($G = -154.97011$ Hartrees).



LV (Continued).

D. Solvated cis,cis isomers A_3S_n , $n = 1-3$, $S = Me_2O$ ($G = -154.97011$ Hartrees).



^a Only selected hydrogens shown for clarity.

^b η^3 -Syn azaallyl moiety not found.

^c η^3 -Anti azaallyl moiety turned into η^1 -anti upon geometry optimization.

^d Optimization of **XLX** converges to its isomer **XLIX**.

LVI. Selected bond lengths (Å) and angles (deg) calculated for unsolvated trimers **A₃S**.^{a, b}

	XXXIII	XXXIV	XXXV	XXXVI	XXXVII	XXXVIII
Li1-N1 ^b	2.00	1.96	2.28	2.21	2.29	1.98
Li1-N3 ^b	2.21	2.05	1.96	2.00	1.96	2.05
Li2-N1 ^b	2.01	2.00	1.94	1.93	1.95	2.11
Li2-N2 ^b	2.13	2.04	2.04	1.93	2.04	2.16
Li3-N3 ^b	1.93	2.18	2.13	2.01	2.13	1.95
Li3-N2 ^b	1.93	1.99	1.98	2.13	1.98	1.92
Li1-N1-N3	140.9	141.5	134.4	140.9	134.3	138.4
Li2-N1-N2	140.3	144.0	143.7	144.6	143.2	135.7
Li3-N2-N3	144.6	136.3	141.2	140.3	141.1	152.6

	XXXIX	XL	XLI	XLII	XLIII	XLIV
Li1-N1 ^b	1.96	1.99	1.97	1.98	1.95	2.03
Li1-N3 ^b	2.07	1.95	2.02	2.07	1.96	1.98
Li2-N1 ^b	2.12	1.96	2.02	2.10	2.22	2.00
Li2-N2 ^b	2.16	2.01	2.16	2.02	2.00	2.05
Li3-N3 ^b	1.95	1.98	1.96	1.96	2.03	2.02
Li3-N2 ^b	1.93	1.95	1.91	1.95	2.05	1.99
Li1-N1-N3	138.3	144.1	153.0	138.7	147.6	137.7
Li2-N1-N2	137.7	147.3	134.8	141.3	136.5	140.0
Li3-N2-N3	156.1	145.5	145.7	152.6	143.2	139.7

^aSee 3D representations in Section LV for atom numbering.

^bN1-C3-C2, N2-C5-C6, and N3-C9-C10 constitute the azaallylic moieties.

LVI (*Continued*). Selected bond lengths (Å) and angles (deg) calculated for solvated trimers A_3S_n .^{a, b}

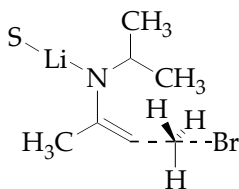
	XLV	XLVI	XLVII	XLVIII	XLIX	LI	LII	LIII	LIV	LV
Li1-N1 ^b	2.02	2.05	2.06	2.02	2.05	2.05	2.07	2.10	2.06	2.06
Li1-N3 ^b	1.95	2.06	2.08	1.96	2.09	2.07	2.14	2.05	2.12	2.08
Li2-N1 ^b	2.07	2.16	2.07	2.10	1.99	2.09	2.07	2.04	2.13	2.08
Li2-N2 ^b	2.07	2.09	2.06	2.14	2.03	2.15	1.98	1.99	2.06	2.06
Li3-N3 ^b	2.13	2.08	2.03	2.11	2.14	2.09	2.00	2.01	1.99	2.07
Li3-N2 ^b	2.12	1.97	1.97	2.11	2.11	2.07	2.04	2.07	2.04	2.08
Li1-N1-N3	142.7	134.8	132.4	147.1	131.0	136.0	132.2	135.8	136.9	135.3
Li2-N1-N2	137.2	140.1	133.0	131.2	150.8	99.8	141.7	144.8	129.6	98.9
Li3-N2-N3	148.1	92.6	154.2	128.2	131.1	137.2	142.3	86.2	144.0	99.8
Li-O (av)	1.97	2.00	2.00	2.01	2.02	2.05	2.00	1.98	2.01	2.06

^aSee 3D representations in Section LV for atom numbering.

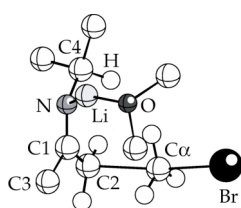
^bN1-C3-C2, N2-C5-C6, and N3-C9-C10 constitute the azaallylic moieties.

LVII. Optimized geometries and free energies (G , Hartrees) of monomer-based transition structures $[\text{AS}_n\text{CH}_3\text{Br}]^\ddagger$.^{a,b}

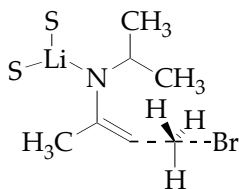
A. Syn alkylations $[\text{AS}_n\text{CH}_3\text{Br}]^\ddagger$. $n = 1-3$. $\text{S} = \text{Me}_2\text{O}$, $G = -154.97011$ Hartrees. MeBr , $G = -2613.76945$ Hartrees.



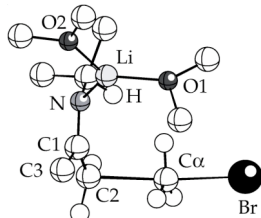
A



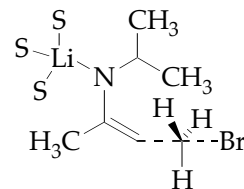
-3066.71919



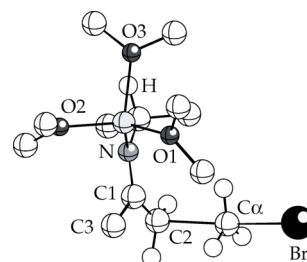
B



-3221.69655

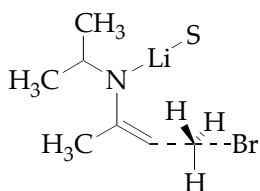


C

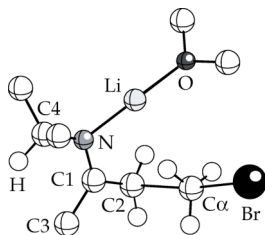


-3376.64811

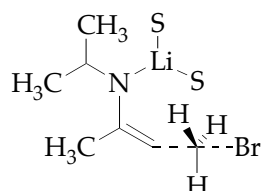
B. Anti alkylations $[\text{AS}_n\text{CH}_3\text{Br}]^\ddagger$.



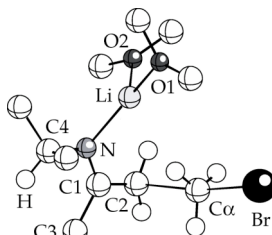
D



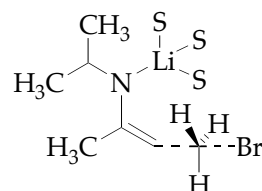
-3066.72378



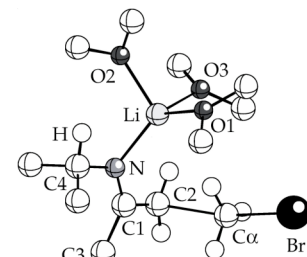
E



-3221.69413



F



-3376.64535

^a Only selected hydrogens shown for clarity.

^b Only most stable conformers shown.

LVIII. Selected bond lengths (Å) and angles (deg) calculated for monomer-based transition structures **A-F**.^{a, b}

	A	B	C	D	E	F
Li-N ^b	1.89	1.94	1.99	1.91	1.94	2.02
Li-C1 ^b	2.64	2.80	2.95	2.33	2.80	2.92
Li-C2 ^b	---	---	---	2.24	2.97	3.13
Li-O1	1.88	1.95	2.06	1.89	1.95	2.04
Li-O2	---	1.93	2.03	---	1.94	2.05
Li-O3	---	---	2.03	---	---	2.12
N-C1	1.34	1.34	1.34	1.33	1.34	1.34
C1-C2	1.40	1.40	1.40	1.43	1.41	1.40
C2-C α	2.33	2.34	2.31	2.35	2.34	2.36
C α -Br	2.42	2.40	2.41	2.40	2.37	2.35
C2-C α -Br	172.8	175.5	175.5	177.3	172.3	171.5
Li-N-C1	108.4	116.0	123.4	90.2	115.7	119.3

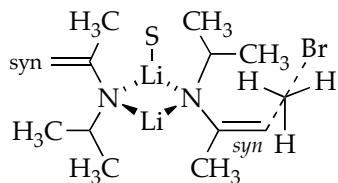
^aSee 3D representations in Section **LVII** for atom numbering.

^bN-C1-C2 constitutes the azaallylic moiety.

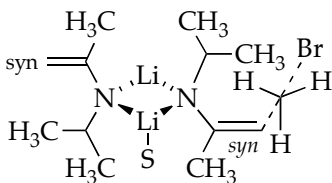
LIX. Optimized geometries and free energies (G , Hartrees) of dimer-based transition structures $[A_2S_n\cdot CH_3Br]^\ddagger$.^{a,b}

A. Exo alkylations $[A_2S_n\cdot CH_3Br]^\ddagger$.

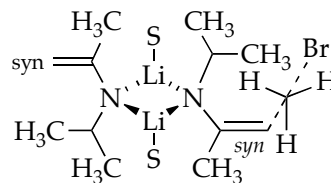
$n = 1-2$. $S = Me_2O$, $G = -154.97011$ Hartrees. $MeBr$, $G = -2613.76945$ Hartrees.



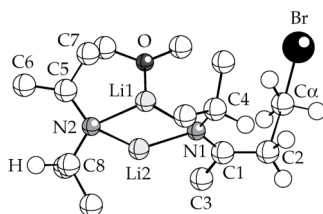
G



H

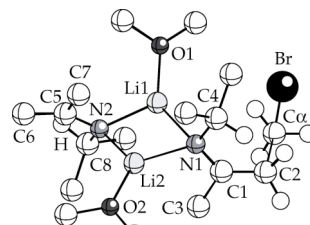


I

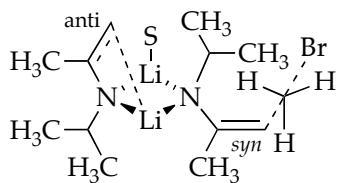


$[A_2S\cdot CH_3Br]^\ddagger$
trans,syn,syn
-3364.74847

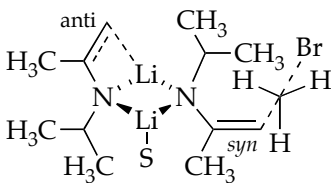
$[A_2S\cdot CH_3Br]^\ddagger$
trans,syn,syn
not found^c



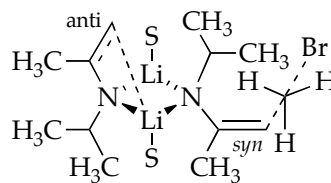
$[A_2S_2\cdot CH_3Br]^\ddagger$
trans,syn,syn
-3519.72375



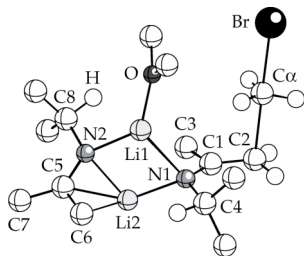
J



K

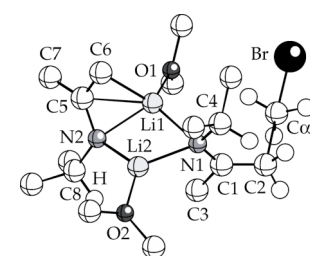


L



$[A_2S\cdot CH_3Br]^\ddagger$
trans,anti,syn
-3364.74785

$[A_2S\cdot CH_3Br]^\ddagger$
trans,anti,syn
not found^c



$[A_2S_2\cdot CH_3Br]^\ddagger$
trans,anti,syn
-3519.72658

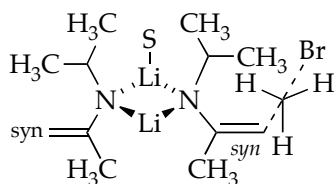
^a Only selected hydrogens shown for clarity.

^b Only most stable conformers shown.

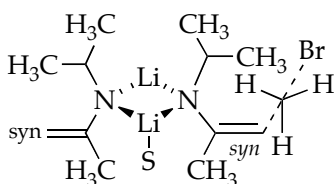
^c TS optimization collapsed into an endo isomer following a Li-Br interaction (see below).

LIX (Continued).

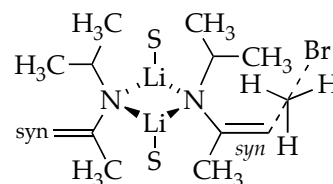
A. Exo alkylations $[A_2S_nCH_3Br]^{\ddagger}$



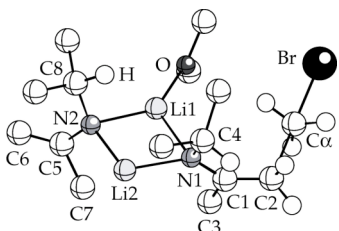
M



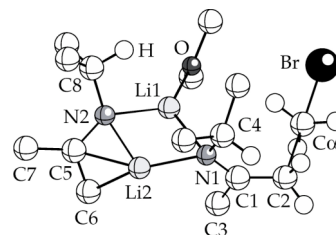
N



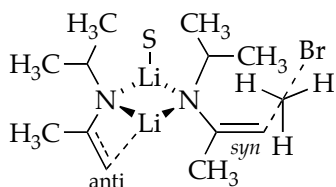
O



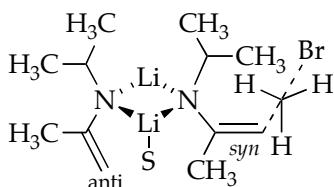
$[A_2SCH_3Br]^{\ddagger}$
cis,syn,syn
-3364.74500



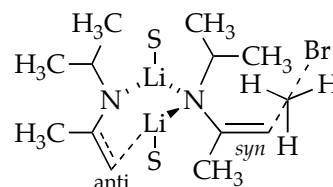
$[A_2S_2CH_3Br]^{\ddagger}$
cis,syn,syn
-3519.72146



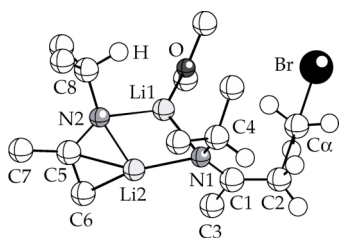
P



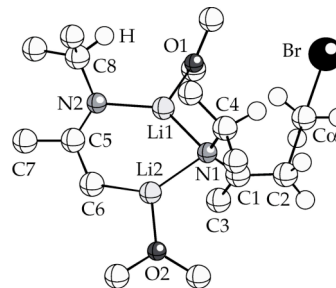
Q



R



$[A_2SCH_3Br]^{\ddagger}$
cis,anti,syn
-3364.75455



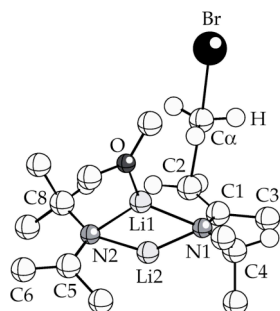
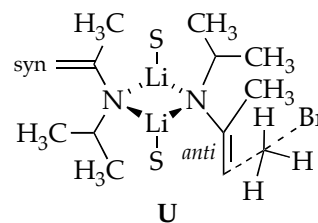
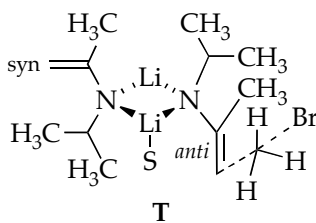
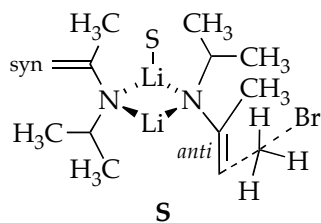
$[A_2S_2CH_3Br]^{\ddagger}$
cis,anti,syn
-3519.72033^d

^c TS optimization collapsed into an endo isomer following a Li-Br interaction (see below).

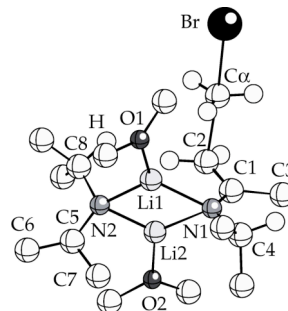
^dThe isomer with an intact Li_2N_2 core couldn't be located.

LIX (Continued).

A. Exo alkylations $[A_2S_nCH_3Br]^{\ddagger}$

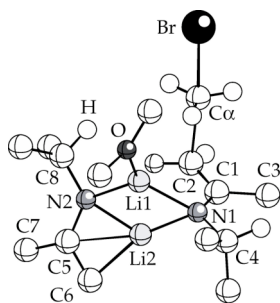
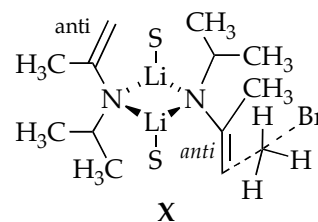
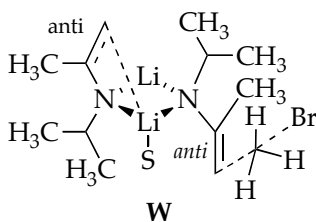
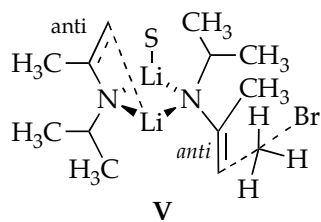


$[A_2SCH_3Br]^{\ddagger}$
trans,syn,anti
-3364.74039

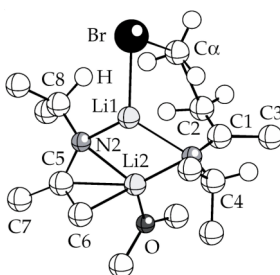


$[A_2S_2CH_3Br]^{\ddagger}$
trans,syn,anti
-3519.72313

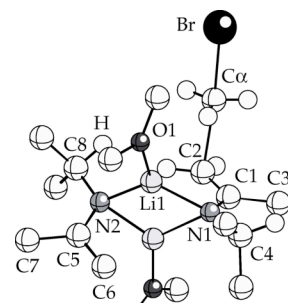
$[A_2SCH_3Br]^{\ddagger}$
trans,syn,anti
not found^c



$[A_2SCH_3Br]^{\ddagger}$
trans,anti,anti
-3364.75287



$[A_2SCH_3Br]^{\ddagger}$
trans,anti,anti
-3364.75307

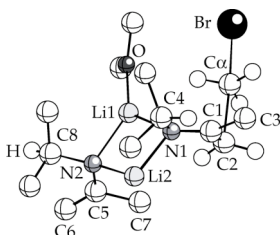
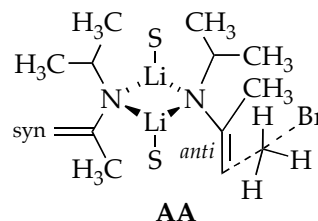
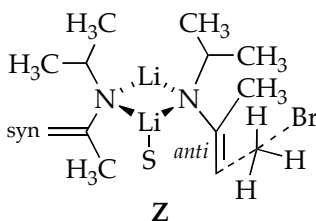
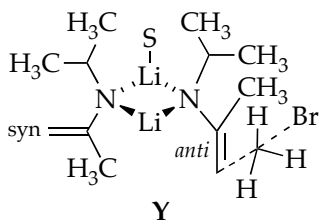


$[A_2S_2CH_3Br]^{\ddagger}$
trans,anti,anti
-3519.72486

^c TS optimization collapsed into an endo isomer following a Li-Br interaction (see below).

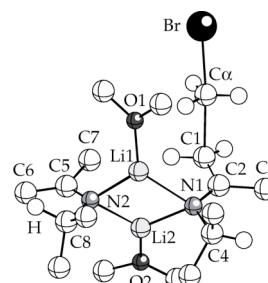
LIX (Continued).

A. Exo alkylations $[A_2S_nCH_3Br]^{\ddagger}$

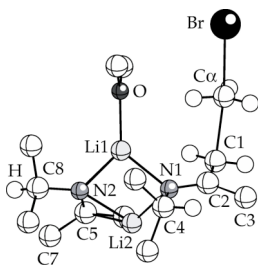
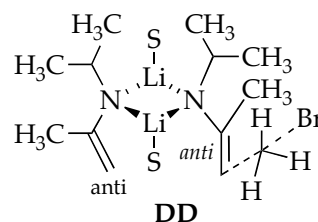
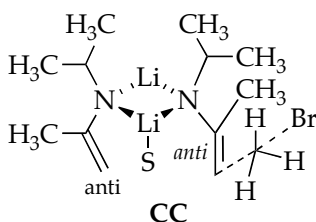
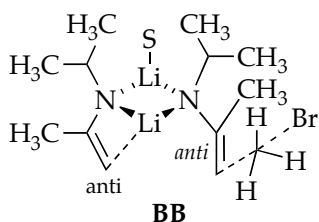


$[A_2SCH_3Br]^{\ddagger}$
cis,syn,anti
-3364.74707

$[A_2SCH_3Br]^{\ddagger}$
cis,syn,anti
not found^c

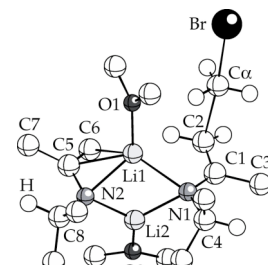


$[A_2S_2CH_3Br]^{\ddagger}$
cis,syn,anti
-3519.72518



$[A_2SCH_3Br]^{\ddagger}$
cis,anti,anti
-3364.75528

$[A_2SCH_3Br]^{\ddagger}$
cis,anti,anti
not found^c



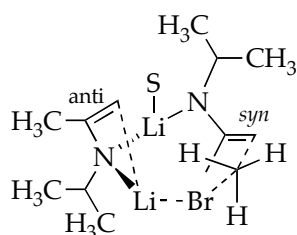
$[A_2S_2CH_3Br]^{\ddagger}$
cis,anti,anti
-3519.72609

^c TS optimization collapsed into an endo isomer following a Li-Br interaction (see below).

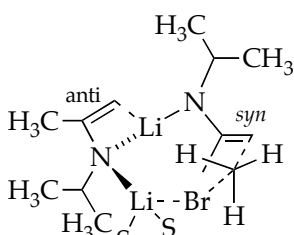
LIX (Continued).

B. Endo alkylations $[A_2S_nCH_3Br]^\ddagger$.

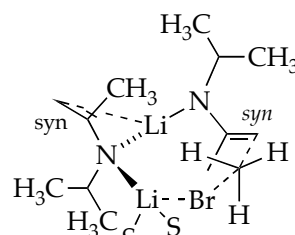
$n = 1-2$. $S = Me_2O$, $G = -154.97011$ Hartrees. $MeBr$, $G = -2613.76945$ Hartrees.



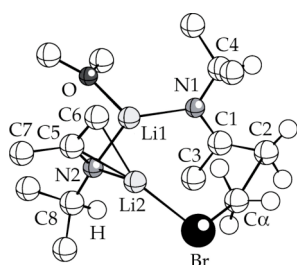
EE



FF



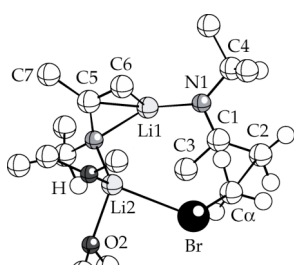
GG



$[A_2SCH_3Br]^\ddagger$

anti,syn

-3364.76278



$[A_2SCH_3Br]^\ddagger$

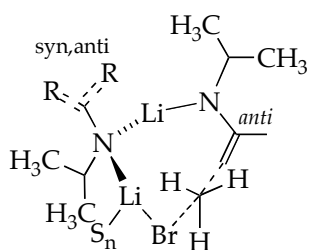
anti,syn

-3519.72627^c

$[A_2S_2CH_3Br]^\ddagger$

syn,syn

not found



HH

$[A_2S_nCH_3Br]^\ddagger$

syn or *anti,anti*

not found^c

^cIsomers, including species with different solvation numbers, couldn't be located.

^eEndo alkylations of anti lithioimine subunits collapsed into their exo isomers or couldn't be located.

LX. Selected bond lengths (Å) and angles (deg) calculated for dimer-based transition structures **G-FF**.^{a,b}

	G	I	J	L	M	O	P	R	S	U
Li1-N1	2.16	2.27	2.15	2.34	2.23	2.16	2.15	2.15	2.15	2.13
Li1-N2	2.08	2.00	2.02	2.08	2.01	1.98	2.00	1.96	2.06	1.99
Li2-N1	1.97	2.05	2.00	2.03	1.97	2.02	2.01	2.05	2.03	2.09
Li2-N2	1.91	2.03	1.99	1.98	1.93	2.00	2.01	3.32	1.93	2.02
C2-C α	2.18	2.23	2.25	2.26	2.26	2.24	2.25	2.22	2.20	2.20
C α -Br	2.48	2.44	2.45	2.45	2.47	2.46	2.45	2.47	2.46	2.46
Li1-N1-N2	100.6	103.1	103.1	100.0	100.4	101.5	103.6	127.0	102.7	105.6
Li2-N1-N2	114.0	110.4	110.3	111.3	113.6	105.9	108.3	82.7	112.3	106.0
C2-C α -Br	178.3	176.6	177.5	178.2	179.5	138.3	179.3	178.9	172.5	174.7
Li-O (av)	1.91	1.94	1.92	1.94	1.91	1.92	1.93	1.95	1.91	1.93

	V	W	X	Y	AA	BB	DD	EE	FF
Li1-N1	2.12	2.28	2.10	2.15	2.20	2.13	2.23	1.91	1.94
Li1-N2	2.00	2.00	2.00	2.00	2.02	2.05	2.09	2.05	2.04
Li2-N1	2.03	2.16	2.14	2.01	2.07	2.04	2.07	---	---
Li2-N2	2.02	2.07	2.02	2.01	2.03	2.03	2.01	1.98	2.05
C2-C α	2.21	2.42	2.24	2.25	2.25	2.24	2.26	2.60	2.51
C α -Br	2.45	2.43	2.43	2.45	2.43	2.43	2.04	2.31	2.36
Li-Br	---	---	---	---	---	---	---	2.59	2.78
Li1-N1-N2	105.5	102.7	106.4	103.6	105.4	104.3	101.6	145.2	152.5
Li2-N1-N2	108.2	106.0	104.4	108.3	109.8	108.8	110.7	---	---
C2-C α -Br	173.9	101.2	175.3	179.3	175.1	172.5	175.2	167.8	167.9
Li-O (av)	1.93	1.98	1.95	1.91	1.92	1.93	1.94	1.94	2.04

^aSee 3D representations in Section **LIX** for atom numbering.

^bN-C1-C2, and N2-C5-C6 constitutes the azaallylic moieties.

Part 5: GIAO Computational Studies

LXI. Calculated chemical shifts (δ , ppm)^a and coupling constants (J , Hz) for monomers **AS_n**.^{b, c}

Structure	no π / no S		no π / S		π / no S		π / S	
	$J_{\text{Li-N}}$	δ_{Li}	$J_{\text{Li-N}}$	δ_{Li}	$J_{\text{Li-N}}$	δ_{Li}	$J_{\text{Li-N}}$	δ_{Li}
I	6.6	0.0	---	---	---	---	---	---
II	---	---	3.6	-0.7	---	---	---	---
III	---	---	6.9	-0.5	---	---	---	---
IV	---	---	6.8	-0.4	---	---	---	---
V	---	---	---	---	3.2	0.8	---	---
VI	---	---	---	---	---	---	2.9	-0.5
VII	---	---	---	---	---	---	2.0	-1.1
VIII	---	---	6.4	0.1	---	---	---	---

^aChemical shifts are referenced to the calculated shielding value of monomer **I**.

^bSee Chart 2 for atom numbering.

^cN, C(1) and C(2) constitute the azaallylic moiety.

LXII. Calculated chemical shifts (δ , ppm) and coupling constants (J , Hz) for dimers A_2S_n .^{a,b}

Structure	no π / no S		no π / S		π / no S		π / S	
	J_{Li-N}	δ_{Li}	J_{Li-N}	δ_{Li}	J_{Li-N}	δ_{Li}	J_{Li-N}	δ_{Li}
IX	4.0	0.0	---	---	---	---	---	---
X	3.7	-0.2	---	---	1.7	0.1	---	---
XI	---	---	---	---	2.1	-0.7	---	---
XII	---	---	---	---	3.4	-0.7	---	---
XIII	4.1	0.0	---	---	---	---	---	---
XIV	3.4	0.6	---	---	1.6	-0.7	---	---
XV	---	---	---	---	1.7	-0.2	---	---
XVII	5.1	0.0	3.3	0.0	---	---	---	---
XVIII	---	---	4.6	0.0	1.9	0.1	---	---
XIX	---	---	---	---	2.5	-0.6	1.4	-1.5
XX	---	---	5.2	0.2	1.9	-0.9	---	---
XXI	5.4	0.4	3.2	0.3	---	---	---	---
XXII	---	---	3.2	0.2	1.8	-0.5	---	---
XXIII	---	---	---	---	2.1	-0.5	---	---
XXV	---	---	4.3	0.2	---	---	2.1	-1.1
XXVI	---	---	5.4	0.1	---	---	1.8	-1.0
XXVII	---	---	---	---	---	---	1.9	-1.5
XXIX	---	---	4.4	0.3	---	---	---	---
XXX	---	---	5.3	0.4	---	---	2.1	-1.1
XXXI	---	---	---	---	---	---	3.3	0.2
av	4.3	0.1	4.3	0.1	2.1	-0.5	2.1	-1.0
σ	0.7	0.3	0.9	0.2	0.5	0.3	0.6	0.6

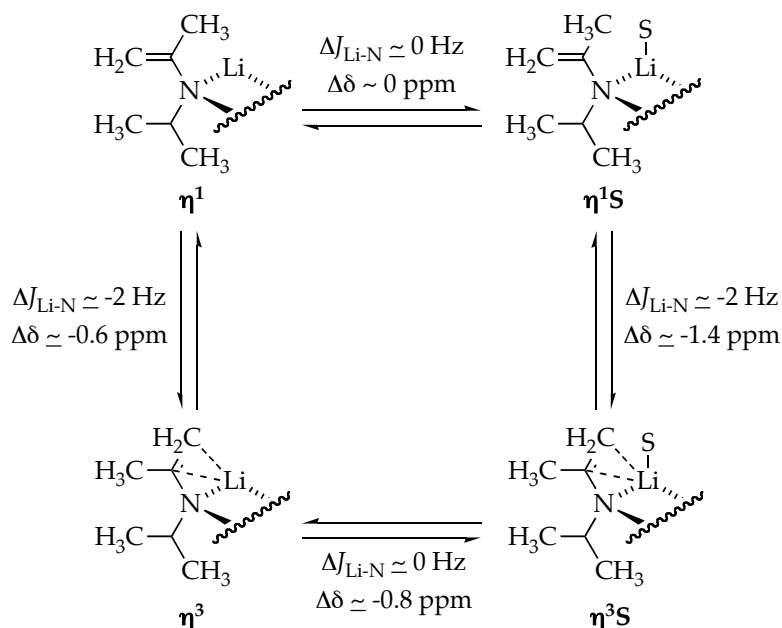
^aChemical shifts are referenced to the calculated shielding value of dimer IX. ^bSee Chart 2 for atom numbering. ^cN, C(1) and C(2) constitute the azaallylic moiety. ^dDouble π complexation not included.

LXIII. Calculated chemical shifts (δ , ppm) and coupling constants (J , Hz) for trimers A_3S_n .^{a,b}

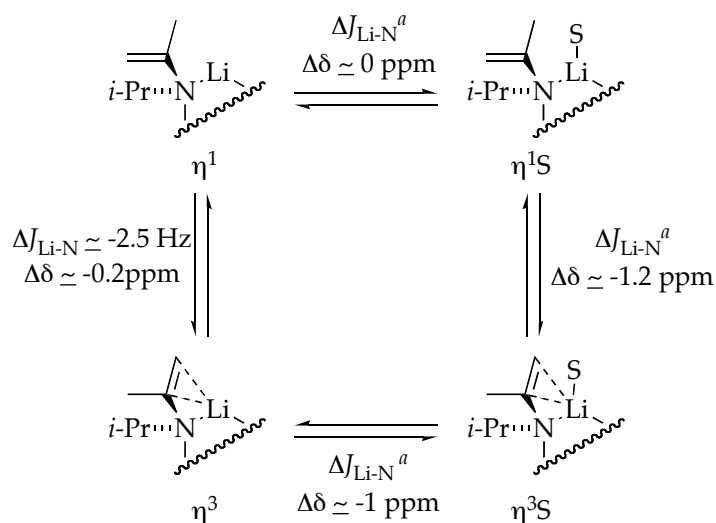
Structure	no π / no S		no π / S		π / no S		π / S	
	J_{Li-N}	δ_{Li}	J_{Li-N}	δ_{Li}	J_{Li-N}	δ_{Li}	J_{Li-N}	δ_{Li}
XXXIII	---	0.0	---	---	1.0 ^c	-1.1 ^c	---	---
XXXIV	---	---	---	---	1.1 ^c	-1.2 ^c	---	---
XXXV	---	---	---	---	1.7 ^c	-0.8 ^c	---	---
XXXVI	---	0.0	---	---	2.2 ^c	-0.7 ^c	---	---
XXXVII	---	0.0	---	---	2.2 ^c	-1.2 ^c	---	---
XXXVIII	---	0.1	---	---	1.9 ^d	-0.7 ^d	---	---
XXXIX	---	0.1	---	---	2.0 ^d	-0.7 ^d	---	---
XL	4.7 ^c	0.6 ^c	---	---	---	---	---	---
XLI	4.5 ^c	0.5 ^c	---	---	0.6	-0.3	---	---
XLII	4.6	0.3	---	---	1.4 ^c	-0.8 ^c	---	---
XLIII	3.8	1.3	---	---	1.9 ^c	-0.5 ^c	---	---
XLIV	---	---	---	---	1.9 ^c	-0.5 ^c	---	---
XLV	---	---	---	0.2	2.2 ^d	-0.3 ^d	---	---
XLVI	---	---	---	-0.1	2.1 ^d	-0.6 ^d	---	---
XLVII	---	---	---	-0.1	---	-0.7 ^c	---	---
XLVIII	---	---	---	---	---	-0.2 ^c	---	-1.7
XLIX	---	---	---	-0.2	---	-0.1 ^c	---	-1.5
LI	---	---	---	-0.7 ^c	---	---	---	-1.6
LII	---	---	---	---	1.9 ^c	-0.3 ^c	2.7	-1.4
LIII	---	---	4.6	-0.2	2.0 ^c	-0.2 ^c	---	---
LIV	---	---	---	-0.7	---	-0.1	---	-1.1
LV	---	---	---	-0.5 ^c	---	---	---	---
av	4.4	0.3	4.6	-0.3	1.7	-0.6	2.7	-1.5
σ	0.4	0.4	---	0.3	0.5	0.3	---	0.2

^aChemical shifts are referenced to the calculated shielding value (90.2) for the no π / no S Li atom in trimer XXXIII. ^bN1-C1-C2, N2-C5-C6, and N3-C9-C10 constitute the azaallylic moieties. ^cAverage values. ^dDouble π complexation not included. ^eThe size of the system precluded the calculation of coupling constants.

LXIV. Effect of solvation and π -complexation upon calculated chemical shifts (δ , ppm) and coupling constants (J , Hz) for dimers A_2S_n .



LXV. Effect of solvation and π -complexation upon calculated chemical shifts (δ , ppm) and coupling constants (J , Hz) for trimers A_3S_n ^a



^a ΔJ_{Li-N} values of statistical significance not calculated due to low populations.

Part 6: X-Ray Crystal Data

LXVI. X-ray crystal data for lithioimine *trans*-**12** (A_2S_2 , $S = Me_2EtN$, Figure 5).

Table 1. Crystal data and structure refinement.

Identification code	ar4	
Empirical formula	C16 H31 Li N2	
Formula weight	258.37	
Temperature	173(2) K	
Wavelength	0.71073 Å	
Crystal system	Triclinic	
Space group	P-1	
Unit cell dimensions	a = 9.2212(11) Å	$\alpha = 82.311(5)^\circ$.
	b = 9.3182(11) Å	$\beta = 72.770(5)^\circ$.
	c = 10.5245(13) Å	$\gamma = 70.616(6)^\circ$.
Volume	814.14(17) Å ³	
Z	2	
Density (calculated)	1.054 Mg/m ³	
Absorption coefficient	0.060 mm ⁻¹	
F(000)	288	
Crystal size	0.40 x 0.30 x 0.20 mm ³	
Theta range for data collection	2.03 to 30.59°.	
Index ranges	-13<=h<=12, -13<=k<=13, -15<=l<=13	
Reflections collected	18562	
Independent reflections	4910 [R(int) = 0.0398]	
Completeness to theta = 30.59°	98.1 %	
Absorption correction	Semi-empirical from equivalents	
Max. and min. transmission	0.9881 and 0.9763	
Refinement method	Full-matrix least-squares on F ²	
Data / restraints / parameters	4910 / 0 / 283	
Goodness-of-fit on F ²	1.076	
Final R indices [I>2sigma(I)]	R1 = 0.0494, wR2 = 0.1447	
R indices (all data)	R1 = 0.0710, wR2 = 0.1576	
Largest diff. peak and hole	0.312 and -0.225 e.Å ⁻³	

Table 2. Atomic coordinates ($\times 10^4$) and equivalent isotropic displacement parameters ($\text{\AA}^2 \times 10^3$). $U(\text{eq})$ is defined as one third of the trace of the orthogonalized U^{ij} tensor.

	x	y	z	$U(\text{eq})$
Li(1)	4059(2)	4681(2)	996(2)	24(1)
N(1)	3937(1)	6862(1)	159(1)	19(1)
N(2)	1918(1)	4119(1)	1933(1)	27(1)
C(1)	2891(1)	8110(1)	-473(1)	20(1)
C(2)	2561(1)	7566(1)	-1635(1)	22(1)
C(3)	1469(1)	8863(1)	-2303(1)	26(1)
C(4)	2136(1)	10195(1)	-2765(1)	29(1)
C(5)	2452(1)	10753(1)	-1608(1)	29(1)
C(6)	3566(1)	9442(1)	-976(1)	27(1)
C(7)	3948(1)	7127(1)	1423(1)	21(1)
C(8)	2601(1)	8355(1)	2277(1)	30(1)
C(9)	3049(5)	8653(3)	3538(3)	32(1)
C(10)	3670(4)	7151(4)	4272(3)	36(1)
C(9')	2444(3)	8134(4)	3758(2)	36(1)
C(10')	4079(3)	7797(4)	3984(2)	37(1)
C(11)	5215(1)	6261(1)	3368(1)	32(1)
C(12)	5120(1)	6194(1)	1972(1)	24(1)
C(13)	1744(2)	3370(2)	845(2)	40(1)
C(14)	589(2)	5473(2)	2278(2)	42(1)
C(15)	1984(2)	3000(2)	3079(1)	35(1)
C(13')	1987(8)	2814(8)	1445(8)	43(2)
C(14')	583(9)	5465(9)	1535(10)	51(2)
C(15')	1373(7)	4150(8)	3460(5)	43(2)
C(16)	2543(2)	3395(2)	4121(1)	59(1)

Table 3. Bond lengths [\AA] and angles [$^\circ$].

Li(1)-N(1)#1	2.0821(17)
Li(1)-N(1)	2.0850(17)
Li(1)-N(2)	2.1306(18)
Li(1)-C(7)	2.3452(18)
Li(1)-C(12)	2.4285(19)
Li(1)-Li(1)#1	2.441(3)
N(1)-C(7)	1.3883(11)
N(1)-C(1)	1.4672(11)
N(1)-Li(1)#1	2.0821(17)
N(2)-C(13')	1.357(6)
N(2)-C(14)	1.4346(18)
N(2)-C(15)	1.4867(15)
N(2)-C(13)	1.4898(18)
N(2)-C(15')	1.537(5)
N(2)-C(14')	1.551(7)
C(1)-C(2)	1.5281(13)
C(1)-C(6)	1.5329(13)
C(2)-C(3)	1.5338(12)
C(3)-C(4)	1.5239(15)
C(4)-C(5)	1.5223(15)
C(5)-C(6)	1.5312(13)
C(7)-C(12)	1.3674(12)
C(7)-C(8)	1.5268(14)
C(8)-C(9')	1.514(2)
C(8)-C(9)	1.584(3)
C(9)-C(10)	1.524(5)
C(10)-C(11)	1.499(3)
C(9')-C(10')	1.518(4)
C(10')-C(11)	1.555(3)
C(11)-C(12)	1.5076(13)
C(15)-C(16)	1.474(2)
C(15')-C(16)	1.396(6)
N(1)#1-Li(1)-N(1)	108.30(7)
N(1)#1-Li(1)-N(2)	121.65(8)

N(1)-Li(1)-N(2)	119.85(8)
N(1)#1-Li(1)-C(7)	124.12(8)
N(1)-Li(1)-C(7)	35.92(4)
N(2)-Li(1)-C(7)	114.21(7)
N(1)#1-Li(1)-C(12)	104.74(7)
N(1)-Li(1)-C(12)	63.24(5)
N(2)-Li(1)-C(12)	124.78(8)
C(7)-Li(1)-C(12)	33.23(4)
N(1)#1-Li(1)-Li(1)#1	54.20(6)
N(1)-Li(1)-Li(1)#1	54.09(6)
N(2)-Li(1)-Li(1)#1	150.79(12)
C(7)-Li(1)-Li(1)#1	77.69(8)
C(12)-Li(1)-Li(1)#1	80.35(8)
C(7)-N(1)-C(1)	115.59(7)
C(7)-N(1)-Li(1)#1	118.44(7)
C(1)-N(1)-Li(1)#1	120.51(7)
C(7)-N(1)-Li(1)	82.31(7)
C(1)-N(1)-Li(1)	139.30(7)
Li(1)#1-N(1)-Li(1)	71.70(7)
C(13')-N(2)-C(14)	129.2(3)
C(13')-N(2)-C(15)	75.8(4)
C(14)-N(2)-C(15)	111.48(12)
C(13')-N(2)-C(13)	32.1(4)
C(14)-N(2)-C(13)	109.48(13)
C(15)-N(2)-C(13)	107.15(11)
C(13')-N(2)-C(15')	113.9(4)
C(14)-N(2)-C(15')	72.9(3)
C(15)-N(2)-C(15')	42.6(3)
C(13)-N(2)-C(15')	138.9(3)
C(13')-N(2)-C(14')	109.6(5)
C(14)-N(2)-C(14')	30.2(3)
C(15)-N(2)-C(14')	134.8(3)
C(13)-N(2)-C(14')	82.4(4)
C(15')-N(2)-C(14')	102.0(4)
C(13')-N(2)-Li(1)	109.9(3)
C(14)-N(2)-Li(1)	110.53(10)

C(15)-N(2)-Li(1)	115.78(9)
C(13)-N(2)-Li(1)	101.79(9)
C(15')-N(2)-Li(1)	116.0(2)
C(14')-N(2)-Li(1)	104.6(3)
N(1)-C(1)-C(2)	111.64(7)
N(1)-C(1)-C(6)	112.86(8)
C(2)-C(1)-C(6)	108.56(7)
C(1)-C(2)-C(3)	112.03(8)
C(4)-C(3)-C(2)	112.00(8)
C(5)-C(4)-C(3)	110.36(8)
C(4)-C(5)-C(6)	110.27(8)
C(5)-C(6)-C(1)	112.55(8)
C(12)-C(7)-N(1)	119.81(8)
C(12)-C(7)-C(8)	118.27(8)
N(1)-C(7)-C(8)	121.71(8)
C(12)-C(7)-Li(1)	76.73(7)
N(1)-C(7)-Li(1)	61.77(6)
C(8)-C(7)-Li(1)	130.18(8)
C(9')-C(8)-C(7)	115.04(11)
C(9')-C(8)-C(9)	30.58(11)
C(7)-C(8)-C(9)	111.83(13)
C(10)-C(9)-C(8)	110.2(3)
C(11)-C(10)-C(9)	107.3(3)
C(8)-C(9')-C(10')	108.8(2)
C(9')-C(10')-C(11)	110.2(2)
C(10)-C(11)-C(12)	113.31(13)
C(10)-C(11)-C(10')	30.05(12)
C(12)-C(11)-C(10')	110.44(11)
C(7)-C(12)-C(11)	125.81(9)
C(7)-C(12)-Li(1)	70.04(7)
C(11)-C(12)-Li(1)	132.72(8)
C(16)-C(15)-N(2)	114.53(12)
C(16)-C(15')-N(2)	116.1(4)
C(15')-C(16)-C(15)	44.9(3)

Symmetry transformations used to generate equivalent atoms: #1 -x+1,-y+1,-z

Table 4. Anisotropic displacement parameters ($\text{\AA}^2 \times 10^3$). The anisotropic displacement factor exponent takes the form: $-2\pi^2 [h^2 a^{*2} U^{11} + \dots + 2 h k a^* b^* U^{12}]$

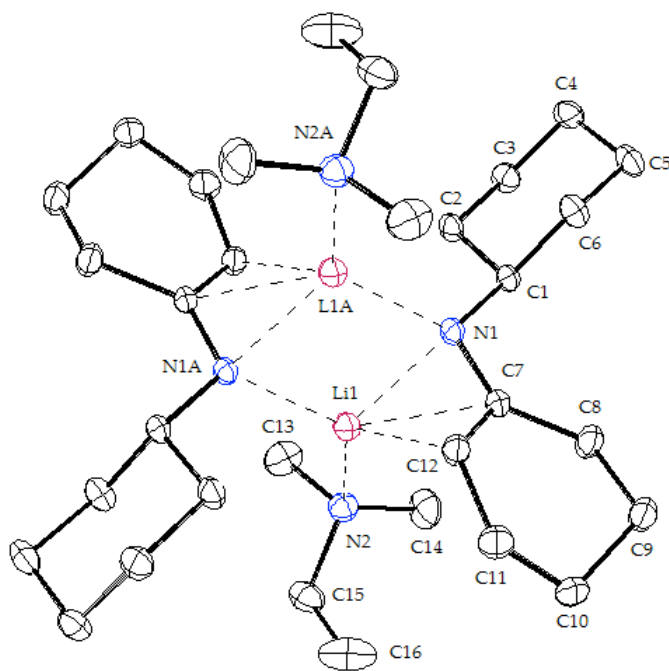
	U ¹¹	U ²²	U ³³	U ²³	U ¹³	U ¹²
Li(1)	24(1)	21(1)	24(1)	0(1)	-4(1)	-4(1)
N(1)	21(1)	16(1)	19(1)	0(1)	-7(1)	0(1)
N(2)	25(1)	28(1)	27(1)	0(1)	-5(1)	-9(1)
C(1)	20(1)	15(1)	21(1)	0(1)	-7(1)	-1(1)
C(2)	24(1)	17(1)	25(1)	0(1)	-10(1)	-2(1)
C(3)	27(1)	25(1)	27(1)	2(1)	-13(1)	-3(1)
C(4)	32(1)	24(1)	26(1)	7(1)	-9(1)	-2(1)
C(5)	32(1)	18(1)	35(1)	5(1)	-11(1)	-5(1)
C(6)	29(1)	20(1)	34(1)	3(1)	-14(1)	-7(1)
C(7)	24(1)	16(1)	20(1)	-1(1)	-6(1)	-3(1)
C(8)	35(1)	25(1)	25(1)	-7(1)	-9(1)	3(1)
C(9)	43(2)	24(1)	25(1)	-7(1)	-11(1)	0(1)
C(10)	52(2)	29(2)	20(1)	-1(1)	-11(1)	-5(1)
C(9')	36(1)	40(1)	24(1)	-11(1)	-2(1)	-5(1)
C(10')	48(1)	38(2)	25(1)	-9(1)	-13(1)	-9(1)
C(11)	42(1)	30(1)	25(1)	0(1)	-17(1)	-7(1)
C(12)	28(1)	20(1)	22(1)	-3(1)	-10(1)	-2(1)
C(13)	40(1)	50(1)	37(1)	-6(1)	-8(1)	-24(1)
C(14)	27(1)	35(1)	54(1)	-4(1)	-5(1)	1(1)
C(15)	35(1)	34(1)	36(1)	8(1)	-7(1)	-15(1)
C(13')	42(4)	42(4)	48(4)	-9(3)	-6(3)	-21(3)
C(14')	39(4)	47(4)	63(5)	6(4)	-25(4)	-1(3)
C(15')	43(4)	63(5)	24(2)	-2(3)	-4(2)	-22(3)
C(16)	57(1)	90(1)	37(1)	19(1)	-18(1)	-36(1)

Table 5. Hydrogen coordinates ($\times 10^4$) and isotropic displacement parameters ($\text{\AA}^2 \times 10^{-3}$)

	x	y	z	U(eq)
H(9A)	3877	9174	3252	39
H(9B)	2095	9324	4144	39
H(10A)	3842	7342	5110	43
H(10B)	2890	6578	4491	43
H(9'A)	2013	7278	4124	43
H(9'B)	1699	9066	4218	43
H(10C)	3977	7743	4951	44
H(10D)	4531	8628	3571	44
H(13A)	783	3049	1164	60
H(13B)	2682	2478	573	60
H(13C)	1653	4091	82	60
H(14A)	-384	5195	2710	63
H(14B)	460	6101	1470	63
H(14C)	785	6049	2890	63
H(15A)	904	2902	3485	42
H(15B)	2702	1994	2742	42
H(13D)	998	2563	1880	65
H(13E)	2897	1983	1621	65
H(13F)	2114	2953	483	65
H(14D)	-451	5287	1932	76
H(14E)	793	5547	563	76
H(14F)	561	6413	1859	76
H(16A)	2554	2605	4836	89
H(16B)	1823	4376	4482	89
H(16C)	3624	3469	3737	89
H(2B)	2072(14)	6747(14)	-1307(11)	32(3)
H(12)	5991(14)	5505(13)	1421(11)	26(3)
H(3A)	380(14)	9218(13)	-1597(11)	29(3)
H(6B)	4598(15)	9035(15)	-1662(12)	34(3)
H(1)	1851(14)	8524(13)	191(11)	29(3)
H(4A)	3139(14)	9891(14)	-3474(12)	30(3)

H(2A)	3617(14)	7097(13)	-2307(11)	28(3)
H(5A)	1425(15)	11157(14)	-906(12)	37(3)
H(6A)	3787(14)	9826(14)	-239(13)	38(3)
H(4B)	1409(16)	11043(16)	-3115(13)	47(4)
H(3A)	1262(15)	8471(14)	-3042(13)	36(3)
H(5B)	2879(16)	11620(16)	-1897(13)	46(4)
H(8B)	2593(16)	9382(16)	1837(14)	48(4)
H(11B)	5258(19)	5275(19)	3847(15)	65(4)
H(11A)	6262(17)	6404(15)	3330(13)	45(4)
H(8A)	1566(18)	8239(16)	2297(14)	53(4)

LXVII. Ortep drawing of lithioimine *trans*-12 (A_2S_2 , S = Me₂EtN)



Part 7. References

- S-1. Glueck, D. S.; Wu, J; Hollander, F. J; Bergman, R. G. *J. Am. Chem. Soc.* **1991**, *113*, 2041.
- S-2. Lazbin, I. M.; Koser, G. F. *J. Org. Chem.* **1986**, *51*, 2669.
- S-3. G. F. Koser; R. H. Wettach. *J. Org. Chem.* **1977**, *42*, 1476.
- S-4. Kim, Y.-J.; Bernstein, M. P.; Galiano-Roth, A. S.; Romesberg, F. E.; Fuller, D. J.; Harrison, A. T.; Collum, D. B.; Williard, P. G. *J. Org. Chem.* **1991**, *56*, 4435.

(18) Gaussian 03, Revision B.04, Frisch, M. J.; Trucks, G. W.; Schlegel, H. B.; Scuseria, G. E.; Robb, M. A.; Cheeseman, J. R.; Montgomery, Jr., J. A.; Vreven, T.; Kudin, K. N.; Burant, J. C.; Millam, J. M.; Iyengar, S. S.; Tomasi, J.; Barone, V.; Mennucci, B.; Cossi, M.; Scalmani, G.; Rega, N.; Petersson, G. A.; Nakatsuji, H.; Hada, M.; Ehara, M.; Toyota, K.; Fukuda, R.; Hasegawa, J.; Ishida, M.; Nakajima, T.; Honda, Y.; Kitao, O.; Nakai, H.; Klene, M.; Li, X.; Knox, J. E.; Hratchian, H. P.; Cross, J. B.; Bakken, V.; Adamo, C.; Jaramillo, J.; Gomperts, R.; Stratmann, R. E.; Yazyev, O.; Austin, A. J.; Cammi, R.; Pomelli, C.; Ochterski, J. W.; Ayala, P. Y.; Morokuma, K.; Voth, G. A.; Salvador, P.; Dannenberg, J. J.; Zakrzewski, V. G.; Dapprich, S.; Daniels, A. D.; Strain, M. C.; Farkas, O.; Malick, D. K.; Rabuck, A. D.; Raghavachari, K.; Foresman, J. B.; Ortiz, J. V.; Cui, Q.; Baboul, A. G.; Clifford, S.; Cioslowski, J.; Stefanov, B. B.; Liu, G.; Liashenko, A.; Piskorz, P.; Komaromi, I.; Martin, R. L.; Fox, D. J.; Keith, T.; Al-Laham, M. A.; Peng, C. Y.; Nanayakkara, A.; Challacombe, M.; Gill, P. M. W.; Johnson, B.; Chen, W.; Wong, M. W.; Gonzalez, C.; and Pople, J. A.; Gaussian, Inc., Wallingford CT, 2004.